Disentangling the processes driving microbial community assembly on a marine plant

By

MELISSA ROSE KARDISH
DISSERTATION

Submitted in partial satisfaction of the requirements for the degree of

DOCTOR OF PHILOSOPHY

in

Population Biology

in the

OFFICE OF GRADUATE STUDIES

of the

UNIVERSITY OF CALIFORNIA

DAVIS

Approved:

_____

John J. Stachowicz, Chair

_____

Jonathan A. Eisen

_____

Edwin D. Grosholz

Committee in Charge

2021

TABLE OF CONTENTS

ACKNOWLEDGEMENTS

More people than I thought possible contributed to my ability to complete this dissertation and I owe all of them an enormous debt of gratitude.

First, Jay, thank you for welcoming me as a bit of an unusual student into your lab. I am really excited about all the work we were able to accomplish and appreciate your unending support and patience. Thank you for helping me explore new science and build up so much of what we know about this system now with me.

To the Stachowicz Lab, I could not imagine this dissertation without you. I loved collaborating with you, learning from your experience in these systems, and exploring your science. Thank you for your love and generosity. Special thanks to Nicole and Katie – it was wonderful to get to do my PhD in parallel with both of you.

To all the undergrads who assisted me on these projects, I truly appreciate your patience and dedication. I truly loved watching you learn and grow throughout your undergrad into your paths going forward. Special thanks to Mackenzie, Therese, Felicia, Harley, Hailey, Liz, Tina, Brian, Kelly, and Daniel for your efforts in the lab and the field.

To the broader UC Davis community, thank you for helping me grow and push past where I thought I could. From CMSI and the Data Lab to CPB and my PBGG cohort to my committee,

you all pushed me to question my ideas, try new approaches, and find questions that were broadly interesting inside and outside of my dissertation.

To the support structures at UC Davis, especially the EVE office to BML to UC Davis Facilities, none of this would have been possible without your support and availability to help whenever there was an issue.

To my many funding sources, including National Science Foundation Graduate Research Fellowship Program, XSEDE, ARCS, Center for Population Biology, Hardman Foundation, and S.O. Mast Scholarship, thank you for supporting my work financially.

To my friends and family (science and non-science!), thank you for your support, reality checks, interest, and encouragement throughout my degree. I appreciate your availability, time, and love more than you know.

To Lowell, my bootstrap value, who else would support me making stats jokes everywhere in my life? Thank you for your support and your ready ear as I talked through many a problem these last several years.

Finally, I would like to dedicate this dissertation to the memory of my grandfather, John Burroughs, the very first PhD I knew and one of the best question askers I've ever met.

ABSTRACT

The role of microbiomes in host ecology is increasingly recognized as a potentially important force driving the ecology and dynamics of a broad range of ecosystems. However, these communities are often so complex that determining the factors (environment, dispersal, host-interactions) driving these assembled communities can be difficult. In my dissertation, I explored various factors might be driving the assembly surface microbiome of Zostera marina, eelgrass. Eelgrass is a marine angiosperm found in coastal waters across the Northern Hemisphere and provides a variety of ecosystem services including sedimentation, habitat creation and carbon sequestration. I have investigated patterns of surface communities of bacteria on both leaves that are largely surrounded by seawater and roots that grow in anoxic, highly sulfidic sediments to understand how these communities connect and modulate eelgrass's interactions with its environment.

In Chapter 1, I begin by identifying and exploring what the unique components of the eelgrass microbiome are by using artificial mimics. I deployed above and belowground mimics and found roots and leaves, but especially roots, host unique microbial communities compared to mimics. Based on differences in taxa between mimics and plant tissue, I suggest that leaf-associated microbiomes may have key roles in mediating plant-microalgal-pathogen interactions and that root-associated taxa with enhanced associations with sulfur and nitrogen cycling may ameliorate environmental stress. Furthermore, in this chapter, I identify future candidates for manipulation to further identify their specific roles on eelgrass.

In Chapter 2, I examined the role of host vs. environment in structure and assembly of eelgrass microbial communities. Through a reciprocal transplant experiment, I found that even on a fine scale, microbial communities quickly resemble where they are transplanted to rather

than where they are transplanted from. Additionally, I found that degree of phylogenetic community clustering varied by site suggesting environmental differences drove different community processes across these sites.

Finally, in Chapter 3, I take these associations into the lab to experiment with reduced diversity environments. Through manipulations of source microbial pools via autoclaving sediments and host specific associates via bleaching root surfaces, I identify that most microbial communities are sourced from their adjacent sediments. In this reduced diversity environment in autoclaved sediments, I also identify that communities are more variable than in normal source environments and that genotype of plant has a role in determining the microbial community present. This suggests that while source and environment are critical in determining microbial community structure, there is also a role in plant-microbe feedbacks that structures assembly of host-associated microbial communities in seagrass.

Through these experiments, I determine that environment plays a predominant role in the assembly of these microbial communities on both leaves and roots. I suggest that there are also smaller, but important roles of interactions with host plant and dispersal in structuring these communities. Continuing work will focus on disentangling how different plant traits influence microbial communities within different and variable environments.

More than a stick in the mud: Eelgrass leaf and root bacterial communities are distinct from those on physical mimics

Authors: Melissa R. Kardish, John. J. Stachowicz

Originality-Significance Statement

We show that eelgrass establishes a distinct microbial community from a physical mimic on both its leaves and roots. This is, to our knowledge, the first comparison of seagrass to a mimicked physical environment. Insights from our study establish bacterial targets for future functional studies of seagrass-microbiome interactions.

Summary

We examine the role of physical structure vs. biotic interactions in structuring host-associated microbial communities on a marine angiosperm, *Zostera marina*, eelgrass. Across several months and sites, we compared microbiomes on physical mimics of eelgrass roots and leaves to those on intact plants. We find large, consistent differences in the microbiome of mimics and plants, especially on roots, but also on leaves. Key taxa that are more abundant on leaves have been associated with microalgal and macroalgal disease and merit further investigation to determine their role in mediating plant-microalgal-pathogen interactions. Root associated taxa were associated with sulfur and nitrogen cycling, potentially ameliorating environmental stresses for the plant. Our work identifies targets for future work on the functional role of the seagrass microbiome in promoting the success of these angiosperms in the sea.

Introduction

The role of microbiomes in host ecology is increasingly recognized as a potentially important force driving the ecology and dynamics of a broad range of ecosystems. Host-microbe

interactions range in strength and direction (McFall-Ngai *et al.*, 2013; Hammer *et al.*, 2019) with microbes providing net benefits to their hosts in some cases, parasitizing hosts or other members of the microbial community in others, and participating in many symbiotic relationships in between these extremes (Trivedi *et al.*, 2020). Yet hundreds or thousands of microbial taxa associate with any given host, and we generally know little about the extent to which most associations rely on specific host traits such as morphology, physiology or metabolites. In most cases, our knowledge is limited to comparing host-associated microbes with a larger environmental pool, such as soils, and identifying taxa over-represented on hosts compared to the environment (Knights *et al.*, 2011; Fahimipour *et al.*, 2017; Xiong *et al.*, 2021). These approaches often identify hundreds of taxa positively associated with hosts, still leaving a major challenge for developing an understanding of the extent to which particular microbes interact closely with, and impact, hosts. However, this approach does not distinguish the role of the provision of physical structure vs. host-specific biology; incorporating this level of distinction would identify taxa that require not just the structure but the presence of a living host and therefore a greater potential for reciprocal interactions with the host. One way to distinguish the relative importance of physical structure from living organisms is to use physical mimics to assess how microbial communities develop differently in the absence of biotic interactions with the host.

Mimicking environments to learn more about host-microbe interactions -- whether through simple physical models, reconstituting biochemical environments, or even using germ-free organisms -- has been used across a diversity of taxa to assess critical members microbial communities as well as to assess how the overall structure of their communities vary under stress. For example, in terrestrial plants, finely mimicked leaf surfaces have led to insights on

where *E. coli* resides on spinach leaves based on water retention on structural mimics (Zhang *et al.*, 2014) and an artificial human gut has been used to demonstrate interactions between anti-inflammatory bacteria and epithelial cells (Zhang *et al.*, 2021). While often used to understand how an organism interacts with the microbes, these mimics can also be used to describe community shifts that would occur without the host, identify key partners, and consider differences in assembly (e.g., Lee *et al.*, 2019).

Host-associated microbial communities have been identified across organisms to assemble in distinct non-random ways though the degree of specificity varies (Taylor *et al.*, 2004; Ambika Manirajan *et al.*, 2016). Microbial associates can be highly specific (e.g., the bobtail squid and *Vibrio fisherii, McFall-Ngai and Ruby, 1991)* or might be transitory/happenstance associations (e.g., high numbers of soil bacteria in Lycaenid butterfly gut microbiomes; (Whitaker *et al.*, 2016). In addition a host can interact with a microbiome with different levels of restrictiveness: a host might harbor a highly restricted environment potentially heavily modified by a host (e.g., a gut microbiome; Garland *et al.*, 1982; Rinninella *et al.*, 2019) or a less restrictive environment where even with environmental modification from the host many microbes could enter the community (e.g., skin microbiome; Byrd *et al.*, 2018). Distinguishing among these types of microbial communities may offer insight into the intensity of interactions with a host. For instance, if we distinguish that a less restrictive surface had a microbiome unassociated specifically with a host, we might infer limited direct unique interactions with that host.

We investigate the role of physical structure vs. biotic interactions in structuring the surface microbiomes of seagrass, specifically, the eelgrass, *Zostera marina*. Eelgrass is a marine flowering plant; its roots and rhizomes grow in highly sulfidic sediment and its leaves, while

primarily exposed to seawater, can be periodically exposed to air at low tides (Jørgensen, 1982). Seagrass leaves are distinct from terrestrial angiosperms in several ways, including absence of stomata as well as primary exposure to seawater rather than air (Olsen *et al.*, 2016). Our previous work showed broad overlap in the composition of leaf and water microbiomes (Fahimipour *et al.*, 2017), but did find some microbes preferentially associated with leaves. Comparison of microbiomes among species of seagrass that grow in the same environment show that some harbor distinct microbial communities on their leaves from other species (Garcias-Bonet *et al.*, 2020) while some seagrass species have broad overlap in their microbiomes (Ugarelli *et al.*, 2017; Kaimenyi *et al.*, 2018). At least some taxa are disproportionately found on seagrass compared to water, though it is not clear the extent to which leaf microbiomes differ from those that accumulate on inert surfaces in marine systems, where biofilms develop on surfaces at a fast rate (Fischer *et al.*, 2014). Mimicked seagrass leaves have long been used to investigate community structures and show similar macroinvertebrate (Healey and Hovel, 2004), fish (Bell *et al.*, 1985) and microalgal communities (Horner, 1987; Pinckney and Micheli, 1998) to natural seagrass and provide an obvious approach for distinguishing substrate generalists from seagrass-specific associates. We adopt this approach to narrow the functionally important microbiome of seagrass leaves from the pool of over a hundred of taxa known to be enriched on leaves relative to surrounding seawater.

Similarly, root surfaces have bacterial communities distinct from adjacent sediments (Fahimipour et al 2017), but it is not yet clear again how much physical structure vs host biology influences this. Roots inhabit anoxic and highly sulfidic sediments that without mitigation can lead to sulfide intrusion decreasing plant growth and health (Hasler-Sheetal and Holmer, 2015). Various mechanisms exist to mitigate this environment and reduce sulfide intrusion into the plant

including radial oxygen loss (ROL) from growing roots (Pedersen *et al.*, 2004), direct partnerships with sulfide-oxidizing bacteria (Smith *et al.*, 2004), and three-way symbiosis with lucinid clams hosting sulfide-oxidizing bacteria (van der Heide *et al.*, 2012; de Fouw *et al.*, 2018). However direct association of seagrass with sulfur oxidizers is known (Fahimipour *et al.*, 2017) and given the leak of oxygen and sugars out of the roots (Sogin *et al.*, 2021), it seems likely that the plant plays an important role in root microbe assembly. Examining mimicked root environments is less common in seagrass than use of seagrass leaves and has focused on sediment stabilization processes (Temmink *et al.*, 2020) rather than influence on biotic community structure.

Here, we explicitly test whether seagrass roots and leaves assemble microbiomes that are distinct from physical mimics at a range of sites and seasons with a harbor. By comparing live plants with biologically inactive surfaces mimicking some physical aspects of their environment, we test explicitly whether seagrass cultivates a unique microbiome on its leaves and/or roots. Differences in the bacterial communities between physically mimicked environments and plants could indicate bacteria that might be either attracted by specific biological aspects of a plant or that might be selected by plants for biologically important roles. Thus, such an approach can identify the role of the plant in microbial assembly and hint at specific key processes, while also potentially identifying microbial partners that may play key functional roles in the seagrass microbiome for future experimentation.

Results

The bacterial assemblages associated with leaves and roots differed from those on their corresponding physical mimics in alpha diversity and/or community composition. However, the extent of this differentiation of eelgrass microbiomes from passive substrates was stronger in roots than leaves, and there were still many amplicon sequence variants (ASVs) shared between mimics and live plants (Figures 1.1 and 1.2). These differences among substrates were highly consistent across four sites and three time points (see results below), despite previously identified seasonal and site-specific microbial components at these sites (Chapter 2), indicating a strong impact of live plants on the microbiome. Thus, we focus our presentation of results on the consistent effects of substrate across sites and time (each of which is controlled for in our statistical models).

Leaves

Leaf mimics had greater ASV richness than leaves (negative binomial glm with crossed random effects for month and site, estimate = 0.19738, standard error = 0.05802, z-value 3.402, $p = 0.0007$; Figure 1.1A). The ASV composition of the leaf and mimic communities was different (PERMANOVA, $F = 12.09$, $p = 0.001$, $r^2 = 0.13$, Figure 1.2A), though there was no difference in variance among-leaf vs. among-mimic communities (betadisper ANOVA, $p = 0.73$). When examining core ASVs (present in at least 50% of samples of a type at at least 1% detection rate), we found that roughly half the ASVs found on leaves were not found on any other substrate (77 of 168 ASVs; 46%) while most of the remaining were shared with those on leaf mimics (88 of 168, 52%). (Figure 1.1B). This degree of overlap in core taxa was the greatest of any pairwise comparison among sample types; The same patterns were present when we examined all ASVs rather than just the core (Supplemental Figure 1.S1). Predicted Metacyc pathways, based on a cross-domain database of metabolic pathways and enzymes (Caspi *et al.*,

2014), also differed between leaves and mimics (PERMANOVA, $r^2 = 0.05488$, $F = 4.7035$, $p = 0.001$), though this effect was weaker than for the sequence based compositional differences (Figure 1.2B).

Through analysis of specific ASVs that varied between leaves and leaf mimics via DESEQ2, we found 92 ASVs were relatively more abundant on leaves and 49 were relatively more abundant on mimics. Only three families contained more than ten ASVs that varied between mimics and leaves (Table 1.1): Flavobacteriaceae (eight higher on leaves, eight higher on mimics), Rhodobacteraceae (23 higher on leaves, 13 higher on mimics), and Saprospiraceae (16 higher on leaves, none higher on mimics). Within these families several genera were represented by multiple ASVs. These included *Kordia* (three ASVs higher on leaves, none on mimics), *Ulvibacter* (two higher on leaves, two higher on mimics), *Octadecabacter* (one higher on leaves, one higher on mimics), *Sedimentitalea* (one higher on leaves, one on mimics), *Tateyamaria* (one higher on leaves, one on mimics), *Yoonia-Loktanella* (two higher on leaves), *Lewinella* (three higher on leaves) and *Rubidimonas* (two higher on leaves). Many other families contained fewer than 3 ASVs that varied between leaves and mimics (Table 1.1, Supplemental Table 1.S1), and within these nine genera contained multiple ASVs that varied between leaves and mimics (Supplemental Table 1.S2). All taxa that varied can be found in Supplemental Table 1.S3.

When we examined predicted pathways that changed between the leaf and leaf mimic microbiomes, we identified 53 pathways that changed, 16 upregulated in leaf microbiomes and 37 upregulated on mimic microbiomes (Supplemental Table 1.4). These predicted pathways included differences in amino acid degradation, starch degradation, and denitrification; however, these predicted pathways did not always indicate expected differences among plants and mimic

communities or produce clear candidate predicted pathways, likely at least in part due to limits in prediction of environmental microbial pathways, so we have focused on taxonomic differences.

Roots

Despite strong compositional differences between roots and root mimics (PERMANOVA, $F = 31.511$, $p = 0.001$, $r^2 = 0.307$; Figure 1.3A), these substrates did not differ in ASV richness (negative binomial glm with crossed random effects for site and month, $p = 0.28$, Figure 1.1A) or variance (betadisper ANOVA, $p = 0.29$). When including sediments in the comparisons, richness did not differ among the three groups in richness (negative binomial glm with crossed random effects for site and month, $p = 0.31$) but microbiome variance among samples was less among sediment samples than either of the other two groups (betadisper ANOVA, $p < 0.001$, Tukey's HSD sediment vs mimic $p = 0.0001$, vs roots $p = 0.004$); ASV composition on roots, mimics and sediment were compositionally distinct (PERMANOVA $r^2 = 0.3480348$, $F = 37.90152$, $p = 0.001$, see Supplemental Table 1.S5 for pairwise comparisons). When we examine overlap in predicted Metacyc pathways, we found that there was a significant difference between roots, sediments and mimics (PERMANOVA, $r^2 = 0.18903$, $F = 12.534$, $p = 0.001$), though this effect was weaker than for the sequence based compositional differences (Figure 1.3B, See Supplemental Table 1.S5 for pairwise differences).

When examining core ASVs (present in at least 50% of samples of a given type at at least 1% detection rate), we found that roots and sediments largely harbored distinct bacterial communities, by ASV (Figure 1.1B), though root mimics had few ASVs unique to its core microbiome (only 2 ASVs unique to root mimics); again, we saw the same patterns when including all ASVs in these analyses, and not just the core (Supplemental Figure 1.S1). Of 256 ASVs in the core root microbiome, 111 or 43% were found only on roots and 181 (71%) were

found only on roots and in sediments. Only 52 core root ASVs (20%) were shared between roots and root mimics. When we examined all ASVs (without core restrictions), root mimics had more taxa unique to their sample type, indicating considerable variability in communities assembled on root mimics and a large contribution of rare ASVs (Supplemental Figure 1.S1).

We found many ASVs varied in abundance between these groups (457 between sediments and mimics, 505 between roots and sediments, and 486 between roots and mimics). Of these, the majority were at higher relative abundances on roots or sediments compared to mimics (comparing roots to mimics, 437 were higher on roots, and 49 were higher on mimics; comparing sediment to mimics, 359 were higher in sediments, 98 were higher on mimics; comparing roots to sediments 265 were higher on roots, 240 were higher in sediments; see Table 1.1 for families with the most representatives, Supplemental Table 1.S6 for more details and Supplemental Table 1.S7 for all ASVs that varied). The families that had the largest number of taxa vary among sample types included Spirochaetaceae (71 ASVs), Bactoroidetes BD2-2 (87 ASVs), Desulfosarcinaceae (103 ASVs), Desusulfocapsaceae (109 ASVs), and Flavobacteriaceae (114 ASVs). Within the families Spirochaetaceae, Bactoroidetes, and Desulfosarcinaceae most ASV were at greater relative abundance on roots than mimics (Table 1.1). In Flavobacteriaceae, roughly equal numbers of ASVs were more abundant in roots vs mimics vs. sediment. A few families showed an abundance of ASVs on roots compared to both sediments and mimics including: Desulfobacteraceae, Lachnospiraceae, Marinilabiliaceae, Moduliflexaceae, and Prolixibacteraceae (Supplemental Table 1.S6).

While the predicted pathways that varied were numerous and not particularly remarkable (as indicated in Supplemental Table 1.S8), we found that indicated pathways were generally indicated to be upregulated on mimics in pairwise comparisons (133 predicted pathways higher

in mimics compared to 32 in sediments, and 137 higher on mimics compared to 35 on roots). Again we anticipate that due to limits in prediction of environmental microbial pathways these may be limited (especially seeing lower numbers of predicted pathways enriched where we saw more taxa enriched), so we have focused on the taxonomic differences we identified.

Discussion

We found large and consistent differences in the microbiome between seagrass and structural mimics both on above- and belowground surfaces. This builds on previous work that showed distinction between microbiomes on water and leaf surfaces and sediment and root surfaces (Fahimipour *et al.*, 2017), showing definitively that microbiomes respond not just to plant physical structure but also the biological activity associated with the host. Previous work also showed strong geographic variation in the microbiome of seagrasses at medium and large scales (Fahimipour *et al.*, 2017; Hurtado-McCormick *et al.*, 2019) yet, we find consistent differences between mimics and plants across four close sites and three time periods from early to late summer. These findings were consistent for both roots and leaves. This confirms a need for understanding of how these communities are cultivated/built, their interactions with the plants, and ultimate influence on plant fitness.

Leaves are differentiated from passive mimics

While we saw a >50% overlap in core taxa between the mimics and leaves, we found that they were compositionally distinct (both taxonomically and functionally) and even showed differences in alpha diversity (more ASVs were found on the average mimic than the average leaf). Epiphytic algae also have higher alpha diversity on mimicked compared to natural seagrass

and differences in the relative abundance of major microalgal groups between mimic and leaves (Pinckney and Micheli, 1998). These differences in communities between leaves and mimics likely represent either microbial preferences for different surfaces or selection by plants. The reduced alpha diversity on real leaves suggests that there may be some selection by leaves, but also some bacterial preferences as the leaf microbiome is not simply a subset of that on mimics (Figure 1.1B). While these mimics were not perfect physical mimics, we did find they captured a large portion of the eelgrass leaf community.

This contrasts with mimicked environments from other marine organismal phyllospheres. Recent work in kelp indicated an enrichment of common seawater taxa on artificial substrate (agar infused with and without kelp), no difference in taxonomic diversity on artificial substrates compared to kelp, and increases in aerobic taxa on the surface of kelp blades (Weigel and Pfister, 2021). We found none of these patterns on seagrass and seagrass mimics, instead finding no enrichment for common taxa on seagrass compared to mimics, higher taxonomic diversity on mimics, and no compelling evidence that compositional differences we observed were due to differences in aerobic conditions. The distinction from our study could be driven by the accumulation of epiphytic algal communities on both seagrass leaves and mimics that could render the mimic surfaces highly aerobic; there also is less carbon released by seagrasses than macroalgae (Barrón *et al.*, 2014) which likely further distinguishes microbe-host interactions in seagrass from those in kelp.

Terrestrial work mimicking plants has largely focused on even more precisely recreating leaf environments when using artificial surfaces in comparisons (Doan and Leveau, 2015). Use of mimics to test the effect of terrestrial plant leaf morphology on microbiota has indicated that the physical structure plays an important role in influencing the microbiome via moisture

retention (Doan *et al.*, 2020), a mechanism that is irrelevant to the submerged microbiome of aquatic plant leaves. Like leaves of terrestrial plants, seagrass leaves exude amino acids (Jørgensen *et al.*, 1981) and dissolved organic carbon (Wetzel and Penhale, 1979) which create a uniquely rich environment potentially shaping their microbial communities including some predicted amino acid degradation pathways we identified (Supplemental Table 1.S4). These and other potentially seagrass-curated microbial partners could allow us to identify mechanisms in the future that have allowed seagrasses to persist in these extreme environments with a host of new biotic interactions as well ranging from microalgae to marine microbial communities. Future experiments could also investigate interactions involving microbial attachment and facilitation or deterrence by plant exudates as has been explored in terrestrial systems (Zhang *et al.*, 2014; Doan and Leveau, 2015; Warning and Datta, 2017) to compare differences that have arisen with transitions to sea.

Finally, while our limited functional evidence does not indicate clear functional differences, the specific taxa that we observe on leaves may have speculatively important roles that are worthy of further investigation. The repeated enrichment of certain ASVs on leaves versus mimics suggests that they might be good targets for experimentation. Some — such as *Kordia spp.* — are likely algicidal bacteria that has been isolated during red tides (Sohn *et al.*, 2004) and could be cultivated by seagrass to manage epiphyte loads; we have also previously identified different *Kordia* ASVs at higher relative abundance under warmed and cooled temperature treatments (Schenck et al. submitted). The two Saprospiraceae that we saw multiple representatives within a genera only present on leaves (*Lewinella spp.* and *Rubidimonas spp.*) are both genera comprised of aerobic heterotrophs previously isolated from marine environments that can metabolize complex starches (McIlroy and Nielsen, 2014) and have previously been

associated higher levels in macroalgal diseases (Zozaya-Valdés *et al.*, 2017). While these bacteria are associated more strongly with seagrass, further investigation is needed to determine how they interact with seagrass, seagrass diseases and seagrass epiphytes -- as they may be cultivated partners in removing unwanted epiphytes or could be negatively affecting eelgrass as well.

Root microbes are vastly different from those in sediment and on root mimics

That root microbiomes differed from mimics was not surprising given that roots exude both organic (e.g., sugars) and inorganic (e.g., oxygen) compounds that have major influences on microbiota. In fact, sugar concentrations associated with seagrass roots can be exceedingly high yet may not metabolized by bacteria due to the presence of inhibitory phenolic compounds (Sogin *et al.*, 2021). Similarly, the combination of oxygen leakage from root tips and surrounding sulfidic sediments promotes sulfur oxidizing bacteria (Brodersen *et al.*, 2018; Martin *et al.*, 2019). Given these plant-caused environmental differences from surrounding sediments, it does not seem surprising that root mimics microbiomes did not resemble those on roots. However, as in leaves, we captured the surface microbiome of a physical structure buried in sediment. There was no clear "core" of root mimic communities and while there was no evidence of a difference in alpha diversity, our taxonomic analyses showed that taxa that varied between mimics and sediments or roots were generally higher in relative abundance on root surfaces or in sediments than on the mimics. Given the lower abundances, we were surprised to see the opposite result in functional predictions where predicted pathways were generally upregulated on mimics. However, given the more limited functional predictions (including the lack of upregulation sulfate reduction related predicted pathways on roots and sediments compared to mimics despite increases in taxonomic relative abundance of sulfate reducing

bacteria) and rapidly changing taxonomy of some of these groups (Waite *et al.*, 2020), the bacteria on mimics might be better described than other groups. However, based on taxonomy we have identified several families containing ASVs worthy of further investigation including Desulfobacteraceae and Prolixibacteraceae, both of which were overrepresented on roots compared to mimics and sediments and involved in sulfate-reduction and nitrogen cycling respectively.

Terrestrial experiments investigating rhizosphere microbial communities through creation of artificial environments have added root exudates through capillaries (e.g., addition of oxalic acid into soils frees carbon; Keiluweit *et al.*, 2015), and similar experiments could test the roles of exudates and oxygen extrusion independently and in combination to further determine the mechanisms by which microbial communities on the surfaces of roots are assembled, particularly how they sustain these plants in highly anoxic sediments. Based on the taxa we identified, it is likely that seagrass root bacterial communities, like those of terrestrial plants, are structured by a resource exchange between hosts and microbes. While there are many differences in what these resources are and partnerships look like (e.g., eelgrass do not have associations with arbuscular mycorrhizal fungi (Nielsen *et al.*, 1999; Ettinger and Eisen, 2019) and land plants live in well oxygenated soils instead of sulfidic anoxic sediments), aquatic and land angiosperms participate in a resource exchange that drives microbial community structures in the rhizosphere (for review of land plants see Jacoby *et al.*, 2017). This suggests that it is likely that root microbes are not only affected by the eelgrass, but affect eelgrass itself, perhaps through sulfur metabolism (Fahimipour *et al.*, 2017). While no studies have directly tested the effect of root microbiome on seagrass growth, the oxidation of sulfides by lucinid bivalve - bacterial symbiosis has been implicated as a major influence on seagrass success in anoxic sediments (van der Heide *et al.*,

2012). Direct tests implicating changing rhizosphere microbial communities with changes in plant performance would be necessary to explicitly test these roles but starting with isolates from many of the families we saw preferentially on seagrass roots compared to mimics and sediments seem likely candidates to have specific adaptations that might deal with both potential phenolic challenges.

Overall conclusions

We found robust evidence of differences between mimics and plant tissues in various environments in seagrass. These large differences suggest that there is a unique environment created by the plant that creates these distinct communities either as part of active partnerships or through inhibition of certain microbes or unique characteristics of that environment preferred by some microbes. Unlike in terrestrial plant surfaces, water retention is unlikely to play a role in driving microbe assembly in aquatic leaves. Seagrass leaf microbiomes may be structured more like microbiomes in terrestrial and marine root microbiomes, by exudates of plants and their influence on the environment. Further experiments with more detailed or realistic mimics could isolate the mechanisms by which these microbiomes are structured and function.

Finally, despite the differences emphasized here, there is vast overlap between these communities even on simple substrates, especially on leaves and their mimics. This designates a manageable number of taxa to further examine to see what factors are driving their unique assemblies. With a continued and rising interest in microbial communities in general and the role of microbial communities associated with seagrasses specifically, extensions of this work point towards associations that should be further explored for understanding holobiont dynamics across species ranges.

Experimental Procedures

Field methods

In July 2015, we deployed artificial substrates to characterize the microbiome of a leaf and root mimics compared with those on live plants (see Supplemental Figure 1.S2 for site locations). We conducted this experiment at four eelgrass beds within Bodega Harbor within 2 km of each other yet vary in distance from the mouth of the harbor, which sets up a gradient of increasing temperature (2˚ C mean temperature difference among sites), decreasing water flow, and progressively finer sediment grain size that result in each site harboring distinct eelgrass microbial communities on seagrass that vary among seasons (Kardish and Stachowicz unpublished data). We used 0.75 m long, 4 mm wide green polypropylene ribbons attached to a vexar mesh anchored into sediments to mimic artificial leaf substrates, a standard technique that has been used for over 40 years to mimic the physical habitat provided by eelgrass to isolate the role of physical structure in structuring the epiphytic, epifaunal and fish communities that inhabit eelgrass (Barber *et al.*, 1979). These ribbons mimic the physical structure of seagrass leaves in a bed with a similar length, width and accumulation of epiphytes. We also deployed artificial root substrates (4 in. twist ties twisted around the same vexar mesh as ribbons) that went to the depth where most root biomass is found at these sites (approximately 2-5 cm) to examine the community that accumulates on a physical structure at a similar depth in sediment. Neither artificial substrate was preinoculated with microbial communities though they were planted (attached to a vexar mesh) inside a seagrass bed immediately adjacent to live plants. We sampled undisturbed plants near the mimics for comparison. We also sampled plants that had been taken from these sites, taken back to the Bodega Marine lab, attached to the same vexar screens as the

mimics and planted back into the field. These results parallel the results presented in the main text comparing mimics and undisturbed plants; parallel analyses can be found in Appendix 1.A. We sampled after one, two and three months after deployment, which is sufficient time for transplanted eelgrass to take on microbial characteristics of a new site (Kardish and Stachowicz unpublished data). For leaves and leaf mimics, we took a 2 cm clip of leaf or ribbon at approximately 15 cm above the sediment surface. For the root mimics, we took a 2 cm clip from the bottom of the twist tie (at approximately the same depth as root samples). For roots, we detached ~10 roots from the rhizome. For sediment samples, we took a small sediment sample from approximately 2 cm under the sediment surface (a similar depth to roots sampled). Samples were immediately placed on dry ice and were frozen at -80˚ C within a few hours of sampling until extraction, and all instruments were alcohol sterilized in between samples. At each of the four sites, across three timepoints, we sampled three sediment samples, three mimic samples (for each of leaf and root mimics), and four plant samples (leaf and root). Due to the identifiable nature of these sample types, we were unable to blind ourselves to sample type during sampling or extraction.

Molecular Methods and Bioinformatic analysis

We extracted DNA with the MoBio PowerSoil DNA kit from leaves, roots, and sediments. To get the surface of the leaves and roots only, we vortexed each frozen sample with 500ul of MilliQ water and then added that liquid to the bead tubes and proceeded with the standard extraction protocol (full protocol available at github.mkardish/Transplants/Lab_Protocols). For sediments, we added a small amount of sediment (approximately 0.25 mg) directly to the bead tube. We amplified and sequenced the V4-V5 region of the 16S rRNA gene on an Illumina MiSeq to identify bacteria present at the

Integrated Microbiome Resource at Dalhousie University with primers 515F and 926R (Walters *et al.*, 2016; Comeau *et al.*, 2017).

Bioinformatic Analysis

We ran all bioinformatic and statistical analyses in R (version 4.0.3). We used a standard dada2 pipeline to error check our reads and to identify amplicon sequence variants (Callahan *et al.*, 2016). We used only forward reads in our subsequent analyses (280 base pairs). We identified ASV taxonomy based on the SILVA database (Quast *et al.*, 2013) and built a phylogeny of ASVs using alignments built with DECIPHER (Wright, 2015) then a tree built with FastTree2 (Price *et al.*, 2010) then converted to ultrametric (Britton *et al.*, 2007). We then rooted the bacterial tree with an archaeal outgroup (Callahan *et al.*, 2016).

We also examined the functional potential of the metagenomes of our samples using PICRUSt2 (Douglas *et al.*, 2020). While these predictions come with major caveats for environmental samples due to underrepresentation in the database, we used this approach to infer potential metabolic pathways based on similarities to known metabolisms and compare these among tissue types.

Sampling and sequencing success

We identified 7,696 bacterial ASVs across 192 leaf, root, mimic and sediment samples after quality filtering samples to 3,752,142 reads. Root samples contained between 390 and 1,013 bacterial ASVs on their surface (we measured 47 root samples with read depth between 11,522 and 49,735 reads), Root mimics samples contained between 81 and 790 bacterial ASVs on their surface (we measured 26 root mimic samples with read depth between 2,037 and 37,793 reads), Sediment samples contained between 270 and 843 bacterial ASVs on their surface (we

measured 36 sediment root samples with read depth between 10,771 and 40,343 reads), leaf samples contained between 191 and 841 bacterial ASVs on their surface (we measured 48 leaf samples with read depth between 5,961 and 61,896 reads) and leaf mimic samples which contained between 195 and 717 bacterial ASVs (35 leaf mimic samples with between 4,587 and 31,648 reads per sample)

Statistics

We analyzed the compositional changes in our dataset based on phylogenetic similarity among samples by normalizing samples via a phylogenetic isometric log transform described in (Silverman *et al.*, 2017) and implemented in the R-package "philr". This allows a compositional transformation of the phylogenetic data -- comparing differential weights at nodes throughout the bacterial tree as opposed to just ASVs. We then calculated the Euclidean distance among samples before using PERMANOVA to determine differences among sample types controlling for month and site by constraining permutations. We tested homogeneity of group dispersions with the betadispr function in 'vegan'.

To measure bacterial richness, we rarified all samples to 2950 reads samples which we repeated 200 times (McMurdie and Holmes, 2014) and used each sample's average "Observed ASVs" in our analysis as our measure of bacterial richness in a sample. We tested differences in Observed ASVs using the negative binomial mixed model with crossed random effects implemented in lme4 : Observed ASVs ~ Sample Type + (Sample Type | Site)+(Sample Type | Month) (Bates *et al.*, 2015). We also visualized overlap in these observed ASVs using upSet which allowed us to identify the numbers of overlapping and non-overlapping ASVs across sample types (Conway *et al.*, 2017).

To identify which ASVs varied between samples we performed a likelihood ratio test in DESeq2 comparing models of ~ Site + Month + Sample Type with ~ Site + Month (separately for above and belowground samples) after geometric mean centering raw ASV abundances (Love *et al.*, 2014). We then examined the contrast between sample types to identify which ASVs varied in each compartment.

We treated functional data compositionally as well, using PERMANOVA to analyze differences in pathway composition among samples after a centered log-ratio transformation. We then used DESeq2 with the same models as for taxonomic differences to test for predicted pathway differences among sample types.

Data Accessibility

All scripts used to analyze this data are available at www.github.com/mkardish/Mimics and sequences have been deposited under the NCBI BioProject ID PRJNA731931.

Acknowledgements

We would like to thank J. Eisen and E. Grosholz for their comments on this manuscript. We would like to thank A. Alexiev for assistance with extractions and A. Firl for assistance in sequencing. We would like to thank the Stachowicz Lab for their expertise and assistance in field work. This work was funded by the UC Davis Center for Population Biology, the National Science Foundation Graduate Research Fellowship (to M. Kardish) and a grant from the Gordon and Betty Moore Foundation. This work used the Extreme Science and Engineering Discovery

Environment (XSEDE) on the Comet at SDSC through an allocation to M. Kardish TG-DEB160008.

References

Ambika Manirajan, B., Ratering, S., Rusch, V., Schwiertz, A., Geissler-Plaum, R., Cardinale, M., and Schnell, S. (2016) Bacterial microbiota associated with flower pollen is influenced by pollination type, and shows a high degree of diversity and species-specificity. *Environ Microbiol* **18**: 5161–5174.

Barber, W.E., Greenwood, J.G., and Crocos, P. (1979) Artificial seagrass—a new technique for sampling the community. *Hydrobiologia* **65**: 135–140.

Barrón, C., Apostolaki, E.T., and Duarte, C.M. (2014) Dissolved organic carbon fluxes by seagrass meadows and macroalgal beds. *Frontiers in Marine Science* **1**: 42.

Bates, D., Mächler, M., Bolker, B., and Walker, S. (2015) Fitting Linear Mixed-Effects Models Using lme4. *Journal of Statistical Software, Articles* **67**: 1–48.

Bell, J.D., Steffe, A.S., and Westoby, M. (1985) Artificial seagrass: How useful is it for field experiments on fish and macroinvertebrates? *J Exp Mar Bio Ecol* **90**: 171–177.

Britton, T., Anderson, C.L., Jacquet, D., Lundqvist, S., and Bremer, K. (2007) Estimating divergence times in large phylogenetic trees. *Syst Biol* **56**: 741–752.

Brodersen, K.E., Siboni, N., Nielsen, D.A., Pernice, M., Ralph, P.J., Seymour, J., and Kühl, M. (2018) Seagrass rhizosphere microenvironment alters plant-associated microbial community composition. *Environ Microbiol* **20**: 2854–2864.

Byrd, A.L., Belkaid, Y., and Segre, J.A. (2018) The human skin microbiome. *Nat Rev Microbiol* **16**: 143–155.

Callahan, B.J., McMurdie, P.J., Rosen, M.J., Han, A.W., Johnson, A.J.A., and Holmes, S.P. (2016) DADA2: High-resolution sample inference from Illumina amplicon data. *Nat Methods* **13**: 581–583.

Caspi, R., Altman, T., Billington, R., Dreher, K., Foerster, H., Fulcher, C.A., et al. (2014) The MetaCyc database of metabolic pathways and enzymes and the BioCyc collection of Pathway/Genome Databases. *Nucleic Acids Res* **42**: D459–71.

Comeau, A.M., Douglas, G.M., and Langille, M.G.I. (2017) Microbiome Helper: a Custom and Streamlined Workflow for Microbiome Research. *mSystems* **2.**:

Conway, J.R., Lex, A., and Gehlenborg, N. (2017) UpSetR: an R package for the visualization of intersecting sets and their properties. *Bioinformatics* **33**: 2938–2940.

Doan, H.K. and Leveau, J.H.J. (2015) Artificial Surfaces in Phyllosphere Microbiology. *Phytopathology* **105**: 1036–1042.

Doan, H.K., Ngassam, V.N., Gilmore, S.F., Tecon, R., Parikh, A.N., and Leveau, J.H.J. (2020) Topography-Driven Shape, Spread, and Retention of Leaf Surface Water Impacts Microbial Dispersion and Activity in the Phyllosphere. *Phytobiomes Journal* **4**: 268–280.

Douglas, G.M., Maffei, V.J., Zaneveld, J.R., Yurgel, S.N., Brown, J.R., Taylor, C.M., et al. (2020) PICRUSt2 for prediction of metagenome functions. *Nat Biotechnol* **38**: 685–688.

Ettinger, C.L. and Eisen, J.A. (2019) Characterization of the Mycobiome of the Seagrass, Zostera marina, Reveals Putative Associations With Marine Chytrids. *Front Microbiol* **10**: 2476.

Fahimipour, A.K., Kardish, M.R., Lang, J.M., Green, J.L., Eisen, J.A., and Stachowicz, J.J. (2017) Globalscale structure of the eelgrass microbiome. *Appl Environ Microbiol* **83.**:

Fischer, M., Friedrichs, G., and Lachnit, T. (2014) Fluorescence-based quasicontinuous and in situ monitoring of biofilm formation dynamics in natural marine environments. *Appl Environ Microbiol* **80**: 3721–3728.

de Fouw, J., van der Heide, T., van Belzen, J., Govers, L.L., Cheikh, M.A.S., Olff, H., et al. (2018) A facultative mutualistic feedback enhances the stability of tropical intertidal seagrass beds. *Sci Rep* **8**: 1–10.

Garcias-Bonet, N., Eguíluz, V.M., Díaz-Rúa, R., and Duarte, C.M. (2020) Host-association as major driver of microbiome structure and composition in Red Sea seagrass ecosystems. *Environ Microbiol*.

Garland, C.D., Nash, G.V., and McMeekin, T.A. (1982) Absence of surface-associated microorganisms in adult oysters (Crassostrea gigas). *Appl Environ Microbiol* **44**: 1205–1211.

Hammer, T.J., Sanders, J.G., and Fierer, N. (2019) Not all animals need a microbiome. *FEMS Microbiol Lett* **366.**:

Hasler-Sheetal, H. and Holmer, M. (2015) Sulfide intrusion and detoxification in the seagrass zostera marina. *PLoS One* **10**: 1–19.

Healey, D. and Hovel, K.A. (2004) Seagrass bed patchiness: effects on epifaunal communities in San Diego Bay, USA. *J Exp Mar Bio Ecol* **313**: 155–174.

van der Heide, T., Govers, L.L., de Fouw, J., Olff, H., van der Geest, M., van Katwijk, M.M., et al. (2012) A Three-Stage Symbiosis Forms the Foundation of Seagrass Ecosystems. *Science* **336**: 1432–1434.

Horner, S.M.J. (1987) Similarity of epiphyte biomass distribution on Posidonia and artificial seagrass leaves. *Aquat Bot* **27**: 159–167.

Hurtado-McCormick, V., Kahlke, T., Petrou, K., Jeffries, T., Ralph, P.J., and Seymour, J.R. (2019) Regional and Microenvironmental Scale Characterization of the Zostera muelleri Seagrass Microbiome. *Front Microbiol* **10**: 1011.

Jacoby, R., Peukert, M., Succurro, A., Koprivova, A., and Kopriva, S. (2017) The Role of Soil Microorganisms in Plant Mineral Nutrition-Current Knowledge and Future Directions. *Front Plant Sci* **8**: 1617.

Jørgensen, B.B. (1982) Mineralization of organic matter in the sea bed – the role of sulphate reduction. *Nature* **296**: 643–645.

Jørgensen, N.O.G., Blackburn, T.H., Henriksen, K., and Bay, D. (1981) The importance of Posidonia oceanica and Cymodocea nodosa as contributors of free amino acids in water and sediment of seagrass beds. *Mar Ecol* **2**: 97–112.

Kaimenyi, D.K., De Villiers, E.P., Ngoi, J., Ndiso, J.B., and De Villiers, S.M. (2018) Microbiome of two predominant seagrass species of the Kenyan coast, Enhalus acoroides and Thalassodendron ciliatum, PeerJ Preprints.

Keiluweit, M., Bougoure, J.J., Nico, P.S., Pett-Ridge, J., Weber, P.K., and Kleber, M. (2015) Mineral protection of soil carbon counteracted by root exudates. *Nat Clim Chang* **5**: 588–595.

Knights, D., Kuczynski, J., Charlson, E.S., Zaneveld, J., Mozer, M.C., Collman, R.G., et al. (2011) Bayesian community-wide culture-independent microbial source tracking. *Nat Methods* **8**: 761–763.

Lee, C., Tell, L.A., Hilfer, T., and Vannette, R.L. (2019) Microbial communities in hummingbird feeders are distinct from floral nectar and influenced by bird visitation. *Proc Biol Sci* **286**: 20182295.

Love, M.I., Huber, W., and Anders, S. (2014) Moderated estimation of fold change and dispersion for RNA-seq data with DESeq2. *Genome Biol* **15**: 550.

Martin, B.C., Bougoure, J., Ryan, M.H., Bennett, W.W., Colmer, T.D., Joyce, N.K., et al. (2019) Oxygen loss from seagrass roots coincides with colonisation of sulphide-oxidising cable bacteria and reduces sulphide stress. *ISME J* **13**: 707–719.

McFall-Ngai, M., Hadfield, M.G., Bosch, T.C.G., Carey, H.V., Domazet-Lošo, T., Douglas, A.E., et al. (2013) Animals in a bacterial world, a new imperative for the life sciences. *Proc Natl Acad Sci U S A* **110**: 3229–3236.

McFall-Ngai, M.J. and Ruby, E.G. (1991) Symbiont Recognistion and Subsequent Morphogenesis as Early Events in an Animal-Bacterial Mutualism. *Science* **254**: 1491–1494.

McIlroy, S.J. and Nielsen, P.H. (2014) The Family Saprospiraceae. In *The Prokaryotes: Other Major Lineages of Bacteria and The Archaea*. Rosenberg, E., DeLong, E.F., Lory, S., Stackebrandt, E., and Thompson, F. (eds). Berlin, Heidelberg: Springer Berlin Heidelberg, pp. 863–889.

McMurdie, P.J. and Holmes, S. (2014) Waste not, want not: why rarefying microbiome data is inadmissible. *PLoS Comput Biol* **10**: e1003531.

Nielsen, S.L., Thingstrup, I., and Wigand, C. (1999) Apparent lack of vesicular–arbuscular mycorrhiza (VAM) in the seagrasses Zostera marina L. and Thalassia testudinum Banks ex König. *Aquat Bot* **63**: 261–266.

Olsen, J.L., Rouzé, P., Verhelst, B., Lin, Y.-C., Bayer, T., Collen, J., et al. (2016) The genome of the seagrass Zostera marina reveals angiosperm adaptation to the sea -- Supps. *Nature* **61**: 5985–5991.

Pedersen, O., Binzer, T., and Borum, J. (2004) Sulphide intrusion in eelgrass (Zostera marina L.). *Plant Cell Environ* **27**: 595–602.

Pinckney, J.L. and Micheli, F. (1998) Microalgae on seagrass mimics: Does epiphyte community structure differ from live seagrasses? *J Exp Mar Bio Ecol* **221**: 59–70.

Price, M.N., Dehal, P.S., and Arkin, A.P. (2010) FastTree 2--approximately maximum-likelihood trees for large alignments. *PLoS One* **5**: e9490.

Quast, C., Pruesse, E., Yilmaz, P., Gerken, J., Schweer, T., Yarza, P., et al. (2013) The SILVA ribosomal RNA gene database project: improved data processing and web-based tools. *Nucleic Acids Res* **41**: D590–6.

Rinninella, E., Raoul, P., Cintoni, M., Franceschi, F., Miggiano, G.A.D., Gasbarrini, A., and Mele, M.C. (2019) What is the Healthy Gut Microbiota Composition? A Changing Ecosystem across Age, Environment, Diet, and Diseases. *Microorganisms* **7.**:

Silverman, J.D., Washburne, A.D., Mukherjee, S., and David, L.A. (2017) A phylogenetic transform enhances analysis of compositional microbiota data. *Elife* **6**: 1–20.

Smith, A.C., Kostka, J.E., Devereux, R., and Yates, D.F. (2004) Seasonal composition and activity of sulfate-reducing prokaryotic communities in seagrass bed sediments. *Aquat Microb Ecol* **37**: 183–195.

Sogin, E.M., Michellod, D., Gruber-Vodicka, H., Bourceau, P., Geier, B., Meier, D.V., et al. (2021) Sugars dominate the seagrass rhizosphere. *bioRxiv* 797522.

Sohn, J.H., Lee, J.-H., Yi, H., Chun, J., Bae, K.S., Ahn, T.-Y., and Kim, S.-J. (2004) Kordia algicida gen. nov., sp. nov., an algicidal bacterium isolated from red tide. *Int J Syst Evol Microbiol* **54**: 675–680.

Taylor, M.W., Schupp, P.J., Dahllöf, I., Kjelleberg, S., and Steinberg, P.D. (2004) Host specificity in marine sponge-associated bacteria, and potential implications for marine microbial diversity. *Environ Microbiol* **6**: 121–130.

Temmink, R.J.M., Christianen, M.J.A., Fivash, G.S., Angelini, C., Boström, C., Didderen, K., et al. (2020) Mimicry of emergent traits amplifies coastal restoration success. *Nat Commun* **11**: 3668.

Trivedi, P., Leach, J.E., Tringe, S.G., Sa, T., and Singh, B.K. (2020) Plant-microbiome interactions: from community assembly to plant health. *Nat Rev Microbiol* **18**: 607–621.

Ugarelli, K., Chakrabarti, S., Laas, P., and Stingl, U. (2017) The Seagrass Holobiont and Its Microbiome. *Microorganisms* **5**: 1–28.

Waite, D.W., Chuvochina, M., Pelikan, C., Parks, D.H., Yilmaz, P., Wagner, M., et al. (2020) Proposal to reclassify the proteobacterial classes Deltaproteobacteria and Oligoflexia, and the phylum Thermodesulfobacteria into four phyla reflecting major functional capabilities. *Int J Syst Evol Microbiol* **70**: 5972–6016.

Walters, W., Hyde, E.R., Berg-Lyons, D., Ackermann, G., Humphrey, G., Parada, A., et al. (2016) Improved Bacterial 16S rRNA Gene (V4 and V4-5) and Fungal Internal Transcribed Spacer Marker Gene Primers for Microbial Community Surveys. *mSystems* **1.**:

Warning, A.D. and Datta, A.K. (2017) Mechanistic understanding of non-spherical bacterial attachment and deposition on plant surface structures. *Chem Eng Sci* **160**: 396–418.

Weigel, B.L. and Pfister, C.A. (2021) Oxygen metabolism shapes microbial settlement on photosynthetic kelp blades compared to artificial kelp substrates. *Environ Microbiol Rep* **13**: 176–184.

Wetzel, R.G. and Penhale, P.A. (1979) Transport of carbon and excretion of dissolved organic carbon by leaves and roots/rhizomes in seagrasses and their epiphytes. *Aquat Bot* **6**: 149–158.

Whitaker, M.R.L., Salzman, S., Sanders, J., Kaltenpoth, M., and Pierce, N.E. (2016) Microbial Communities of Lycaenid Butterflies Do Not Correlate with Larval Diet. *Front Microbiol* **7**: 1920.

Wright, E.S. (2015) DECIPHER: harnessing local sequence context to improve protein multiple sequence alignment. *BMC Bioinformatics* **16**: 322.

Xiong, C., Zhu, Y.-G., Wang, J.-T., Singh, B., Han, L.-L., Shen, J.-P., et al. (2021) Host selection shapes crop microbiome assembly and network complexity. *New Phytol* **229**: 1091–1104.

Zhang, B., Luo, Y., Pearlstein, A.J., Aplin, J., Liu, Y., Bauchan, G.R., et al. (2014) Fabrication of biomimetically patterned surfaces and their application to probing plant-bacteria interactions. *ACS Appl Mater Interfaces* **6**: 12467–12478.

Zhang, J., Huang, Y.-J., Yoon, J.Y., Kemmitt, J., Wright, C., Schneider, K., et al. (2021) Primary human colonic mucosal barrier crosstalk with super oxygen-sensitive Faecalibacterium prausnitzii in continuous culture. *Med (N Y)* **2**: 74–98.e9.

Zozaya-Valdés, E., Roth-Schulze, A.J., Egan, S., and Thomas, T. (2017) Microbial community function in the bleaching disease of the marine macroalgae Delisea pulchra. *Environ Microbiol* **19**: 3012–3024.

Figures and Tables

Figure 1.1: (A) Mean amplicon sequence variant (ASV) richness found in each type of sample we measured. Raw data as well as means and standard errors are presented. Leaf mimic bacterial communities had a higher mean richness than leaf bacterial communities ($p < 0.001$); root mimic, root, and sediment bacterial communities did not differ in mean community richness. (B) Overlap among core bacterial communities showing shared ASVs present in each sample type in at least 50% of samples at a 1% detection rate. Diagram is a barplot of shared community memberships, equivalent to a Venn diagram.

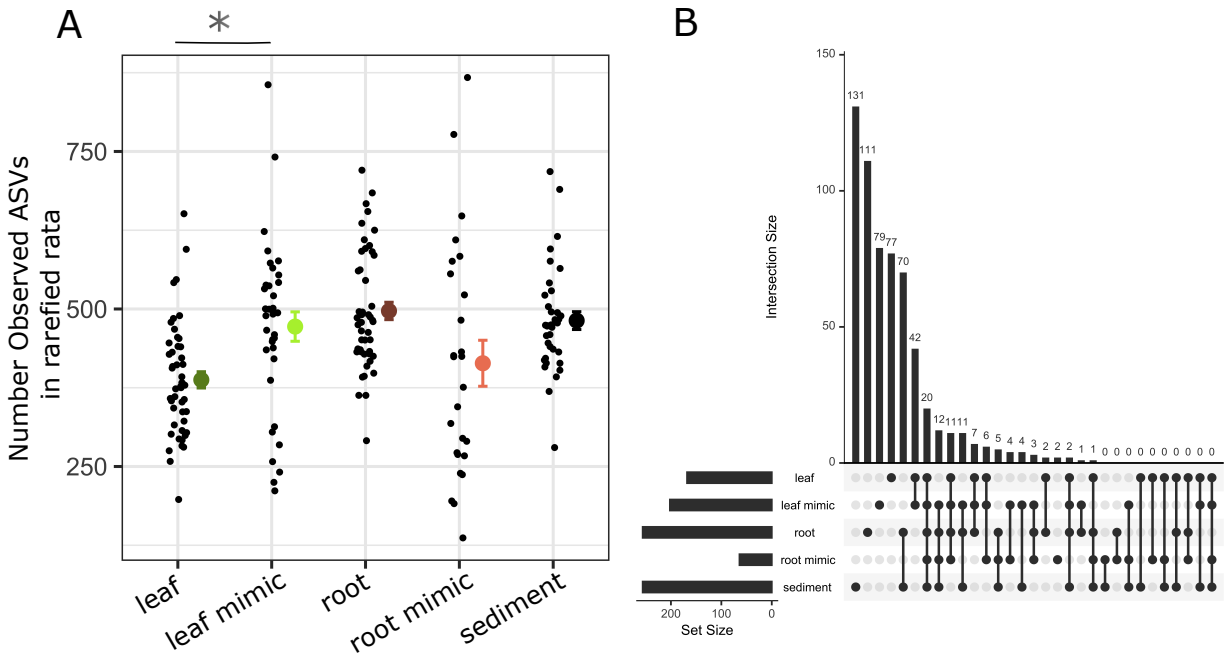

Figure 1.2: (A) Ordination of bacterial community structure based on principal coordinate analysis of phylogenetic-isometric log-ratio transformed distances. (B) Ordination of predicted Metacyc pathways structure based on principal coordinate analysis of centered log-ratio transformed distances. Bright green points are communities on leaf mimics and dark green points are communities on leaves. Leaf and leaf mimic communities in both analyses are distinct from each other (PERMANOVA $p < 0.001$).

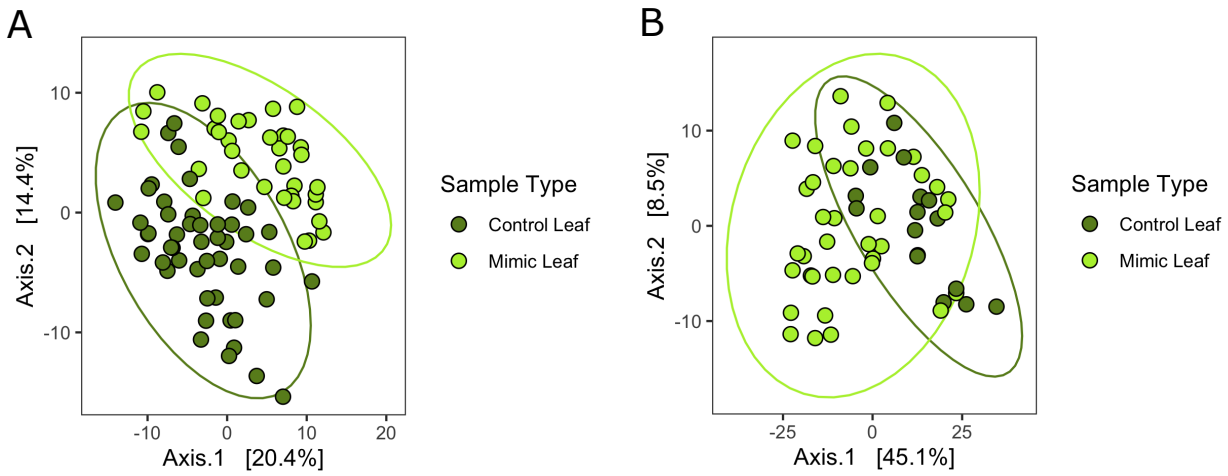

Figure 1.3: (A) Ordination of bacterial community structure based on principal coordinate analysis of phylogenetic-isometric log-ratio transformed distances. (B) Ordination of predicted Metacyc pathways structure based on principal coordinate analysis of centered log-ratio transformed distances. Red-orange points are communities on root mimics, dark brown points are communities on roots, and grey points are communities in sediments. All communities are distinct from each other in each analysis (PERMANOVA $p < 0.001$).

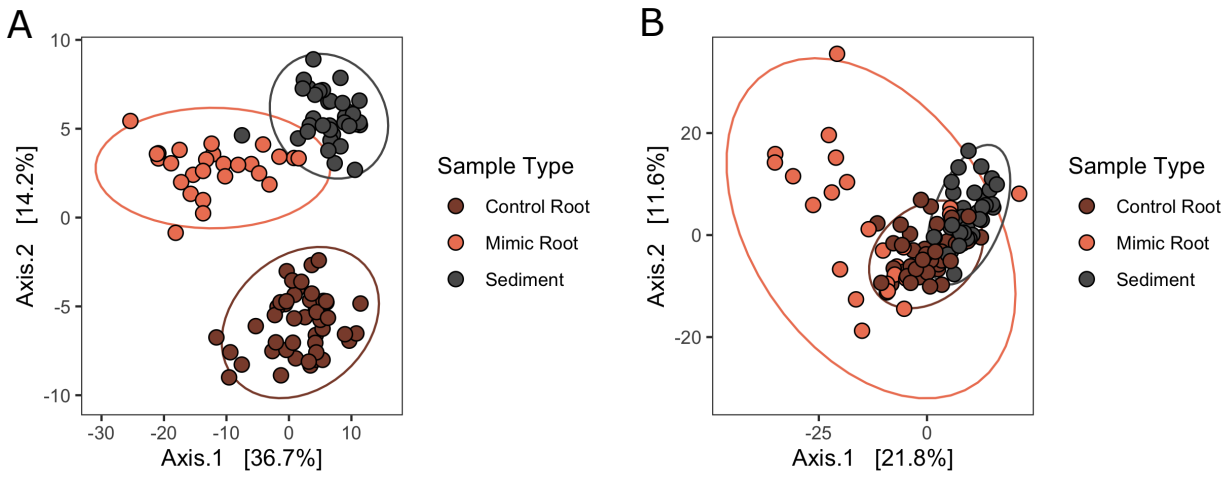

Table 1.1: For both leaves and root communities, the five families that had the most ASVs vary between mimics and seagrass substrate. See Supplemental Tables 1.1 and 1.6 for complete lists for leaves and roots respectively.

Leaves		
Family	**Higher on leaves**	**Higher on mimics**
Rhodobacteraceae	23	13
Flavobacteriaceae	8	8
Saprospiraceae	16	0
Granulosicoccaceae	4	2
Alteromonadaceae	5	0

Roots						
Family	**Higher on roots**	**Higher on mimics**	**Higher on mimics**	**Higher in sediment**	**Higher on roots**	**Higher in sediment**
Desulfocapsaceae	40	0	8	25	27	9
Flavobacteriaceae	24	13	19	20	21	17
Desulfosarcinaceae	34	0	0	35	8	26
Bacteroidetes_BD2-2	31	1	0	25	16	14
Spirochaetaceae	23	0	1	21	15	11

Supplemental Figures and Tables

Supplemental Figure 1.S1: Overlap among all ASVs present in each sample type. Diagram is a barplot of shared community memberships, equivalent to a Venn diagram.

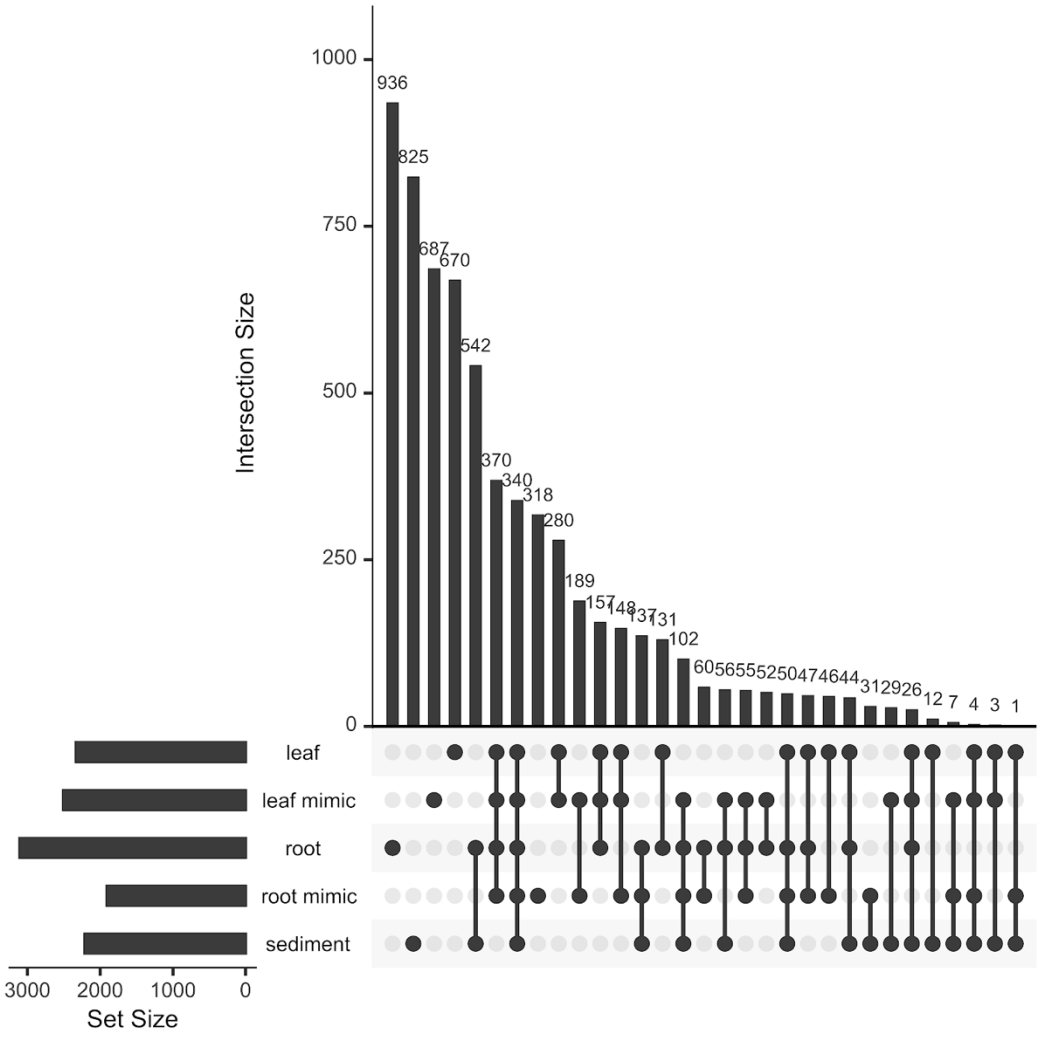

Supplemental Figure 1.S2: Map of sampling sites in Bodega Harbor, Bodega Bay, CA, USA.

Supplemental Table 1.S1: For leaf bacterial communities, the family-level identification of ASVs that varied significantly between mimics and seagrass substrate determined by DESeq2.

Family	Higher on leaves	Higher on mimics
Alteromonadaceae	5	0
Arenicellaceae	1	1
Blastocatellaceae	0	1
Cellvibrionaceae	1	0
Colwelliaceae	2	0
Crocinitomicaceae	5	0
Cryomorphaceae	3	0
Desulfocapsaceae	0	1
DEV007	0	2
Flavobacteriaceae	8	8
Fokiniaceae	1	0
Gimesiaceae	0	1
Granulosicoccaceae	4	2
Hyphomicrobiaceae	0	1
Hyphomonadaceae	2	1
Kangiellaceae	1	0
Marinomonadaceae	1	0
Methylophagaceae	1	0
Methylophilaceae	3	1
Micavibrionaceae	0	2
Microtrichaceae	0	1
Nitrincolaceae	2	0
NS9_marine_group	1	0
Oleiphilaceae	1	0
Phormidesmiaceae	0	1
Pirellulaceae	4	1
Rhizobiaceae	1	2
Rhodobacteraceae	23	13
Rhodothermaceae	1	0
Rickettsiaceae	1	0
Rubinisphaeraceae	0	2
Rubritaleaceae	0	1
Saprospiraceae	16	0
Sphingomonadaceae	0	2
Spirosomaceae	1	0
Spongiibacteraceae	1	0
Sulfurovaceae	0	2

Terasakiellaceae	1	0
Thiomicrospiraceae	1	0
Trueperaceae	0	1
Unknown_Family	0	1
Woeseiaceae	0	1

Supplemental Table 1.S2: For leaf bacterial communities, the genus-level identification of ASVs that varied significantly between mimics and seagrass substrate determined by DESeq2.

Family	Genus	Higher on leaves	Higher on mimics
Alteromonadaceae	Glaciecola	4	0
Alteromonadaceae	Salinimonas	1	0
Arenicellaceae	Arenicella	1	1
Blastocatellaceae	Blastocatella	0	1
Cellvibrionaceae	Agaribacterium	1	0
Colwelliaceae	Colwellia	2	0
Crocinitomicaceae	Crocinitomix	1	0
Crocinitomicaceae	Fluviicola	3	0
Cryomorphaceae	Vicingus	1	0
Flavobacteriaceae	Aquibacter	0	1
Flavobacteriaceae	Aurantivirga	1	0
Flavobacteriaceae	Changchengzhania	1	0
Flavobacteriaceae	Kordia	3	0
Flavobacteriaceae	Maribacter	0	1
Flavobacteriaceae	Polaribacter	1	0
Flavobacteriaceae	Psychroserpens	0	1
Flavobacteriaceae	Ulvibacter	2	2
Fokiniaceae	MD3-55	1	0
Granulosicoccaceae	Granulosicoccus	4	2
Hyphomicrobiaceae	Filomicrobium	0	1
Hyphomonadaceae	Hellea	1	0
Hyphomonadaceae	Hyphomonas	0	1
Hyphomonadaceae	Litorimonas	1	0
Marinomonadaceae	Marinomonas	1	0
Methylophilaceae	Methylotenera	3	1
Microtrichaceae	Sva0996_marine_group	0	1
Oleiphilaceae	Oleiphilus	1	0
Phormidesmiaceae	Phormidesmis_ANT.LACV5.1	0	1
Pirellulaceae	Blastopirellula	3	1
Pirellulaceae	Rhodopirellula	1	0
Rhizobiaceae	Pseudahrensia	1	2
Rhodobacteraceae	Celeribacter	0	1
Rhodobacteraceae	Jannaschia	0	1
Rhodobacteraceae	Octadecabacter	1	1
Rhodobacteraceae	Phaeobacter	0	1
Rhodobacteraceae	Roseovarius	0	1

Rhodobacteraceae	Sedimentitalea	1	1
Rhodobacteraceae	Sulfitobacter	0	1
Rhodobacteraceae	Tateyamaria	1	1
Rhodobacteraceae	Thiobacimonas	0	1
Rhodobacteraceae	Yoonia-Loktanella	2	0
Rickettsiaceae	Candidatus_Megaira	1	0
Rubinisphaeraceae	Planctomicrobium	0	1
Rubritaleaceae	Persicirhabdus	0	1
Saprospiraceae	Lewinella	3	0
Saprospiraceae	Phaeodactylibacter	1	0
Saprospiraceae	Portibacter	1	0
Saprospiraceae	Rubidimonas	2	0
Sphingomonadaceae	Parasphingopyxis	0	1
Spirosomaceae	Taeseokella	1	0
Sulfurovaceae	Sulfurovum	0	2
Thiomicrospiraceae	endosymbionts	1	0
Trueperaceae	Truepera	0	1
Woeseiaceae	Woeseia	0	1

Supplemental Table 1.S3: For leaf bacterial communities, all ASVs that varied significantly between mimics and seagrass substrate determined by DESeq2, including magnitude of differences. See Supplemental File SupplementalTable1.S3.csv.

Supplemental Table 1.S4: For leaf bacterial communities, all Metacyc predicted pathways that varied significantly between mimics and seagrass substrate determined by DESeq2, including magnitude of differences.

Pathway	log2-fold Change
nitrifier denitrification	3.57517042
superpathway of polyamine biosynthesis III	2.81827993
CMP-pseudaminate biosynthesis	2.62893542
nylon-6 oligomer degradation	1.64149213
formaldehyde oxidation I	1.19448623
formaldehyde assimilation II (RuMP Cycle)	1.18703389
thiazole biosynthesis II (Bacillus)	1.17319111
coenzyme M biosynthesis I	1.06840996
superpathway of thiamin diphosphate biosynthesis II	0.98492463
methyl ketone biosynthesis	0.93025842
L-arginine degradation II (AST pathway)	0.87076592
glucose and glucose-1-phosphate degradation	0.71012766
ectoine biosynthesis	0.68464435
norspermidine biosynthesis	0.59741725
ADP-L-glycero-β-D-manno-heptose biosynthesis	0.59480138
superpathway of polyamine biosynthesis I	0.50117322
catechol degradation II (meta-cleavage pathway)	-0.5051274
L-tryptophan degradation XII (Geobacillus)	-0.5311326
catechol degradation I (meta-cleavage pathway)	-0.5785306
acetylene degradation	-0.599038
2-aminophenol degradation	-0.6086563
catechol degradation to β-ketoadipate	-0.6123384
superpathway of pyridoxal 5'-phosphate biosynthesis and salvage	-0.6160838
superpathway of sulfur oxidation (Acidianus ambivalens)	-0.7083875
reductive acetyl coenzyme A pathway	-0.8598703
meta cleavage pathway of aromatic compounds	-0.8753625
adenosylcobalamin biosynthesis II (late cobalt incorporation)	-0.9123838
androstenedione degradation	-0.9491612
superpathway of salicylate degradation	-0.9500477
methanogenesis from acetate	-0.9597901
catechol degradation III (ortho-cleavage pathway)	-0.968522
aromatic compounds degradation via β-ketoadipate	-0.968522
formaldehyde assimilation I (serine pathway)	-0.9774884
superpathway of 2,3-butanediol biosynthesis	-0.9804931

D-galactarate degradation I	-1.0428591
superpathway of D-glucarate and D-galactarate degradation	-1.0428591
pyruvate fermentation to acetone	-1.0446446
isopropanol biosynthesis	-1.0943399
superpathway of (R,R)-butanediol biosynthesis	-1.1560577
superpathway of L-aspartate and L-asparagine biosynthesis	-1.2056707
glycerol degradation to butanol	-1.2387094
superpathway of N-acetylneuraminate degradation	-1.2987337
superpathway of N-acetylglucosamine, N-acetylmannosamine and N-acetylneuraminate degradation	-1.407782
creatinine degradation II	-1.4875672
D-glucarate degradation I	-1.4888527
1,5-anhydrofructose degradation	-1.5852009
allantoin degradation to glyoxylate III	-1.6402326
mono-trans, poly-cis decaprenyl phosphate biosynthesis	-1.6413193
cob(II)yrinate a,c-diamide biosynthesis I (early cobalt insertion)	-2.4457325
methylaspartate cycle	-2.4547742
coenzyme B biosynthesis	-2.718622
chondroitin sulfate degradation I (bacterial)	-3.8564041
starch degradation III	-5.3764083

Supplemental Table 1.S5: Results of pairwise PERMANOVA tests distinguishing compositional differences among roots, root mimics, and sediments in both ASV composition and composition of predicted Metacyc pathways.

			df	Sum Of Squares	R^2	F-Statistic	Pr(>F)
Based on taxonomy	Root vs. Mimic	Sample Type	1	4716.5	0.307	31.511	**0.001**
		Residual	71	10627.2	0.693		
		Total	72	15343.7	1		
	Mimic vs. Sediment	Sample Type	1	5659.8	0.424	44.22	**0.001**
		Residual	60	7679.5	0.576		
		Total	61	13339.3	1		
	Root vs. Sediment	Sample Type	1	3234.5	0.248	26.722	**0.001**
		Residual	81	9804.5	0.752		
		Total	82	13039.1	1		
Based on predicted function	Root vs. Mimic	Sample Type	1	4991	0.114	9.1228	**0.001**
		Residual	71	38841	0.886		
		Total	72	43831	1		
	Mimic vs. Sediment	Sample Type	1	8250	0.196	14.592	**0.001**
		Residual	60	33924	0.804		
		Total	61	42174	1		
	Root vs. Sediment	Sample Type	1	4865	0.148	14.093	**0.001**
		Residual	81	27963	0.852		
		Total	82	32829	1		

Supplemental Table 1.S6: For belowground bacterial communities, the family-level identification of ASVs that varied significantly among mimics, seagrass and sediment determined by DESeq2.

Family	Higher on roots	Higher on mimics	Higher on mimics	Higher on sediment	Higher on roots	Higher on sediment
4572-13	3	0	0	2	1	2
Acanthopleuribacteraceae	2	0	0	1	1	1
Anaerolineaceae	12	0	1	11	3	10
Arcobacteraceae	2	0	1	0	2	0
Arenicellaceae	0	1	0	1	0	1
Bacteroidetes_BD2-2	31	1	0	25	16	14
Calditrichaceae	10	1	0	11	1	10
Cellvibrionaceae	1	0	1	0	1	0
Christensenellaceae	3	0	0	3	2	1
Chromatiaceae	4	0	0	4	0	4
Crocinitomicaceae	1	0	2	0	2	0
Cyclobacteriaceae	3	0	0	3	0	3
Desulfatiglandaceae	4	0	0	4	0	4
Desulfobacteraceae	9	0	0	5	7	2
Desulfobulbaceae	8	0	1	7	4	5
Desulfocapsaceae	40	0	8	25	27	9
Desulfococcaceae	1	0	0	1	1	0
Desulfolunaceae	1	0	0	1	0	1
Desulfomonilaceae	0	1	0	1	0	1
Desulfosarcinaceae	34	0	0	35	8	26
Desulfovibrionaceae	3	0	0	1	3	0
Ectothiorhodospiraceae	1	1	0	2	0	2
Fermentibacteraceae	3	0	0	3	1	2
Fibrobacteraceae	1	0	0	1	1	0
Flavobacteriaceae	24	13	19	20	21	17
Fusibacteraceae	1	0	0	1	1	0
Gemmatimonadaceae	1	0	0	1	0	1
Geopsychrobacteraceae	2	0	1	0	2	0
Halieaceae	9	0	1	9	1	9
Halomonadaceae	0	2	2	0	2	0
Hungateiclostridiaceae	3	0	0	3	1	2
Hyphomonadaceae	0	2	2	0	2	0
Ignavibacteriaceae	1	0	0	1	0	1

Kiritimatiellaceae	3	1	0	3	2	1
Lachnospiraceae	8	0	3	3	8	0
Latescibacteraceae	1	0	0	3	0	3
Lentimicrobiaceae	7	0	0	7	1	3
Leptospiraceae	1	0	0	1	1	0
Marinifilaceae	6	0	0	2	6	0
Marinilabiliaceae	9	0	0	8	6	3
Marinomonadaceae	1	0	1	0	1	0
Melioribacteraceae	7	0	0	6	3	4
Methylophagaceae	2	0	1	1	2	0
Methylophilaceae	1	0	2	0	2	0
Moduliflexaceae	19	0	0	14	16	3
MSBL8	5	0	1	4	2	2
Nitrincolaceae	1	0	0	1	1	0
NS11-12_marine_group	0	1	1	0	1	0
Pedosphaeraceae	1	0	0	1	0	1
PHOS-HE36	2	0	0	3	0	3
Pirellulaceae	9	1	2	10	2	9
Prolixibacteraceae	16	0	1	11	10	3
Puniceicoccaceae	2	0	1	0	2	0
Rhizobiaceae	4	0	3	0	5	0
Rhodobacteraceae	5	4	17	0	17	0
Rickettsiaceae	1	0	1	0	1	0
Rubinisphaeraceae	0	1	2	0	2	0
S15A-MN91	1	0	0	1	1	0
Sandaracinaceae	1	0	0	1	0	1
Saprospiraceae	5	5	6	5	6	3
SB-5	11	0	0	8	6	5
Sedimenticolaceae	8	2	1	9	4	6
SG8-4	3	0	0	2	1	2
Shewanellaceae	0	1	1	0	1	0
Spirochaetaceae	23	0	1	21	15	11
Spirosomaceae	0	1	1	0	1	0
Spongiibacteraceae	2	1	2	1	2	1
Sulfurimonadaceae	6	1	1	1	6	1
Sulfurovaceae	1	0	1	0	1	0
Syntrophotaleaceae	1	0	0	1	1	0
Thermoanaerobaculaceae	13	0	0	14	0	14
Thioalkalispiraceae	1	1	0	4	0	4
Thiohalorhabdaceae	1	0	0	1	0	1
Thiomicrospiraceae	7	2	0	9	1	8

Thiotrichaceae	2	5	5	4	5	4
Unknown_Family	9	0	1	10	1	10
Vibrionaceae	1	0	1	0	1	0
Woeseiaceae	3	0	0	3	0	3

Supplemental Table 1.S7: For belowground bacterial communities, all ASVs that varied significantly among mimics, seagrass and sediment determined by DESeq2, including magnitude of differences. See Supplemental Files SupplementalTable1.S7.xlsx.

Supplemental Table 1.S8: For belowground bacterial communities, all Metacyc predicted pathways that varied significantly among mimics, seagrass and sediment determined by DESeq2, including magnitude of differences.

Pathway	Root vs. Mimic	Mimic vs. Sediment	Root vs. Sediment
β-alanine biosynthesis II	-2.707	6.111	3.404
1,4-dihydroxy-2-naphthoate biosynthesis I	-0.734	NA	NA
1,4-dihydroxy-6-naphthoate biosynthesis I	0.895	-0.833	NA
1,4-dihydroxy-6-naphthoate biosynthesis II	0.936	-0.922	NA
2-amino-3-carboxymuconate semialdehyde degradation to 2-oxopentenoate	-1.392	2.038	0.646
2-aminophenol degradation	-2.279	1.971	NA
2-methylcitrate cycle I	-1.101	NA	-0.666
2-methylcitrate cycle II	-0.814	NA	-0.5
2-nitrobenzoate degradation I	-1.351	1.919	0.568
3-phenylpropanoate and 3-(3-hydroxyphenyl)propanoate degradation	-1.066	3.175	2.11
3-phenylpropanoate degradation	-2.55	7.214	4.664
4-coumarate degradation (anaerobic)	NA	0.894	0.511
4-deoxy-L-threo-hex-4-enopyranuronate degradation	NA	NA	0.568
4-hydroxyphenylacetate degradation	-0.697	1.697	1
4-methylcatechol degradation (ortho cleavage)	-2.808	2.565	NA
acetylene degradation	NA	NA	0.599
adenosylcobalamin biosynthesis I (early cobalt insertion)	-0.714	2.256	1.542
adenosylcobalamin biosynthesis II (late cobalt incorporation)	-0.868	2.381	1.512
ADP-L-glycero-β-D-manno-heptose biosynthesis	0.625	-1.079	NA
aerobactin biosynthesis	-0.913	2.622	1.709
allantoin degradation IV (anaerobic)	-5.19	12.389	7.199
allantoin degradation to glyoxylate III	-1.345	1.089	NA
androstenedione degradation	NA	-1.1	-1.165
arginine, ornithine and proline interconversion	0.831	NA	0.59
aromatic biogenic amine degradation (bacteria)	-0.658	0.859	NA
aromatic compounds degradation via β-ketoadipate	-2.45	2.489	NA
benzoyl-CoA degradation II (anaerobic)	2.335	-2.511	NA
Bifidobacterium shunt	-1.207	1.348	NA
biotin biosynthesis II	-1.18	5.052	3.871
catechol degradation I (meta-cleavage pathway)	NA	NA	-0.548
catechol degradation III (ortho-cleavage pathway)	-2.45	2.489	NA
catechol degradation to β-ketoadipate	-1.833	2.268	NA

catechol degradation to 2-oxopent-4-enoate II	-0.686	1.26	0.574
chitin derivatives degradation	NA	0.947	1.405
chlorophyllide a biosynthesis I (aerobic, light-dependent)	-0.72	1.652	0.932
chlorophyllide a biosynthesis II (anaerobic)	-0.768	1.592	0.823
chlorophyllide a biosynthesis III (aerobic, light independent)	-0.768	1.592	0.823
chlorosalicylate degradation	-3.061	5.32	2.259
chondroitin sulfate degradation I (bacterial)	-1.706	2.696	0.99
CMP-legionaminate biosynthesis I	0.934	-1.577	-0.643
CMP-pseudaminate biosynthesis	2.677	3.179	5.856
cob(II)yrinate a,c-diamide biosynthesis I (early cobalt insertion)	NA	1.762	1.522
cob(II)yrinate a,c-diamide biosynthesis II (late cobalt incorporation)	-0.532	1.015	NA
coenzyme B biosynthesis	-3.071	6.334	3.263
coenzyme M biosynthesis I	-0.653	NA	NA
creatinine degradation I	-0.731	1.411	0.68
creatinine degradation II	-1.043	1.966	0.923
D-fructuronate degradation	-0.69	0.755	NA
D-galactarate degradation I	-1.061	0.528	-0.533
D-galacturonate degradation I	NA	0.635	NA
D-glucarate degradation I	-1.669	NA	-1.318
dTDP-N-acetylthomosamine biosynthesis	-1.002	0.717	NA
ectoine biosynthesis	-0.56	0.587	NA
enterobacterial common antigen biosynthesis	-6.585	6.736	NA
enterobactin biosynthesis	-2.12	1.54	-0.58
ergothioneine biosynthesis I (bacteria)	-5.705	4.133	-1.572
ethylmalonyl-CoA pathway	NA	1.609	1.126
factor 420 biosynthesis	-3.584	7.65	4.066
formaldehyde assimilation I (serine pathway)	-1.108	NA	-1.106
formaldehyde assimilation II (RuMP Cycle)	-0.539	1.394	0.855
formaldehyde oxidation I	-0.531	1.373	0.843
galactose degradation I (Leloir pathway)	0.553	NA	NA
gallate degradation I	-1.414	2.933	1.519
gallate degradation II	-1.449	2.968	1.52
GDP-D-glycero-α-D-manno-heptose biosynthesis	1.444	-2.19	-0.746
glucose and glucose-1-phosphate degradation	-0.788	0.798	NA
glucose degradation (oxidative)	-2.795	1.294	-1.501
glutaryl-CoA degradation	0.7	-1.314	-0.614
glycerol degradation to butanol	-1.06	1.965	0.905
glycine betaine degradation I	NA	1.479	1.012
glycogen degradation I (bacterial)	0.541	-0.531	NA

glycogen degradation II (eukaryotic)	-0.826	1.763	0.937
glyoxylate cycle	-0.581	0.505	NA
heterolactic fermentation	-1.206	1.333	NA
hexitol fermentation to lactate, formate, ethanol and acetate	-3.151	3.158	NA
incomplete reductive TCA cycle	0.575	-0.655	NA
isoprene biosynthesis II (engineered)	1.375	-1.53	NA
isopropanol biosynthesis	NA	-0.788	-1.081
ketogluconate metabolism	-2.08	2.904	0.823
L-1,2-propanediol degradation	-3.483	7.5	4.017
L-arabinose degradation IV	-1.091	10.119	9.027
L-arginine degradation II (AST pathway)	-2.36	2.826	NA
L-glutamate degradation V (via hydroxyglutarate)	0.929	-1.452	-0.522
L-histidine degradation II	-0.905	1.758	0.853
L-isoleucine biosynthesis IV	0.648	-0.637	NA
L-lysine biosynthesis II	-3.403	5.364	1.961
L-lysine fermentation to acetate and butanoate	0.561	1.344	1.905
L-methionine biosynthesis I	NA	0.651	NA
L-methionine salvage cycle III	-6.548	9.365	2.817
L-rhamnose degradation I	-0.601	0.575	NA
L-tryptophan degradation IX	-0.755	0.943	NA
L-tryptophan degradation to 2-amino-3-carboxymuconate semialdehyde	-1.013	0.945	NA
L-tryptophan degradation XII (Geobacillus)	-1.826	1.525	NA
L-tyrosine degradation I	-0.69	0.791	NA
L-valine degradation I	-2.825	6.469	3.644
lactose and galactose degradation I	-5.366	8.296	2.93
mannan degradation	NA	0.979	0.8
meta cleavage pathway of aromatic compounds	-2.222	2.442	NA
methanogenesis from acetate	1.383	-1.405	NA
methanol oxidation to carbon dioxide	-1.267	1.652	NA
methyl ketone biosynthesis	-0.595	NA	-0.695
methylaspartate cycle	NA	NA	0.622
methylgallate degradation	-1.426	2.944	1.518
methylphosphonate degradation I	NA	1.155	0.657
mevalonate pathway I	0.62	-0.789	NA
mevalonate pathway II (archaea)	2.767	-2.41	NA
mono-trans, poly-cis decaprenyl phosphate biosynthesis	-4.413	7.054	2.641
mycothiol biosynthesis	-1.242	0.619	-0.623
myo-, chiro- and scillo-inositol degradation	-1.407	2.468	1.061
myo-inositol degradation I	-1.294	2.424	1.13
NAD biosynthesis II (from tryptophan)	-0.799	0.725	NA

NAD salvage pathway II	-3.019	2.894	NA
nicotinate degradation I	-5.063	8.194	3.131
nitrate reduction VI (assimilatory)	-1.019	1.286	NA
nitrifier denitrification	-2.899	1.945	-0.954
norspermidine biosynthesis	-0.953	1.536	0.583
nylon-6 oligomer degradation	-0.85	0.947	NA
octane oxidation	-0.822	0.989	NA
palmitate biosynthesis II (bacteria and plants)	NA	-0.905	-1.09
peptidoglycan biosynthesis II (staphylococci)	-5.146	11.401	6.254
peptidoglycan biosynthesis IV (Enterococcus faecium)	-3.081	3.053	NA
peptidoglycan biosynthesis V (β-lactam resistance)	-3.874	6.005	2.131
phenylacetate degradation I (aerobic)	-2.362	2.021	NA
phospholipases	-1.595	1.442	NA
polymyxin resistance	-3.01	1.664	-1.346
ppGpp biosynthesis	-0.775	1.179	NA
protocatechuate degradation I (meta-cleavage pathway)	-1.35	3.374	2.025
protocatechuate degradation II (ortho-cleavage pathway)	-0.963	1.364	NA
purine nucleotides degradation II (aerobic)	NA	0.761	0.626
purine ribonucleosides degradation	NA	0.974	1.037
pyrimidine deoxyribonucleotides biosynthesis from CTP	1.42	-2.896	-1.476
pyrimidine deoxyribonucleotides de novo biosynthesis III	0.531	NA	NA
pyrimidine deoxyribonucleotides de novo biosynthesis IV	1.396	-2.894	-1.498
pyruvate fermentation to acetate and lactate II	0.607	NA	NA
pyruvate fermentation to acetone	-1.116	NA	-0.677
pyruvate fermentation to butanoate	1.011	-0.849	NA
reductive acetyl coenzyme A pathway	1.077	-1.026	NA
S-adenosyl-L-methionine cycle I	NA	1.435	1.331
S-methyl-5-thio-α-D-ribose 1-phosphate degradation	-6.882	9.53	2.648
spirilloxanthin and 2,2'-diketo-spirilloxanthin biosynthesis	-0.97	2.188	1.218
sucrose degradation II (sucrose synthase)	0.736	-2.09	-1.354
sucrose degradation III (sucrose invertase)	-1.619	2.032	NA
superpathway of (Kdo)2-lipid A biosynthesis	-0.563	-0.78	-1.344
superpathway of (R,R)-butanediol biosynthesis	-0.822	NA	-1.035
superpathway of β-D-glucuronide and D-glucuronate degradation	-0.856	0.788	NA
superpathway of 2,3-butanediol biosynthesis	-0.542	NA	-0.89
superpathway of aerobic toluene degradation	-1.618	1.714	NA
superpathway of bacteriochlorophyll a biosynthesis	-0.717	1.655	0.938
superpathway of C1 compounds oxidation to CO2	NA	3.717	3.424

superpathway of chorismate metabolism	-1.082	NA	-0.77
superpathway of Clostridium acetobutylicum acidogenic fermentation	0.964	-0.791	NA
superpathway of D-glucarate and D-galactarate degradation	-1.061	0.528	-0.533
superpathway of demethylmenaquinol-6 biosynthesis I	-0.559	NA	NA
superpathway of demethylmenaquinol-6 biosynthesis II	1.413	0.828	2.241
superpathway of demethylmenaquinol-8 biosynthesis	-0.555	NA	NA
superpathway of demethylmenaquinol-9 biosynthesis	-0.559	NA	NA
superpathway of fucose and rhamnose degradation	-1.558	3.619	2.061
superpathway of geranylgeranyldiphosphate biosynthesis I (via mevalonate)	0.629	-0.792	NA
superpathway of glycerol degradation to 1,3-propanediol	-0.507	3.473	2.966
superpathway of glycol metabolism and degradation	-1.911	4.578	2.667
superpathway of glyoxylate bypass and TCA	-0.568	NA	NA
superpathway of hexitol degradation (bacteria)	-1.444	1.087	NA
superpathway of hexuronide and hexuronate degradation	-0.937	1.092	NA
superpathway of L-arginine and L-ornithine degradation	-5.65	7.165	1.516
superpathway of L-arginine, putrescine, and 4-aminobutanoate degradation	-5.65	7.165	1.516
superpathway of L-aspartate and L-asparagine biosynthesis	0.576	NA	0.74
superpathway of L-threonine metabolism	-6.335	9.146	2.811
superpathway of menaquinol-10 biosynthesis	-0.508	NA	NA
superpathway of menaquinol-11 biosynthesis	-0.52	NA	NA
superpathway of menaquinol-12 biosynthesis	-0.52	NA	NA
superpathway of menaquinol-13 biosynthesis	-0.52	NA	NA
superpathway of menaquinol-6 biosynthesis I	-0.508	NA	NA
superpathway of menaquinol-8 biosynthesis II	1.413	-0.787	0.626
superpathway of menaquinol-9 biosynthesis	-0.508	NA	NA
superpathway of methylglyoxal degradation	-2.183	3.746	1.563
superpathway of N-acetylglucosamine, N-acetylmannosamine and N-acetylneuraminate degradation	-0.896	NA	-0.715
superpathway of N-acetylneuraminate degradation	-0.663	NA	-0.566
superpathway of phenylethylamine degradation	-2.206	4.726	2.52
superpathway of phylloquinol biosynthesis	-0.712	NA	NA
superpathway of purine deoxyribonucleosides degradation	NA	0.937	0.905
superpathway of pyridoxal 5'-phosphate biosynthesis and salvage	NA	2.341	2.37
superpathway of pyrimidine deoxyribonucleosides degradation	NA	0.648	0.768

superpathway of salicylate degradation	-2.333	2.405	NA
superpathway of sulfolactate degradation	NA	1.819	1.324
superpathway of sulfur oxidation (Acidianus ambivalens)	1.533	-1.735	NA
superpathway of thiamin diphosphate biosynthesis II	1.049	-1.069	NA
superpathway of UDP-glucose-derived O-antigen building blocks biosynthesis	-0.577	1.115	0.537
superpathway of vanillin and vanillate degradation	-1.328	3.437	2.11
TCA cycle VII (acetate-producers)	NA	0.716	NA
teichoic acid (poly-glycerol) biosynthesis	-1.136	4.14	3.004
thiazole biosynthesis II (Bacillus)	1.319	-1.274	NA
toluene degradation III (aerobic) (via p-cresol)	-2.388	2.255	NA
toluene degradation IV (aerobic) (via catechol)	-2.366	2.877	0.511
tRNA processing	NA	-0.591	NA
UDP-2,3-diacetamido-2,3-dideoxy-α-D-mannuronate biosynthesis	0.615	-0.585	NA
vanillin and vanillate degradation I	-1.328	3.437	2.11
vanillin and vanillate degradation II	-1.325	3.426	2.101
vitamin E biosynthesis (tocopherols)	-2.895	7.085	4.19

Appendix 1.A

We also had controls that we transplanted back to sites with mimics (in addition to control plants taken from nearby where mimics were placed). Appendix 1.A repeats the analyses in the main text and produces very similar results in terms of degrees of differences compared to the transplants in the main text. This suggests that these results are robust to our manipulations.

Sampling and sequencing success

We identified 43,118 bacterial ASVs across 247 leaf, root, mimic, and sediment samples after quality filtering samples to 5,165,712 reads. Root samples contained between 328 and 1,026 bacterial ASVs on their surface (we measured 75 root samples with read depth between 7,501 and 79,940 reads), Root mimics samples contained between 85 and 797 bacterial ASVs on their surface (we measured 26 root mimic samples with read depth between 2,056 and 37,853 reads), Sediment samples contained between 271 and 843 bacterial ASVs on their surface (we measured 36 sediment root samples with read depth between 10,775 and 40,346 reads), leaf samples contained between 261 and 716 bacterial ASVs on their surface (we measured 75 leaf samples with read depth between 5,770 and 50,564 reads) and leaf mimic samples which contained between 196 and 724 bacterial ASVs (35 leaf mimic samples with between 4,591 and 31,702 reads per sample).

Results

Leaf mimics have a higher number of ASVs than leaves (negative binomial glm, ANOVA, $p = 0.048$; Appendix Figure 1.A1A). When examining core ASVs (present in at least 50% of samples of a type at at least a 1% detection rate), we found that leaves and leaf mimics

largely harbored distinct bacterial communities, by ASV, while also sharing substantial overlap (Appendix Figure 1.A1B) and more so than other sample types. Of the 212 ASVS in the core leaf microbiome, 107 or 50% were found only on leaves and 97 of the remaining (56% of core leaf ASVs) overlapped with leaf mimic ASVs. While there was not a difference in variance within each sample type (betadisper ANOVA, $p = 0.71$), the composition of the two groups was different (PERMANOVA, $F = 19.61$, $p = 0.001$, $r2 = 0.15$, Appendix Figure 1.A2A). When we examine overlap in predicted Metacyc pathways, we found that there was a significant difference between leaves and mimics (PERMANOVA, $r2 = 0.05411$, $F = 6.1787$, $p = 0.001$), though this effect was weaker than for the sequence based compositional differences (Appendix Figure 1.A2B).

Through analysis of specific ASVs that varied between leaves and leaf mimics via DESEQ2, we found 209 ASV that showed higher relative abundance on leaves and 101 that showed higher relative abundance on mimics. Only four families contained more than ten ASVs that varied between mimics and leaves: Flavobacteriaceae (15 higher on leaves, 17 higher on mimics), Pirellulaceae (eight higher on leaves, four higher on mimics), Rhodobacteraceae (40 higher on leaves, 25 higher on mimics), and Saprospiraceae (39 higher on leaves, one higher on mimics); most families contained fewer than 3 ASVs that varied between leaves and mimics (Appendix Table 1.A1&A2). Within these families several genera were represented by multiple ASVs. These included *Kordia* (three ASVs higher on leaves), *Maribacter* (one higher on leaves, two higher on mimics) *Ulvibacter* (two higher on leaves, two higher on mimics), *Winogradskyella* (one higher on leaves, two higher on mimics), *Blastopirellula* (5 higher on leaves, 2 higher on mimics), *Rhodopirellula* (two higher on leaves), *Octadecabacter* (one higher on leaves, one higher on mimics), *Roseobacter* (one higher on leaves, two higher on mimics),

Sedimentitalea (one higher on leaves, one on mimics), *Sulfitobacter* (three higher on leaves, three higher on mimics), *Tateyamaria* (one higher on leaves, one on mimics), *Yoonia-Loktanella* (four higher on leaves), *Lewinella* (five higher on leaves), *Portibacter* (four higher on mimics), and *Rubidimonas* (three higher on leaves). Six other genera (not in these families) contained multiple ASVs that varied between leaves and mimics (Appendix Table 1.A3). For all ASVs that varied significantly between seagrass leaves and mimics see Appendix Table 1.A4.

When we examined pathways that changed between the leaf and leaf mimic microbiomes, we identified 82 pathways that changed, 16 upregulated in leaf microbiomes and 66 upregulated on mimic microbiomes (Appendix Table 1.A5). These pathways were generally unremarkable (likely at least in part due to limits in prediction of environmental microbial pathways), though did indicate that aerobic environments might not solely limited to leaf microbiomes with an upregulation of the superpathway of sulfur oxidation on mimic leaf surfaces compared to leaf surfaces.

In roots, less surprisingly, we also found differences between the mimic and root communities. We found that despite fewer ASVs found summed across samples in mimics (Appendix Figure 1.A1B), there were generally the same number of ASVs on roots and root mimics (Appendix Figure 1.A1A, negative binomial glm ANOVA, $p = 0.093$, $p = 0.32$ when comparing sediments as well). We found that there was no difference in variance among roots and root mimics (betadisper ANOVA $p = 0.87$), however sediments showed less variance than either of the other two groups (betadisper ANOVA, $p < 0.001$, Tukey's HSD sediment vs mimic $p < 0.001$, vs roots $p < 0.001$). When examining core ASVs (present in at least 50% of samples of a given type at at least 1% detection rate), we found that roots and sediments largely harbored distinct bacterial communities, by ASV (Appendix Figure 1.A1B), though root mimics had fewer

unique core microbiome (only 2 ASVs unique to root mimics). Of 266 ASVS in the core root microbiome, 82 or 31% were found only on roots and 131 (49%) were found only on roots and in sediments. Only 38 core root ASVs (14%) were shared between roots and root mimics. When we examined all ASVs (without core restrictions), root mimics had more taxa unique to their sample type, indicating considerable variability in communities assembled on root mimics (Appendix Figure 1.A3). ASV composition on roots, mimics and sediment were compositionally distinct (PERMANOVA r2 = 0.151 F = 17.672 p = 0.001, see Appendix Table 1.A6 for pairwise comparisons, Appendix Figure 1.A4).

We found many ASVs varied in abundance between these groups (417 between sediments and mimics, 454 between roots and sediments, and 385 between roots and mimics). Of these, the majority were at higher abundances on roots or sediments compared to mimics (comparing roots to mimics, 437 were higher on roots, and 49 were higher on mimics; comparing sediment to mimics, 359 were higher in sediments, 98 were higher on mimics; comparing roots to sediments 265 were higher on roots, 240 were higher in sediments; see Appendix Table 1.A7&8 for more details). The families that had the largest number of taxa vary among sample types included Spirochaetaceae (32 ASVs), Thiotrichaceae (33 ASVs), Bactoroidetes BD2-2 (47 ASVs), Pirellulaceae (56 ASVs), Desulfosarcinaceae (63 ASVs), Desusulfocapsaceae (69 ASVs), Saprospiraceae (73 ASVs), Rhodobacteraceae (125 ASVs) and Flavobacteriaceae (130 ASVs). Number of ASVs at higher or lower relative abundances in these different treatments can be found in Appendix Table 1.A7.While the pathways that varied were numerous and not particularly remarkable (as indicated in Appendix Table 1.A9), we found that indicated pathways were generally indicated to be upregulated on mimics in pairwise

comparisons (141 pathways higher in mimics compared to 32 in sediments, and 69 higher on mimics compared to 11 on roots).

Appendix 1.A Figures and Tables:

Appendix Figure 1.A1: (A) Mean amplicon sequence variant (ASV) richness found in each type of sample we measured. Raw data as well as means and standard errors are presented. Leaf mimic bacterial communities had a higher mean richness than leaf bacterial communities ($p < 0.001$); root mimic, root, and sediment bacterial communities did not differ in mean community richness. (B) Overlap among core bacterial communities showing shared ASVs present in each sample type in at least 50% of samples at a 1% detection rate. Diagram is a barplot of shared community memberships, equivalent to a Venn diagram.

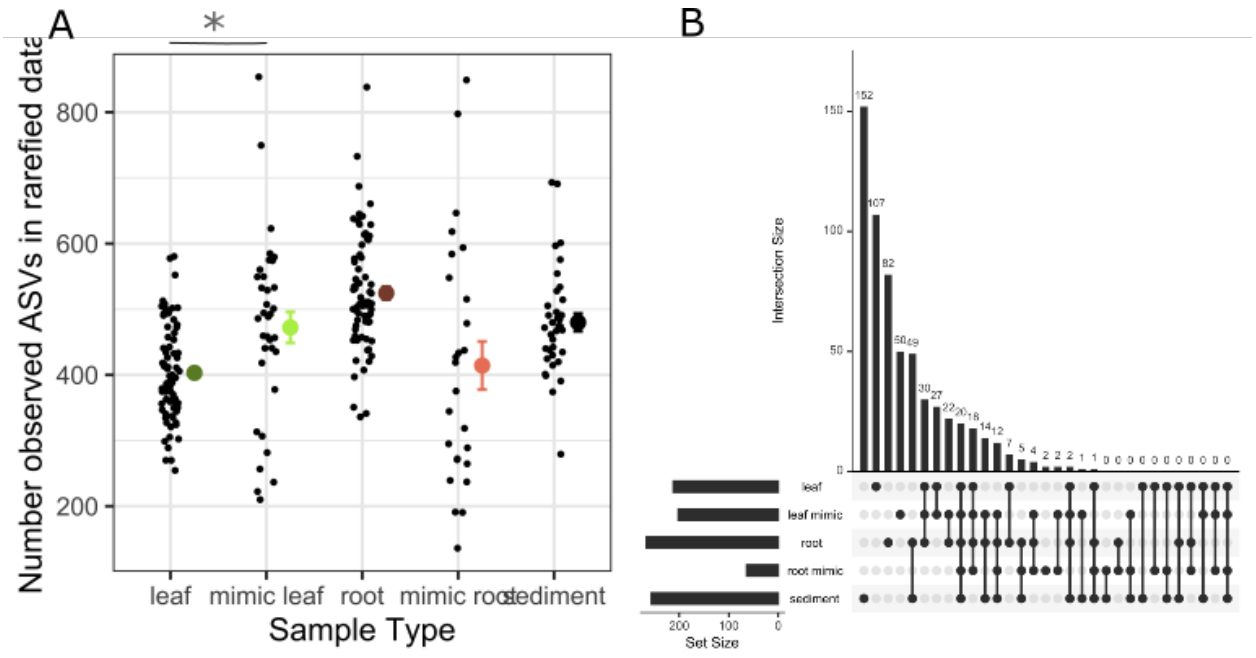

Appendix Figure 1.A2: (A) Ordination of bacterial community structure based on principal coordinate analysis of phylogenetic-isometric log-ratio transformed distances. (B) Ordination of predicted Metacyc pathways structure based on principal coordinate analysis of centered log-ratio transformed distances. Bright green points are communities on leaf mimics and dark green points are communities on leaves. Leaf and leaf mimic communities in both analyses are distinct from each other (PERMANOVA $p < 0.001$).

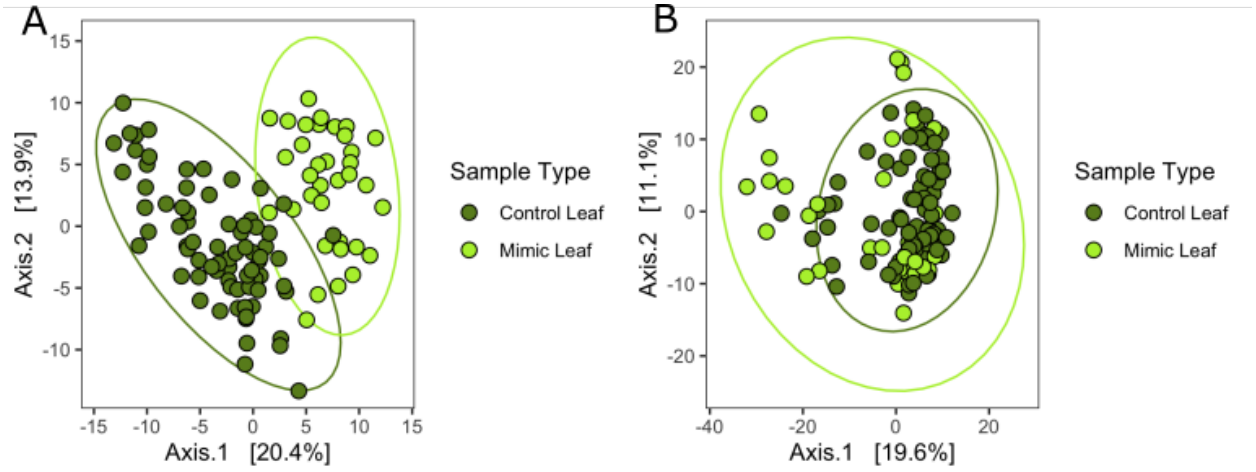

Appendix Figure 1.A3 Overlap among all ASVs present in each sample type. Diagram is a barplot of shared community memberships, equivalent to a Venn diagram.

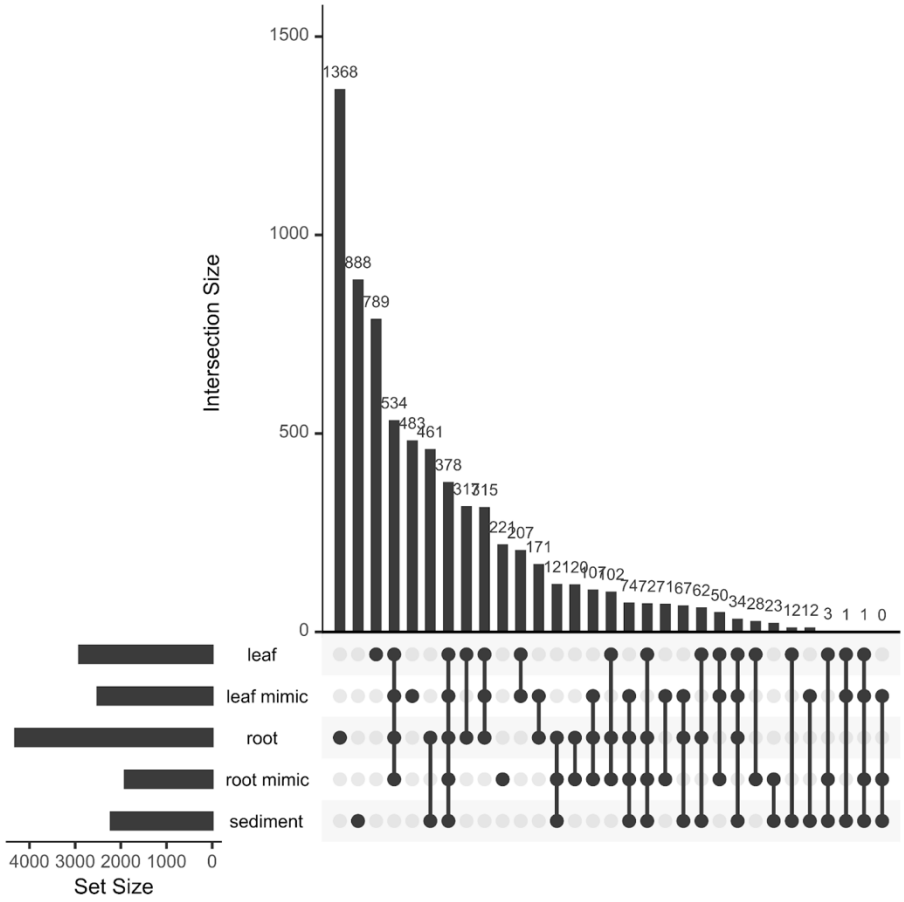

Appendix Figure 1.A4: (A) Ordination of bacterial community structure based on principal coordinate analysis of phylogenetic-isometric log-ratio transformed distances. (B) Ordination of predicted Metacyc pathways structure based on principal coordinate analysis of centered log-ratio transformed distances. Red-orange points are communities on root mimics, dark brown points are communities on roots, and grey points are communities in sediments. All communities are distinct from each other in each analysis (PERMANOVA $p < 0.001$).

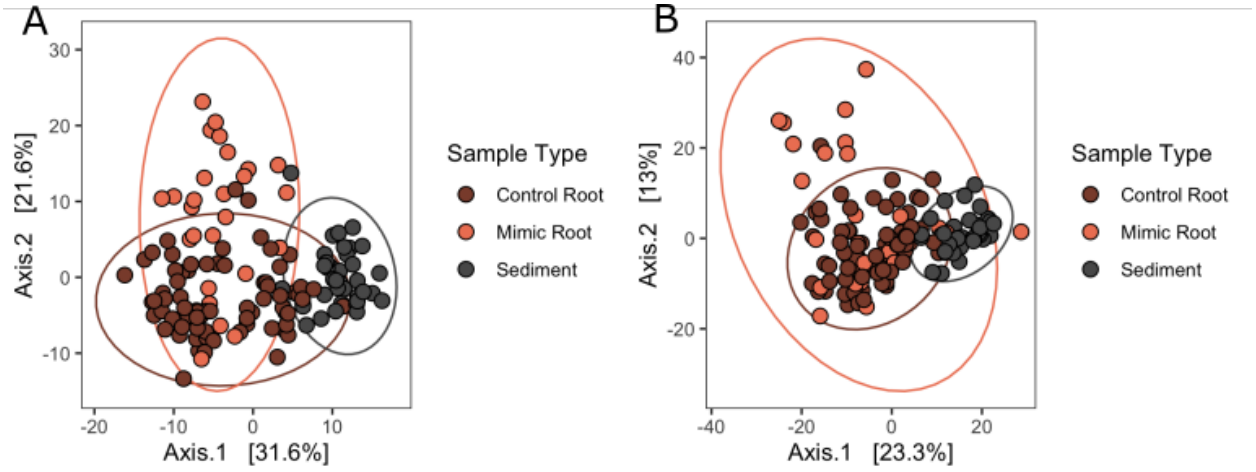

Appendix Table 1.A1: For both leaves and root communities, the five families that had the most ASVs vary between mimics and seagrass substrate. See Appendix Tables 1.A2 and 1.A7 for complete lists for leaves and roots respectively.

Family	Higher on leaves	Higher on mimics
Rhodobacteraceae	40	25
Saprospiraceae	39	1
Flavobacteriaceae	15	17
Pirellulaceae	8	4
Rhizobiaceae	1	8

Family	Higher on roots	Higher on mimics	Higher on mimics	Higher on sediment	Higher on roots	Higher on sediment
Flavobacteriaceae	38	3	32	12	37	8
Rhodobacteraceae	36	3	41	0	45	0
Desulfocapsaceae	24	0	6	15	14	10
Saprospiraceae	19	3	21	4	23	3
Desulfosarcinaceae	14	3	0	23	0	23

Appendix Table 1.A2: For leaf bacterial communities, the family-level identification of ASVs that varied significantly between mimics and seagrass substrate determined by DESeq2.

Family	Higher on leaves	Higher on mimics
37-13	1	0
A4b	1	0
Alteromonadaceae	8	0
Arenicellaceae	1	0
Bdellovibrionaceae	2	0
Bernardetiaceae	1	0
Blastocatellaceae	0	1
Caldilineaceae	2	0
Cellvibrionaceae	3	0
Chromatiaceae	2	1
Colwelliaceae	4	0
Crocinitomicaceae	8	0
Cryomorphaceae	8	0
Cyanobiaceae	0	1
Cyclobacteriaceae	2	0
Desulfobulbaceae	0	1
Desulfocapsaceae	1	5
DEV007	3	3
Flammeovirgaceae	1	0
Flavobacteriaceae	15	17
Fokiniaceae	1	0
Francisellaceae	1	0
Gimesiaceae	0	1
Granulosicoccaceae	5	2
Halieaceae	3	1
Halomonadaceae	0	1
Hyphomicrobiaceae	0	1
Hyphomonadaceae	3	2
Ilumatobacteraceae	0	1
Kangiellaceae	1	0
KD3-93	1	0
Legionellaceae	0	1
Magnetospiraceae	1	0
Marinomonadaceae	1	0
Methylophagaceae	2	0
Methylophilaceae	5	1

Micavibrionaceae	0	2
Microtrichaceae	2	2
Nitrincolaceae	2	0
Nitrosococcaceae	1	0
NS11-12_marine_group	1	0
NS9_marine_group	1	0
Oleiphilaceae	1	0
Opitutaceae	1	0
Phormidesmiaceae	0	1
Phycisphaeraceae	3	0
Pirellulaceae	8	4
Porticoccaceae	1	0
Prolixibacteraceae	2	0
Pseudohongiellaceae	2	0
Rhizobiaceae	1	8
Rhizobiales_Incertae_Sedis	0	1
Rhodobacteraceae	40	25
Rhodothermaceae	1	0
Rickettsiaceae	2	0
Rubinisphaeraceae	1	3
Rubritaleaceae	1	2
Saprospiraceae	39	1
Schleiferiaceae	1	0
Shewanellaceae	0	1
Sphingomonadaceae	3	3
Spirosomaceae	1	0
Spongiibacteraceae	2	0
Sulfurimonadaceae	1	0
Sulfurovaceae	0	3
Tenderiaceae	1	0
Terasakiellaceae	1	0
Thioglobaceae	1	0
Thiotrichaceae	1	1
Unknown_Family	0	2
Woeseiaceae	0	2

Appendix Table 1.A3: For leaf bacterial communities, the genus-level identification of ASVs that varied significantly between mimics and seagrass substrate determined by DESeq2.

Family	Genus	Higher on leaves	Higher on mimics
Alteromonadaceae	Glaciecola	6	0
Alteromonadaceae	Paraglaciecola	1	0
Alteromonadaceae	Salinimonas	1	0
Arenicellaceae	Arenicella	1	0
Bdellovibrionaceae	Bdellovibrio	1	0
Bdellovibrionaceae	OM27_clade	1	0
Bernardetiaceae	Garritya	1	0
Blastocatellaceae	Blastocatella	0	1
Cellvibrionaceae	Agaribacterium	1	0
Cellvibrionaceae	Candidatus_Endobugula	1	0
Chromatiaceae	Candidatus_Thiobios	2	0
Chromatiaceae	Halochromatium	0	1
Colwelliaceae	Colwellia	3	0
Colwelliaceae	Thalassotalea	1	0
Crocinitomicaceae	Crocinitomix	4	0
Crocinitomicaceae	Fluviicola	3	0
Cryomorphaceae	Vicingus	3	0
Cyanobiaceae	Synechococcus_CC9902	0	1
Cyclobacteriaceae	Ekhidna	1	0
Cyclobacteriaceae	Fabibacter	1	0
Desulfobulbaceae	Desulfobulbus	0	1
Flavobacteriaceae	Actibacter	0	1
Flavobacteriaceae	Aquibacter	0	2
Flavobacteriaceae	Aurantivirga	2	0
Flavobacteriaceae	Changchengzhania	1	0
Flavobacteriaceae	Formosa	1	0
Flavobacteriaceae	Jejudonia	0	1
Flavobacteriaceae	Kordia	3	0
Flavobacteriaceae	Lutibacter	0	1
Flavobacteriaceae	Maribacter	1	2
Flavobacteriaceae	NS2b_marine_group	1	0
Flavobacteriaceae	NS3a_marine_group	1	0
Flavobacteriaceae	Polaribacter	1	0

Flavobacteriaceae	Psychroserpens	0	1
Flavobacteriaceae	Robiginitalea	0	1
Flavobacteriaceae	Ulvibacter	2	2
Flavobacteriaceae	Wenyingzhuangia	1	0
Flavobacteriaceae	Winogradskyella	1	2
Fokiniaceae	MD3-55	1	0
Granulosicoccaceae	Granulosicoccus	5	2
Halieaceae	Halioglobus	0	1
Halieaceae	OM60(NOR5)_clade	2	0
Halieaceae	Pseudohaliea	1	0
Halomonadaceae	Halomonas	0	1
Hyphomicrobiaceae	Filomicrobium	0	1
Hyphomonadaceae	Hellea	1	0
Hyphomonadaceae	Hyphomonas	0	1
Hyphomonadaceae	Litorimonas	1	0
Hyphomonadaceae	Robiginitomaculum	1	0
Ilumatobacteraceae	Ilumatobacter	0	1
Magnetospiraceae	Magnetospira	1	0
Marinomonadaceae	Marinomonas	1	0
Methylophagaceae	Marine_Methylotrophic_Group_3	1	0
Methylophilaceae	Methylotenera	5	1
Microtrichaceae	Sva0996_marine_group	1	2
Nitrosococcaceae	Cm1-21	1	0
Oleiphilaceae	Oleiphilus	1	0
Opitutaceae	Diplosphaera	1	0
Phormidesmiaceae	Phormidesmis_ANT.LACV5.1	0	1
Phycisphaeraceae	Phycisphaera	1	0
Phycisphaeraceae	SM1A02	2	0
Pirellulaceae	Blastopirellula	5	2
Pirellulaceae	Pir4_lineage	0	1
Pirellulaceae	Pirellula	0	1
Pirellulaceae	Rhodopirellula	2	0
Pirellulaceae	Rubripirellula	1	0
Porticoccaceae	C1-B045	1	0
Prolixibacteraceae	Draconibacterium	2	0
Pseudohongiellaceae	Pseudohongiella	2	0
Rhizobiaceae	Ahrensia	0	1
Rhizobiaceae	Hoeflea	0	1
Rhizobiaceae	Pseudahrensia	1	4

Rhizobiales_Incertae_Sedis	Anderseniella	0	1
Rhodobacteraceae	Aliiroseovarius	1	0
Rhodobacteraceae	Celeribacter	0	1
Rhodobacteraceae	Jannaschia	0	1
Rhodobacteraceae	Leisingera	0	1
Rhodobacteraceae	Limibaculum	1	0
Rhodobacteraceae	Octadecabacter	1	1
Rhodobacteraceae	Phaeobacter	0	1
Rhodobacteraceae	Planktomarina	0	1
Rhodobacteraceae	Planktotalea	1	0
Rhodobacteraceae	Roseobacter	1	2
Rhodobacteraceae	Roseovarius	0	1
Rhodobacteraceae	Sedimentitalea	1	1
Rhodobacteraceae	Sulfitobacter	3	3
Rhodobacteraceae	Tateyamaria	1	1
Rhodobacteraceae	Thiobacimonas	0	1
Rhodobacteraceae	Tropicimonas	0	1
Rhodobacteraceae	Yoonia-Loktanella	4	0
Rickettsiaceae	Candidatus_Megaira	2	0
Rubinisphaeraceae	Fuerstia	1	0
Rubinisphaeraceae	Planctomicrobium	0	2
Rubritaleaceae	Haloferula	0	1
Rubritaleaceae	Persicirhabdus	0	1
Rubritaleaceae	Roseibacillus	1	0
Saprospiraceae	Aureispira	1	0
Saprospiraceae	Lewinella	5	0
Saprospiraceae	Phaeodactylibacter	1	0
Saprospiraceae	Portibacter	4	0
Saprospiraceae	Rubidimonas	3	0
Schleiferiaceae	Schleiferia	1	0
Shewanellaceae	Shewanella	0	1
Sphingomonadaceae	Altererythrobacter	0	1
Sphingomonadaceae	Erythrobacter	2	0
Sphingomonadaceae	Parasphingopyxis	0	1
Sphingomonadaceae	Sphingorhabdus	1	0
Spirosomaceae	Taeseokella	1	0
Spongiibacteraceae	Dasania	1	0
Sulfurimonadaceae	Sulfurimonas	1	0
Sulfurovaceae	Sulfurovum	0	3

Tenderiaceae	Candidatus_Tenderia	1	0
Thioglobaceae	SUP05_cluster	1	0
Thiotrichaceae	Cocleimonas	0	1
Thiotrichaceae	Leucothrix	1	0
Unknown_Family	Marinicella	0	1
Woeseiaceae	Woeseia	0	2

Appendix Table 1.A4: For leaf bacterial communities, all ASVs that varied significantly between mimics and seagrass substrate determined by DESeq2, including magnitude of differences. See Supplemental Files AppendixATable1.A4.csv

Appendix Table 1.A5: For leaf bacterial communities, all Metacyc predicted pathways that varied significantly between mimics and seagrass substrate determined by DESeq2, including magnitude of differences.

Pathway	log2-fold Change
nitrifier denitrification	3.23766261
superpathway of polyamine biosynthesis III	2.50832917
CMP-pseudaminate biosynthesis	2.38533794
nylon-6 oligomer degradation	1.78133925
thiazole biosynthesis II (Bacillus)	1.10325976
coenzyme M biosynthesis I	1.04456344
formaldehyde oxidation I	0.9590049
formaldehyde assimilation II (RuMP Cycle)	0.9562312
methyl ketone biosynthesis	0.9450924
superpathway of thiamin diphosphate biosynthesis II	0.92452883
ectoine biosynthesis	0.70480998
ADP-L-glycero-β-D-manno-heptose biosynthesis	0.65819635
L-arginine degradation II (AST pathway)	0.63231738
glucose and glucose-1-phosphate degradation	0.60402905
norspermidine biosynthesis	0.57577995
superpathway of polyamine biosynthesis I	0.56942389
superpathway of histidine, purine, and pyrimidine biosynthesis	-0.5242397
thiazole biosynthesis I (E. coli)	-0.5275914
fucose degradation	-0.5326074
catechol degradation to β-ketoadipate	-0.5359885
2-aminophenol degradation	-0.543549
acetylene degradation	-0.5581539
superpathway of Clostridium acetobutylicum acidogenic fermentation	-0.5613171
mannan degradation	-0.5810783
pyruvate fermentation to butanoate	-0.5920957
pyrimidine deoxyribonucleotides de novo biosynthesis II	-0.6078529
nitrate reduction VI (assimilatory)	-0.6120458
superpathway of pyridoxal 5'-phosphate biosynthesis and salvage	-0.6644642
superpathway of purine nucleotides de novo biosynthesis II	-0.6876697
aerobactin biosynthesis	-0.6890469
superpathway of sulfur oxidation (Acidianus ambivalens)	-0.7026774
superpathway of salicylate degradation	-0.8300772
reductive acetyl coenzyme A pathway	-0.8371843

teichoic acid (poly-glycerol) biosynthesis	-0.8410264
catechol degradation III (ortho-cleavage pathway)	-0.8454332
aromatic compounds degradation via β-ketoadipate	-0.8454332
meta cleavage pathway of aromatic compounds	-0.8789704
succinate fermentation to butanoate	-0.8998533
adenosylcobalamin biosynthesis II (late cobalt incorporation)	-0.9365552
androstenedione degradation	-0.9391163
superpathway of 2,3-butanediol biosynthesis	-0.9661671
superpathway of (Kdo)2-lipid A biosynthesis	-0.9733811
methanogenesis from acetate	-0.9792468
superpathway of demethylmenaquinol-6 biosynthesis II	-1.0619267
isopropanol biosynthesis	-1.0728644
superpathway of hexitol degradation (bacteria)	-1.0874184
L-glutamate degradation V (via hydroxyglutarate)	-1.1359106
D-galactarate degradation I	-1.1440026
superpathway of D-glucarate and D-galactarate degradation	-1.1440026
superpathway of (R,R)-butanediol biosynthesis	-1.1442403
pyruvate fermentation to acetone	-1.1605646
formaldehyde assimilation I (serine pathway)	-1.1923269
factor 420 biosynthesis	-1.2158772
isoprene biosynthesis II (engineered)	-1.2826466
glycerol degradation to butanol	-1.3412872
superpathway of N-acetylneuraminate degradation	-1.3670503
superpathway of L-aspartate and L-asparagine biosynthesis	-1.4278134
1,5-anhydrofructose degradation	-1.4325517
superpathway of N-acetylglucosamine, N-acetylmannosamine and N-acetylneuraminate degradation	-1.4891301
coenzyme B biosynthesis	-1.6276845
allantoin degradation to glyoxylate III	-1.6391955
D-glucarate degradation I	-1.6718886
glutaryl-CoA degradation	-1.7367827
L-lysine fermentation to acetate and butanoate	-1.7522809
creatinine degradation II	-1.7894301
glucose degradation (oxidative)	-2.1076198
mono-trans, poly-cis decaprenyl phosphate biosynthesis	-2.2966947
methylaspartate cycle	-2.3760429
L-lysine biosynthesis II	-2.4960889
NAD salvage pathway II	-2.5786537
cob(II)yrinate a,c-diamide biosynthesis I (early cobalt insertion)	-2.7391815
chondroitin sulfate degradation I (bacterial)	-2.8135174
L-glutamate degradation VIII (to propanoate)	-2.8832619

peptidoglycan biosynthesis IV (Enterococcus faecium)	-2.9437995
3-phenylpropanoate and 3-(3-hydroxyphenyl)propanoate degradation to 2-oxopent-4-enoate	-3.0650628
cinnamate and 3-hydroxycinnamate degradation to 2-oxopent-4-enoate	-3.0650628
allantoin degradation IV (anaerobic)	-3.3360909
superpathway of L-arginine, putrescine, and 4-aminobutanoate degradation	-3.5753343
superpathway of L-arginine and L-ornithine degradation	-3.5753343
nicotinate degradation I	-3.8065081
starch degradation III	-5.1566723
peptidoglycan biosynthesis V (β-lactam resistance)	-8.1998858

Appendix Table 1.A6: Results of pairwise PERMANOVA tests distinguishing compositional differences among roots, root mimics, and sediments in both ASV composition and composition of predicted Metacyc pathways.

			df	Sum Of Squares	R^2	F-Statistic	Pr(>F)
Based on taxonomy	Root vs. Mimic	Sample Type	1	2854.7	0.14	16.116	**0.001**
		Residual	99	17536.1	0.86		
		Total	100	20390.8	1		
	Mimic vs. Sediment	Sample Type	1	4684.5	0.371	35.362	**0.001**
		Residual	60	7948.3	0.629		
		Total	61	12632.8	1		
	Root vs. Sediment	Sample Type	1	6239.1	0.275	41.447	**0.001**
		Residual	109	16408	0.725		
		Total	110	22647.1	1		
Based on predicted function	Root vs. Mimic	Sample Type	1	3038	0.051	5.3312	**0.001**
		Residual	99	56417	0.949		
		Total	100	59455	1		
	Mimic vs. Sediment	Sample Type	1	8870	0.193	14.323	**0.001**
		Residual	60	37157	0.807		
		Total	61	46028	1		
	Root vs. Sediment	Sample Type	1	12146	0.212	29.289	**0.001**
		Residual	109	45201	0.788		
		Total	110	57347	1		

Appendix Table 1.A7: For belowground bacterial communities, the family-level identification of ASVs that varied significantly among mimics, seagrass and sediment determined by DESeq2.

Family	Higher on roots	Higher on mimics	Higher on mimics	Higher on sediment	Higher on roots	Higher on sediment
Acanthopleuribacteraceae	1	0	0	1	0	1
Anaerolineaceae	3	0	1	5	1	5
Arenicellaceae	3	1	2	1	3	1
Bacteroidetes_BD2-2	14	1	0	16	3	13
Calditrichaceae	5	3	0	9	0	9
Cellulomonadaceae	1	0	1	0	1	0
Cellvibrionaceae	3	0	2	0	3	0
Chitinophagaceae	1	0	1	0	1	0
Christensenellaceae	2	0	0	1	1	1
Chromatiaceae	3	0	0	4	0	4
Crocinitomicaceae	4	0	5	0	5	0
Cyclobacteriaceae	5	0	1	3	2	3
Desulfobacteraceae	3	0	0	2	1	2
Desulfobulbaceae	2	0	0	4	1	3
Desulfocapsaceae	24	0	6	15	14	10
Desulfosarcinaceae	14	3	0	23	0	23
Desulfovibrionaceae	5	0	0	1	5	0
DEV007	3	0	3	1	4	0
Devosiaceae	1	0	1	0	1	0
Ectothiorhodospiraceae	1	1	0	2	0	2
Flavobacteriaceae	38	3	32	12	37	8
Fusibacteraceae	2	0	0	1	2	0
Gemmatimonadaceae	1	0	0	1	0	1
Gimesiaceae	1	0	1	0	1	0
Granulosicoccaceae	2	1	5	0	5	0
Halieaceae	4	0	1	4	1	4
Halomonadaceae	0	2	2	0	2	0
Hungateiclostridiaceae	3	0	0	3	1	2
Hyphomonadaceae	1	0	4	0	4	0
Kiritimatiellaceae	1	0	0	1	0	1
Kordiimonadaceae	1	0	1	0	1	0
Lachnospiraceae	6	0	2	1	6	0
Latescibacteraceae	0	2	0	3	0	3
Lentimicrobiaceae	3	0	0	3	0	3
Magnetospiraceae	1	0	1	0	1	0

Marinifilaceae	2	0	0	1	2	0
Marinilabiliaceae	5	1	0	6	3	2
Marinomonadaceae	1	0	1	0	1	0
Melioribacteraceae	6	0	1	4	3	3
Methyloligellaceae	1	0	0	1	0	1
Methylophagaceae	2	0	2	0	2	0
Methylophilaceae	4	0	4	0	4	0
Microtrichaceae	2	0	2	0	2	0
MSBL8	1	0	0	2	0	2
Nitrincolaceae	2	0	1	1	2	0
Parvibaculaceae	1	0	1	0	1	0
PHOS-HE36	2	0	0	3	0	3
Pirellulaceae	16	1	13	7	13	6
Prolixibacteraceae	7	0	2	4	6	2
Psychromonadaceae	1	0	1	0	1	0
Puniceicoccaceae	2	0	1	0	2	0
Rhizobiaceae	6	0	6	0	7	0
Rhodobacteraceae	36	3	41	0	45	0
Rubinisphaeraceae	5	0	5	0	5	0
Rubritaleaceae	3	0	3	0	3	0
Sandaracinaceae	1	0	0	1	0	1
Saprospiraceae	19	3	21	4	23	3
SB-5	6	0	0	6	2	4
Schleiferiaceae	1	0	1	0	1	0
Sedimenticolaceae	2	2	1	5	1	5
SG8-4	1	0	0	1	0	1
Shewanellaceae	0	1	1	0	1	0
Sphingomonadaceae	2	0	2	0	3	0
Spirochaetaceae	9	1	0	10	7	5
Spirosomaceae	1	0	2	0	2	0
Spongiibacteraceae	2	0	2	1	2	1
Sulfurovaceae	1	0	1	0	1	0
Syntrophotaleaceae	1	0	0	1	1	0
Thermoanaerobaculaceae	7	0	0	11	0	11
Thioalkalispiraceae	1	2	0	3	0	3
Thiomicrospiraceae	4	1	1	6	1	6
Thiotrichaceae	8	1	9	3	9	3
Trueperaceae	1	0	1	0	1	0
Unknown_Family	5	1	1	6	1	5
Vibrionaceae	1	0	1	0	1	0
Woeseiaceae	2	0	0	2	0	2

Appendix Table 1.A8: For belowground bacterial communities, all ASVs that varied significantly among mimics, seagrass and sediment determined by DESeq2, including magnitude of differences. See Supplemental File AppendixATable1.A8.

Appendix Table 1.A9: For belowground bacterial communities, all Metacyc predicted pathways that varied significantly among mimics, seagrass and sediment determined by DESeq2, including magnitude of differences.

Pathway	Root vs. Mimic	Mimic vs. Sediment	Root vs. Sediment
β-alanine biosynthesis II	NA	5.98028867	6.17916013
1,4-dihydroxy-6-naphthoate biosynthesis I	0.52453186	-0.8382554	NA
1,4-dihydroxy-6-naphthoate biosynthesis II	NA	-0.9208415	NA
1,5-anhydrofructose degradation	NA	0.5822825	0.91678643
2-amino-3-carboxymuconate semialdehyde degradation to 2-oxopentenoate	-0.5324918	2.10192706	1.56943525
2-aminophenol degradation	-1.0096637	2.07887674	1.06921309
2-methylcitrate cycle I	-0.9007436	0.59329576	NA
2-methylcitrate cycle II	-0.7081516	NA	NA
2-nitrobenzoate degradation I	-0.5048366	1.98333606	1.47849943
3-phenylpropanoate and 3-(3-hydroxyphenyl)propanoate degradation to 2-oxopent-4-enoate	-1.3020418	4.07512185	2.77308003
3-phenylpropanoate degradation	-1.3795198	7.21839716	5.83887733
4-coumarate degradation (anaerobic)	NA	0.90868496	1.0680199
4-hydroxyphenylacetate degradation	-0.6235443	1.70481364	1.0812693
4-methylcatechol degradation (ortho cleavage)	-2.1204126	2.63553665	0.51512402
adenosylcobalamin biosynthesis I (early cobalt insertion)	-0.5278635	2.38312108	1.85525759
adenosylcobalamin biosynthesis II (late cobalt incorporation)	NA	2.45438795	2.19260435
ADP-L-glycero-β-D-manno-heptose biosynthesis	NA	-1.0379013	-1.0447171
aerobactin biosynthesis	NA	2.67822173	2.97740096
allantoin degradation IV (anaerobic)	-3.8790422	11.6679446	7.78890236
allantoin degradation to glyoxylate III	-1.0948528	1.20012867	NA
androstenedione degradation	NA	-1.0590578	-0.7936352
aromatic biogenic amine degradation (bacteria)	NA	0.97177605	0.64651199
aromatic compounds degradation via β-ketoadipate	-1.7048087	2.56052172	0.85571297
benzoyl-CoA degradation I (aerobic)	-5.3493261	8.43200767	3.08268157
benzoyl-CoA degradation II (anaerobic)	0.81885539	-3.1649666	-2.3461112
Bifidobacterium shunt	NA	1.36268466	0.9583059
biotin biosynthesis II	-2.2801293	5.1067305	2.82660117
catechol degradation III (ortho-cleavage pathway)	-1.7048087	2.56052172	0.85571297

catechol degradation to β-ketoadipate	-0.8640468	2.3152049	1.4511581
catechol degradation to 2-oxopent-4-enoate II	NA	1.29739008	1.0656568
chitin derivatives degradation	0.83765223	1.23367148	2.07132371
chlorophyllide a biosynthesis I (aerobic, light-dependent)	NA	1.66916567	1.65806178
chlorophyllide a biosynthesis II (anaerobic)	NA	1.63793953	1.6191585
chlorophyllide a biosynthesis III (aerobic, light independent)	NA	1.63793953	1.6191585
chlorosalicylate degradation	-1.5806965	5.29068882	3.70999227
chondroitin sulfate degradation I (bacterial)	-3.5706214	2.1288075	-1.4418139
cinnamate and 3-hydroxycinnamate degradation to 2-oxopent-4-enoate	-1.3020418	4.07512185	2.77308003
CMP-legionaminate biosynthesis I	NA	-1.7170811	-1.7560234
CMP-pseudaminate biosynthesis	0.96889146	2.61729121	3.58618266
cob(II)yrinate a,c-diamide biosynthesis I (early cobalt insertion)	NA	1.95843292	1.70820751
cob(II)yrinate a,c-diamide biosynthesis II (late cobalt incorporation)	NA	1.06300152	1.22997949
coenzyme B biosynthesis	NA	6.33172398	5.84288679
coenzyme M biosynthesis I	NA	0.55913072	NA
creatinine degradation I	NA	1.47125265	1.73472301
creatinine degradation II	NA	2.02886451	2.48406197
D-fructuronate degradation	NA	0.84183251	0.54886057
D-galactarate degradation I	NA	0.5502454	NA
D-galacturonate degradation I	NA	0.68804147	0.60597012
D-glucarate degradation I	-0.7791992	NA	NA
dTDP-N-acetylthomosamine biosynthesis	NA	0.82091307	NA
ectoine biosynthesis	NA	0.6063511	0.7610108
enterobacterial common antigen biosynthesis	-3.9398588	8.08370873	4.1438499
enterobactin biosynthesis	-1.6985363	1.81330954	NA
ergothioneine biosynthesis I (bacteria)	-4.5808794	3.71990392	-0.8609754
ethylmalonyl-CoA pathway	NA	1.63626912	1.93902201
factor 420 biosynthesis	-3.6181246	7.7968298	4.17870521
formaldehyde assimilation II (RuMP Cycle)	NA	1.36498138	1.62215714
formaldehyde oxidation I	NA	1.34472111	1.60981698
gallate degradation I	NA	2.96335443	2.60732399
gallate degradation II	NA	2.9931866	2.60959275
GDP-D-glycero-α-D-manno-heptose biosynthesis	NA	-2.336863	-2.3533359
glucose and glucose-1-phosphate degradation	-0.6154652	0.87514308	NA
glucose degradation (oxidative)	-3.5634038	1.31205774	-2.251346
glutaryl-CoA degradation	-0.8744803	-1.4823571	-2.3568374
glycerol degradation to butanol	-1.2138411	2.11371278	0.89987173

glycine betaine degradation I	NA	1.52630641	1.77967665
glycogen degradation I (bacterial)	NA	-0.5022613	NA
glycogen degradation II (eukaryotic)	NA	1.92811354	1.48703839
glyoxylate cycle	NA	0.59545961	NA
heterolactic fermentation	NA	1.35594303	0.9030291
hexitol fermentation to lactate, formate, ethanol and acetate	-2.3564217	2.93058383	0.57416213
incomplete reductive TCA cycle	NA	-0.6320642	NA
isoprene biosynthesis II (engineered)	NA	-1.596346	-1.2874942
isopropanol biosynthesis	NA	-0.7395089	-0.6601573
ketogluconate metabolism	-1.1100443	2.96513108	1.85508681
L-arabinose degradation IV	NA	9.80122018	9.49234434
L-arginine degradation II (AST pathway)	-2.0305001	2.94130845	0.91080839
L-glutamate degradation V (via hydroxyglutarate)	NA	-1.5896498	-1.8924772
L-histidine degradation II	NA	1.82293122	1.87999775
L-isoleucine biosynthesis IV	NA	-0.6183816	NA
L-lysine biosynthesis II	-2.7233821	5.1544283	2.43104615
L-lysine fermentation to acetate and butanoate	NA	1.47736849	1.57053027
L-methionine biosynthesis I	NA	0.71356601	0.64118985
L-methionine salvage cycle III	-5.7266642	7.85970156	2.1330374
L-rhamnose degradation I	-0.5624761	0.61263037	NA
L-tryptophan degradation IX	NA	1.00068122	0.80181412
L-tryptophan degradation to 2-amino-3-carboxymuconate semialdehyde	NA	1.00325492	0.74569097
L-tryptophan degradation XII (Geobacillus)	-0.7230692	1.62974146	0.90667225
L-tyrosine degradation I	NA	0.85425311	0.81798341
L-valine degradation I	NA	6.3388524	6.49180761
lactose and galactose degradation I	-5.062184	8.28938471	3.22720075
mannan degradation	NA	0.97400331	0.60637761
meta cleavage pathway of aromatic compounds	-1.0709935	2.48553208	1.41453861
methanogenesis from acetate	0.66802212	-1.5177292	-0.8497071
methanol oxidation to carbon dioxide	-0.6092689	1.67128139	1.06201246
methylaspartate cycle	NA	NA	0.72955726
methylgallate degradation	NA	2.96817215	2.59940031
methylphosphonate degradation I	NA	1.21248246	1.44671709
mevalonate pathway I	NA	-0.6973192	NA
mevalonate pathway II (archaea)	1.19113556	-2.5647924	-1.3736568
mono-trans, poly-cis decaprenyl phosphate biosynthesis	-2.1669721	6.66242923	4.49545717
mycothiol biosynthesis	-0.5798133	0.57033211	NA
myo-, chiro- and scillo-inositol degradation	NA	2.56222211	2.29443289
myo-inositol degradation I	NA	2.51159939	2.38726902

NAD biosynthesis II (from tryptophan)	NA	0.7850773	0.59630288
NAD salvage pathway II	-3.216504	3.1998056	NA
nicotinate degradation I	-5.9100989	8.01022674	2.1001278
nitrate reduction VI (assimilatory)	NA	1.33504703	0.94737502
norspermidine biosynthesis	NA	1.58842222	1.33114879
nylon-6 oligomer degradation	NA	0.99787962	0.80549182
octane oxidation	NA	1.03817344	1.15439139
palmitate biosynthesis II (bacteria and plants)	-0.872762	-0.8440889	-1.716851
peptidoglycan biosynthesis II (staphylococci)	-5.788931	12.6352847	6.84635369
peptidoglycan biosynthesis IV (Enterococcus faecium)	-2.3037652	3.02148026	0.71771506
peptidoglycan biosynthesis V (β-lactam resistance)	-3.1421431	5.05225645	1.91011332
phenylacetate degradation I (aerobic)	-1.5928447	2.04828109	NA
phospholipases	-0.7007483	1.74447062	1.04372228
polymyxin resistance	-2.9570821	1.86688576	-1.0901963
ppGpp biosynthesis	NA	1.3237357	0.94719959
protocatechuate degradation I (meta-cleavage pathway)	NA	3.31323514	3.04051865
protocatechuate degradation II (ortho-cleavage pathway)	NA	1.43269458	1.45955473
purine nucleotides degradation II (aerobic)	NA	0.84745319	0.95184059
purine ribonucleosides degradation	NA	1.02596312	1.33210895
pyrimidine deoxyribonucleotides biosynthesis from CTP	NA	-3.2387427	-3.0061164
pyrimidine deoxyribonucleotides de novo biosynthesis IV	NA	-3.2464337	-3.0353371
pyruvate fermentation to acetone	-0.7989368	0.58953572	NA
pyruvate fermentation to butanoate	NA	-0.8480954	-0.6834175
reductive acetyl coenzyme A pathway	0.56299075	-1.0712442	-0.5082534
S-adenosyl-L-methionine cycle I	-0.5730782	1.49674887	0.92367066
S-methyl-5-thio-α-D-ribose 1-phosphate degradation	-6.0971955	7.92182186	1.82462635
spirilloxanthin and 2,2'-diketo-spirilloxanthin biosynthesis	NA	2.2330273	2.28217566
starch degradation III	NA	7.32377146	7.21603178
sucrose degradation II (sucrose synthase)	NA	-2.0756477	-1.9117441
sucrose degradation III (sucrose invertase)	-1.0811735	2.13489002	1.05371654
superpathway of (Kdo)2-lipid A biosynthesis	NA	-0.7054507	-1.1461552
superpathway of β-D-glucuronide and D-glucuronate degradation	NA	0.85148319	0.6319071
superpathway of aerobic toluene degradation	-0.7444703	1.79585096	1.05138063
superpathway of bacteriochlorophyll a biosynthesis	NA	1.67435543	1.69358424

superpathway of C1 compounds oxidation to CO2	0.79775953	4.93409574	5.73185526
superpathway of Clostridium acetobutylicum acidogenic fermentation	NA	-0.7857639	-0.6260313
superpathway of D-glucarate and D-galactarate degradation	NA	0.5502454	NA
superpathway of demethylmenaquinol-6 biosynthesis II	NA	0.81685025	1.18219199
superpathway of fucose and rhamnose degradation	-0.8033356	3.780394	2.97705835
superpathway of geranylgeranyldiphosphate biosynthesis I (via mevalonate)	NA	-0.7049968	NA
superpathway of glycerol degradation to 1,3-propanediol	NA	2.71236968	2.61185182
superpathway of glycol metabolism and degradation	-1.048886	4.77755709	3.72867113
superpathway of hexitol degradation (bacteria)	-1.4325053	1.10451066	NA
superpathway of hexuronide and hexuronate degradation	NA	1.1797743	0.68847957
superpathway of L-arginine and L-ornithine degradation	-4.2622312	7.80495629	3.54272513
superpathway of L-arginine, putrescine, and 4-aminobutanoate degradation	-4.2622312	7.80495629	3.54272513
superpathway of L-threonine metabolism	-5.2246486	8.59332633	3.36867768
superpathway of menaquinol-8 biosynthesis II	0.67518966	-0.7613806	NA
superpathway of methylglyoxal degradation	-1.1952535	3.88225935	2.6870059
superpathway of phenylethylamine degradation	-1.3717238	4.68127965	3.30955587
superpathway of polyamine biosynthesis III	1.12820444	NA	1.40574398
superpathway of purine deoxyribonucleosides degradation	NA	0.99995122	1.24937609
superpathway of pyridoxal 5'-phosphate biosynthesis and salvage	-0.6116537	2.45674032	1.84508665
superpathway of pyrimidine deoxyribonucleosides degradation	NA	0.70003531	1.00034021
superpathway of S-adenosyl-L-methionine biosynthesis	NA	0.51696413	NA
superpathway of salicylate degradation	-1.5799859	2.48032888	0.90034295
superpathway of sulfolactate degradation	NA	1.89159187	2.27801115
superpathway of sulfur oxidation (Acidianus ambivalens)	0.76011508	-1.8921344	-1.1320193
superpathway of thiamin diphosphate biosynthesis II	NA	-1.1289035	-0.8492926
superpathway of UDP-glucose-derived O-antigen building blocks biosynthesis	NA	1.16390318	0.98925039
superpathway of vanillin and vanillate degradation	NA	3.40551039	2.99074115
TCA cycle VII (acetate-producers)	NA	0.78551358	NA
teichoic acid (poly-glycerol) biosynthesis	NA	4.22846527	3.957639

thiazole biosynthesis II (Bacillus)	NA	-1.4247689	-1.0254904
toluene degradation III (aerobic) (via p-cresol)	-1.5757307	2.32241598	0.74668526
toluene degradation IV (aerobic) (via catechol)	-1.3085971	2.94089177	1.63229471
tRNA processing	NA	-0.5698891	NA
UDP-2,3-diacetamido-2,3-dideoxy-α-D-mannuronate biosynthesis	NA	-0.5764018	NA
urea cycle	NA	0.52908568	0.76921194
vanillin and vanillate degradation I	NA	3.40551039	2.99074115
vanillin and vanillate degradation II	NA	3.39293769	2.98479856
vitamin B6 degradation	-4.8624169	6.32522899	1.46281206
vitamin E biosynthesis (tocopherols)	-2.7550338	7.24500287	4.48996911

Local environment drives rapid shifts in composition and phylogenetic clustering of seagrass microbiomes

Authors: Melissa R. Kardish, John. J. Stachowicz

Introduction

Host-associated microbial communities are increasingly identified to have important effects on their host (McFall-Ngai et al. 2013, Hammer et al. 2019). The composition and structure of host-associated microbial communities vary by geographic region (Coleman-Derr et al. 2016, Griffiths et al. 2019), host health (Marzinelli et al. 2015), successional stage (Shade et al. 2013, Copeland et al. 2015, Shi et al. 2015, Wang et al. 2020) and environmental conditions (Avena et al. 2016, Rothschild et al. 2018), but the extent to which the host is a cause of, or faces consequences from, this variation is often unclear (Glasl et al. 2019). Making progress on this question requires an understanding of the forces structuring these communities. Such an understanding will be key toward manipulating the microbes in the interest of enhancing functionality and predicting microbiome composition and function under environmental change. This requires experimental and observational work to disentangle the roles of temporal and environmental variation in driving community structure at different scales.

Microbial communities, like many ecological communities, vary predictably with seasonal and interannual variation in environmental drivers and host characteristics (Copeland et al. 2015, Fuhrman et al. 2015, Weigel and Erwin 2017). Microbial communities often shift composition as environmental conditions change, but whether these changes are due to direct environmental changes or changes in the host is often unclear. For example, coral bacterial communities resemble their new sites when hosts were transplanted among sites for 21 months (Ziegler et al. 2019). Similarly, temporal/seasonal variation was the dominant driver of sponge microbiome composition among nearby sites, despite differences in tidal depth (Weigel and Erwin 2017). Some terrestrial plant common garden studies looking at microbial communities that have run for at least two years (e.g., Wagner et al. 2016) also find a dominance of local

environmental over host characteristics in driving microbial assemblages. However, the coarse temporal resolution of these studies limits the ability to assess how quickly a change in local environment changes microbiomes. Thus, the speed of microbiomes matching novel environments is often unknown, yet is critical for assessing the capacity of the microbiome to buffer the host against a changing environment.

Community composition is determined by the source pool of potential inhabitants in conjunction with numerous abiotic and biotic filters restricting certain members (Weiher and Keddy 1995, Kraft et al. 2015). In order to assess the various roles of different filters, community ecologists have used functional similarity to describe likely niche overlap between members of a guild: using the observed patterns in communities to infer the process of assembly (Cavender-Bares et al. 2004b). When good functional data is not available, as is the case for many uncultured members of metagenomic sequenced communities, phylogenetic similarity can be used, with the assumption that conservation of key traits is held within clades (Webb 2000, Webb et al. 2002, Cavender-Bares et al. 2004a, Kembel et al. 2014). Given these assumptions, if microbial communities are phylogenetically clustered (i.e., more phylogenetically similar than expected by chance), local environmental filtering may exert a dominant influence on microbiomes. Alternatively, if microbiomes are phylogenetically overdispersed (less similar than expected by chance) resource partitioning or inter-taxon facilitation (i.e., cross-feeding, environmental buffering) could be the dominant driver of assembly. Furthermore, comparing phylogenetic clustering (or overdispersion) among sites can allow insights into the contingent nature of community assembly. For example, if at one site there is increased evidence of phylogenetic clustering compared to other sites we might expect that there is either a different environmental filter at that site or a reduction of competition in the microbial community there.

Microbial communities associated with the marine angiosperm eelgrass (*Zostera marina*) are of increasing interest for their role in host ecology and ecosystem functioning. Eelgrass is a foundation species that provides food and habitat for a diversity of animals (Duarte 2002), stabilizes sediment (Fonseca et al. 1982a, 1982b), and mediates nutrient cycling (Moore and Short 2006), and the potential role of the microbiome in mediating these effects will clarify how to best conserve and restore the important functions of eelgrass. Both leaves and roots differ in composition from source pools in water and sediments, but roots are more differentiated from sediment than leaves are from water (Fahimipour et al. 2017). Additionally, there seems to be an enhanced abundance of potentially functionally important sulfide oxidizing bacteria in communities collected from roots (Cúcio et al. 2016). Leaf microbial communities are locally and regionally variable (Fahimipour et al. 2017, Bengtsson et al. 2017) and may reflect other environmental patterns and guild structures (Bengtsson et al. 2017), whereas root microbiomes seem to vary less geographically (Fahimipour et al. 2017). No work in eelgrass to date has tested the role of host versus environment in microbial community structure but we know that there are strong differences in host genotypic composition, genetically-based traits, and environment on spatial scales less than 1km (Hughes et al. 2009, Hughes and Stachowicz 2010, Kamel et al. 2012, Abbott et al. 2018).

To understand the assembly processes of seagrass microbiomes, we performed a reciprocal transplant experiment among four sites within a single 5 km^2 embayment in Bodega Harbor, California, USA, along a gradient from the mouth of the harbor (most oceanic) to the head (most estuarine). This gradient (see Figure 2.1) consists of increasing temperature, decreasing flow, and changing sediment grain size and organic content, all of which potentially influence the root and leaf microbiomes; local adaptation of plants to these differences could also

moderate microbiome assembly. We tracked changes in the bacterial assemblages associated with eelgrass roots and leaves across a time course of three months (July to September) to examine the relative importance of host factors vs environment in determining microbiome composition. We then applied community phylogenetic approaches to assess the role of environmental filtering vs. other processes in structuring bacterial assemblages.

Results

On both roots and leaves, plants strongly resembled destination and not origin site after one month

Leaf bacterial community composition based on phylogenetic isometric log-ratio transformed data from samples transplanted among our four sites quickly resembled destination site (the site to which shoots were transplanted) and not origin site (the site of collection) across our four sites (Figure 2.2, Table 2.1), suggesting that eelgrass microbiomes rapidly change as a function of local conditions. After 1 month, there was also an effect of origin site and its interaction with destination site, though these effects were weaker than the effect of destination site (Figure 2.2A, PERMANOVA results in Table 2.1). After two and three months, there was still a strong effect of destination site, but no effect of origin site or its interaction with destination site (2 months: Figure 2.2B, Table 2.1; 3 months: Figure 2.2C, Table 2.1). There was strong differentiation by destination site across all three time points (Figure 2.2A-C, Table 2.1). This suggests that destination environment, and/or plant changes that happen as a result of the destination environment, were the primary drivers of leaf microbiome and these overwhelmed any residual effect of origin site within 2 months at most. These differences were associated with differences in variance among sites within time points (betadisper, ANOVA $p_1 = 0.0016$, $p_2 =$

0.0003, $p_3 = 0.05127$): after one month, Mason's Marina (MM) had higher within-site variance than all other sites, and after two months was still greater than Doran Beach (DB) and Westside Park (WP) but not Campbell Cove (CC).

As there was a significant interaction between destination and origin sites after one month, we compared all possible combinations of origin and destination sites. Regardless of origin site, bacterial communities differed between all pairwise destination sites after one month (Supplemental Table 2.S1A & 2.S1B for p and R^2 values). After one month, leaves of plants transplanted to DB from MM were distinct from those transplanted from CC or DB. Leaf bacterial communities of plants transplanted to MM from CC and MM were also still distinct from each other (Supplemental Table 2.S2 A & 2.S2 B for pairwise p and R^2 values). All pairwise combinations of leaf bacterial communities after two and three months were distinct from each other by destination site only.

Alpha diversity also varied as a function of destination site, although these differences only emerged after 2 months. After one month, there were no significant differences in amplicon sequence variant (ASV) richness among destination or origin sites (negative binomial GLM, $p > 0.05$, Figure 2.2D). After two months, plants at CC had a higher number of ASVs than those at DB and plants at WP had a higher number of ASVs observed than MM and DB (negative binomial GLM, $p < 0.001$, all significant pairwise comparisons also $p < 0.001$; Figure 2.2E). Finally after three months, WP had a higher number of ASVs than DB and MM ($p_{vsDB} < 0.001$, $p_{vsMM} < 0.001$) and CC had more ASVs than DB ($p < 0.001$, Figure 2.2F). After two months, there was also a small effect of origin site on richness due to differences between plants from CC and MM ($p = 0.040$). Considering all time points, fewer ASVs were present on leaves when at DB as destination site and more bacterial ASVs on leaves when at WP.

Root bacterial communities followed similar patterns as leaves. After one month, destination site had the strongest effect on microbiome composition, but there was also an effect of origin site and an interaction between origin and destination site (Figure 2.3A, PERMANOVA statistics in Table 2.2), but this was absent after two months (Figure 2.3b, Table 2.2) and three months (Figure 2.3C, Table 2.2). After two and three months, microbiomes still showed differences among all destination sites (Figure 2.3). There was no difference in within-site variance among sites at any time point (betadisper ANOVA, $p_1 = 0.0912$, $p_2 = 0.6264$, $p_3 = 0.3975$).

We explored the interaction between destination and origin site on root microbiome after one month, by comparing microbiomes in all possible combinations of origin and destination site at this time point. Regardless of origin site, bacterial communities differed between all pairwise destination sites after one month (all pairwise results (p-values and R^2) can be found in Supplemental Table 2.S3). However, origin site only influenced community composition for some origins at some destinations and only after one month. On roots of plants transplanted to MM, bacterial communities varied when comparing plants from MM vs. any other site while communities on roots of other sites did not differ from each other. The same pattern occurred at WP, where all plants transplanted from WP were distinct from all other sites and all other sites could not be distinguished from each other. At CC, bacterial communities roughly formed two groups with root bacterial communities -- plants from CC and DB hosted similar communities and plants from MM and WP hosted a different distinct community. At DB, we saw no effect of origin site (all pairwise results p-values and R^2s can be found in Supplemental Table 2.S4). There were no differences in alpha diversity among roots by destination after one or three months (negative binomial GLM, $p_1, p_3 > 0.05$), but after two months plants planted at WP had

more ASVs (Figure 2.3D-F; negative binomial GLM, $p_{destination} = 0.007$, $p_{origin} = 0.023$, $p_{destination:origin} = 0.447$; significant pairwise differences: $p_{destination\ CCvsWP} = 0.011$, $p_{destination\ MMvs\ WP}$, $p_{origin\ MMvsWP} = 0.023$).

Most sites show phylogenetic clustering, degree of clustering varies by destination site

Given that all sites are within a few kilometers, and the high degree of tidal exchange within Bodega Harbor, all sites are likely exposed to a very similar pool of colonizing microbes; therefore we expect that the compositional differences among sites we observed are driven by local factors rather than dispersal limitation. From our compositional analyses, we found that sites differed by destination site, indicating that destination environment exerted a dominant influence on community composition (Figure 2.2). This leaves the question open whether environments favor different bacterial communities, interactions are different at different sites or if different members of bacterial communities are better competitors, at different sites. To assess these impacts, we compared the phylogenetic composition of microbiomes using Nearest Relative Index (NRI) which calculates the average phylogenetic distance among all pairs of taxa to give a sense of overall clustering on a tree. We also compared values from different sites, to assess if the degree of clustering vs. dispersion varied among sites with different environmental characteristics.

When we examined leaf and root bacterial communities across sites, we found that these communities were largely phylogenetically clustered; no community showed evidence of phylogenetic overdispersion in NRI (Figures 2.4 and 2.5, Supplemental Table 2.S5). Leaf microbiomes varied in the degree of clustering by site, with communities at the most oceanic sites being least clustered and those at sites that were warmer or with less water flow were most clustered (Figure 2.4). After one month, leaf bacterial communities were more clustered at DB

than CC or WP; DB is the site furthest from the mouth of the harbor (Figure 2.4A). After two months, we observed that communities at MM were the most clustered followed by DB and WP followed by CC which was neither clustered nor overdispersed; MM is the site with the least flow and CC is the site closest to the mouth of the harbor and the coolest site (Figure 2.4B). There was no evidence of differences in phylogenetic clustering among sites after three months (Figure 2.4C). These changes in clustering across months suggests temporal variation in ecological filtering, perhaps due to low tides being less extreme and more nocturnal during September than earlier in the summer. This could have reduced environmental differences due to exposure differences among sites.

Root bacterial communities also showed differences in degree of phylogenetic clustering among sites via NRI (Figure 2.5). Bacterial communities on roots at MM were less clustered than CC or DB sites after one month, after two and three months WP was more clustered than DB or MM. These differences may be associated with temperature differences across sites (DB and MM are warmer than CC and WP) or by sediment grain size (MM has a finer grain size than other sites). Additionally, these results suggest that the differences we saw among root bacterial communities are driven by larger environmental patterns rather than seasonal or tidal differences as there were no differences in clustering over time.

Individual phylogenetic balances reveal variable clades among sites; more in roots than leaves

To determine which ASVs drove the differences among destination sites and identify where these differences might occur, we employed a phylogenetic balance approach to identify where in a phylogenetic tree there are differences among samples. This means we identify which nodes in a phylogenetic tree of ASV 16S sequences are more abundant on one branch of the node at some sites compared to others. Especially as clustering was a common observation, this

allows us to identify the clades that varied among sites rather than just listing variable ASVs, including if differences are at a higher taxonomic level.

These balances ranged in phylogenetic position from the tips of trees containing only 2 ASVs (~0.02% of the ASVs in the pool), to near the base of the tree containing over 96% of ASVs in the case of a leaf node after both one and two months. However, the median balance across samples was relatively small containing 3-4 ASVs within a node for leaf samples (depending on time point) and 5 ASVs per node in root samples (across time points). When we examined placement of nodes that defined differential balances, the phylogenetic placement of nodes was not different from a null distribution except for root bacterial communities after two and three months where nodes that differed were less basal (closer to tips) than expected (Supplemental Table 2.S6). Overall, we found between 5 and 35 balances that identified each site from others within a time point. See Supplemental Figures 2.S2-S7 for specific balances that distinguished specific sites from others within a plant compartment and time point, and Supplemental Figure 2.S1 for interpretive guidance.

As most of these nodes were at the level of differentiating among or within families (>97% did not contain a node that was not best identified to family or lower), we examined which differentiating families were in each plant compartment. We found the families that differed in leaves were different than those that varied in roots (Fisher's Exact Test $p<0.001$, Figure 2.6). The families most representative of differences in root microbiomes among sites include those likely involved in sulfate reduction (including Desulfocapsaceae), sulfur oxidation (Sulfurvaceae) and nitrogen cycling (Prolixbacteraceae); but there were no consistent patterns of certain ASVs distinguishing certain sites across timepoints. While we ran similar analyses in leaves, we did not identify families indicating processes that might differ among sites as we did

in roots for sulfur and nitrogen cycling. We suggest that these families are important in root microbial communities and individual taxa may vary between environments and therefore functions -- however further efforts in culturing members of these communities to allow for better differentiation among members would be required.

Transplant effect present in roots, but not leaves

Finally, we assessed the extent to which the experimental procedure: the process of uprooting, handling, transport and lab processing affected root and leaf microbiomes by comparing the bacterial communities from plants transplanted back to their origin site with undisturbed plants. This allowed us to examine the effect of transplantation as well as investigate differences among sites.

We found that leaf microbiomes were indistinguishable between transplant controls and undisturbed plants at any time point (Table 2.3, Figure 2.7 A-C), and retained the among-site differences described in Figure 2.2. There were no differences in alpha diversity or variance among transplanted plant leaf bacterial communities and untransplanted controls at any timepoint, except after 3 months, when transplanted plants had slightly higher bacterial richness than controls (ANOVA negative binomial GLM, $p_1 = 0.942$, $p_2 = 0.942$, $p_3 = 0.036$; Supplemental Figure 2.S8 A-C).

In contrast, we found persistent differences between root bacterial communities from transplanted and control plants across all three months we sampled (PERMANOVA, Table 2.4, Figure 2.7 D-F). Variance within transplanted plants was only higher than untransplanted control plants at three months (ANOVA, $p = 0.164$, $p_2 = 0.108$, $p_3 = 0.0009$). There were no differences in ASV richness among control and transplanted roots (ANOVA negative binomial GLM, $p_1 = 0.071$, $p_2 = 0.572$, $p_3 = 0.984$) (Supplemental Figures 2.S8 D-E).

As transplanted roots differed from control roots and leaves did not, we confirmed that leaf and root microbial communities on transplants were in fact different from controls due to the transplantation process and that it was not that transplanted root microbial communities resembled like leaves due to removal from sediment during transplantation. We found leaf and root communities of transplanted plants were distinct and transplanted plant root microbiomes more closely resemble control roots microbiomes than transplanted leaf microbiomes. Thus, though there is a transplantation effect in root microbiome, this was not due to them changing to resemble leaves (Supplemental Figure 2.S9, PERMANOVA, $p_{rootvsleaf} = 0.001$), which may just indicate different preferred microbial associations when transplanted.

Discussion

Seagrass beds within a harbor varied in their leaf and root microbiomes, and plants transplanted among these beds rapidly assumed the microbiome of the destination site, usually within a month. Root and leaf microbiomes were phylogenetically clustered within a site, but the degree of clustering varied with sites more stressful for seagrass (warmer, lower water flow, farther from the open ocean) showing a greater degree of clustering. Our balance analysis allowed us to further identify that many of the differences in communities among sites were at shallow nodes indicating fine scale differences in communities. In conjunction with the shifts to match new environments and assuming that traits relevant to environmental tolerances are conserved, we conclude that direct effects of environmental differences among sites drive these differences in microbial community assembly, though we cannot, as yet, conclusively identify the specific factors responsible. Furthermore, we highlight the differences in microbial community composition that can occur on small scales among seagrass beds within the same 5

km^2 embayment.

Terrestrial leaf phyllosphere microbial communities are more phylogenetically clustered on faster growing trees, potentially due to stronger ecological filters or decreased time for microbial succession to play out (Kembel et al. 2014). With this in mind, our evidence of clustering in leaves is not surprising in eelgrass given the very quick turnover of leaf tissue (new leaves produced roughly every 14 days (Sand-Jensen 1975)) which would reduce the amount of time that competition would have to play out on leaf surfaces before the leaf senesces. However, this indicates that there are potentially limited interactions among bacteria on the eelgrass leaf surface and suggests that the environment of the leaf surface and is critical. Recent work in terrestrial phyllospheres emphasizes establishing the patterns of assembly in phyllosphere, but provides little insight into the dominant mechanisms and requires more experimentation (Vacher et al. 2016). Bacterial competition has been suggested as the major driver of community assembly given the low nutrient environments and likely competition for shared resources (Schlechter et al. 2019), though low nutrient environments often produce clustering for traits (Miazaki et al. 2015). While seagrass leaves may be more nutrient rich environments than terrestrial plants due to the abundance of epiphytic algae growing on surfaces that exude excess DOC, the rapid turnover likely reduces the influence of competitive interaction. We suggest that processes of assembly need to take into account the ephemeral nature of these environments and that leaf microbiomes likely adapt rapidly to seasonal and among site variation in environmental conditions. This also could partially explain lower levels of clustering we observed at CC -- more random assembly assembly could be driven by increased exposure time due to slower growth related to cooler temperatures at CC compared to other sites (in July and August DB and MM were more clustered than CC and WP and also both have warmer water temperatures).

Unpublished growth data indicates that plants from CC grew slower than plants at DB (Kardish and Stachowicz unpublished data).

Additionally, there seem to be seasonal differences in leaf bacterial community assembly mechanisms. Our samples were taken at a standard position along the blade. Leaves grew more slowly are turning over slower in September compared to growth in July and August (Kardish and Stachowicz unpublished data), the standardized-sized leaf tissue we sampled would have been exposed for a slightly longer time and provide a more allowing more time for recruitment and biotic interactions to play out resulting in environment being less important, and biotic interactions among bacteria to becoming more important (and therefore NRI indicate more random rather than clustered assembly in September). However, this could also be driven by shallower, shorter, more nocturnal tides in September decreasing variability within environments among these intertidal beds, speeding succession in these communities. Further work would be needed to disentangle which seasonal effects are changing community assembly mechanisms. Seasonal differences are critical to understanding differences in community assembled differences across seasons are understudied in community phylogenetics even in non-microbial systems (see (Fitzgerald et al. 2017) for an example in tropical fish communities) and should be particularly prominent in systems like this where changing plant environment changes the microbiome in less than a month-- a similar time scale to that of seasonal environmental change. Studies of rhizospheric microbial communities are dominated by comparisons to bulk soil communities or across different environments (Whitman et al. 2018, Vieira et al. 2020, Rüger et al. 2021). However, there is some evidence of predictable seasonal changes (Shi et al. 2015), deterministic processes in root development (Rüger et al. 2021), and differences based on diversity of plant host species (Fitzpatrick et al. 2018). We have similarly established that

seagrasses host distinct communities from their surrounding sediments (Fahimipour et al. 2017, Kardish and Stachowicz 2021). We found different amounts of phylogenetic clustering at DB and MM than at WP or CC (the opposite pattern as seen in the first couple months in leaves where DB and MM were more clustered). Unlike in leaves, we were unable to control for approximate amount of environmental exposure or age in roots which limits the conclusions we can draw; however, these clustering differences suggest that root environments may be more distinct than leaf environments among sites.

Finally, we considered which phylogenetic balances drove differences in community structures in both leaves and roots. While we identified many balances that we used to identify different sites within time points, they varied by time point and site (i.e., we did not consistently identify the same balances differentiating certain sites). We found that the nodes that distinguished sites were not consistently shallow or deep within the tree (and generally were not differently placed than expected by chance). When we examined the families that distinguished leaf and root bacterial communities we found several differences, but perhaps most notably were differences within the family *Desulfocapsaceae* in roots. *Desulfocapsaceae* is a family containing known sulfate reducers associated with the top layers of marine sediments was found almost exclusively as an identifying balance in root bacterial community samples (Galushko and Kuever 2021). This bacterial family distinguished roots at CC, MM, and DB from other sites after one month and multiple balances distinguished DB from other sites at time points two and three. This potentially indicates that sulfur cycling at DB requires different members of *Desulfocapsaceae* or a difference in tolerance to an environmental parameter (e.g., the warmer temperatures at DB). This could potentially be explored through further metagenomic work exploring different roles and abilities of members of *Desulfocapsaceae* at these different sites.

Our previous work has identified many bacteria related to sulfur cycling enriched on seagrass roots, and especially noted the presence of sulfur oxidizers enhanced compared to sediments (Fahimipour et al. 2017). The presence of differences among sites in which members of this family are present may indicate differences in sulfide reduction rates immediately near sites or simply community structuring of different members of the community. More direct experimental work at this family in conjunction with different members of this family would be necessary to tease apart any different functions or differences in sulfur reducing abilities, they might have to determine if these are functionally redundant or if they result in differences to functional potential as well.

While previous studies have not considered the effects of transplantation itself on changes in microbial communities, we show a significant effect of transplantation on root microbial communities highlighting that comparing un-transplanted controls is an important consideration in future reciprocal transplant studies of microbiomes. In conjunction with the differences among destination sites and the quick acquisition of bacterial communities from a site, we concluded that these leaf bacterial communities are (1) relatively unaffected by transplantation stress and (2) likely acquire bacteria primarily from their local environment. Root communities, however, differed between control un-transplanted plants and plants transplanted back to their initial site. These differences were initially driven by more variable communities in transplanted vs control plants and higher alpha diversity in transplanted plants. However, these differences in richness and variance disappeared over time, while the effect of transplantation remained. We conclude that root surfaces also acquire bacteria from their local environment but are dramatically affected by transplantation stress in ways that do not vary by site. This could be caused by our methods of transplantation (which involved attachment to vexar to track shoots

and a several day period in seawater (with roots out of sediment)) being more stressful to root bacterial communities than leaf communities resulting in selection for different microbial communities upon transplantation. Regardless, our work emphasizes the importance of measuring undisturbed controls when drawing conclusions about how microbiomes alter in new environments which has not been done in previous microbiome reciprocal transplant experiments, especially in communities that may select for unique communities. To keep these communities more intact, moving plants with their previously-associated sediments may be important to the success in transplantation efforts. However, eelgrass transplantation with or without sediment has shown similar trajectories and convergence of root and rhizosphere microbial communities within 4 weeks (Wang et al. 2020). As this did not include unmoved controls, further investigation would be needed to determine the overall role of transplantation stress on root microbial community structure. As transplanting individual plants is an important mechanism of eelgrass restoration (Zhou et al. 2014, Eriander et al. 2016), understanding the microbiome of transplanting plants, particularly among even similar environments is important, but is relevant to other studies examining microbial shifts under transplantation that also are involved in high levels of habitat restoration (e.g., corals).

Changes in microbiomes potentially buffer hosts against stressful environments (Christian et al. 2015, Trevelline et al. 2019), but understanding the pace of these shifts is critical for assessing whether the host can survive the period of mismatch. We found that eelgrass microbiomes rapidly shift (< 1 month) in response to novel environments, and that these microbiomes, especially in roots, are distinguishable among sites based on taxa associated with key functions of nitrogen and sulfur metabolism. This suggests the potential for the microbiome to buffer the host against a changing environment through rapid community re-assembly. Using

manipulative experiments to assess microbiome functionality in field settings remains a challenging and important goal, and metagenomics studies, while powerful, can be limited in sample size due to costs. In this context, our approach of host transplantation combined with community phylogenetic and phylogenetic balance approaches has suggested some testable functional hypotheses and provides a viable approach for making progress on the functionality of microbiomes in non-model systems in field situations.

Methods

Reciprocal Transplant and Field Methods

We collected plants and reciprocally transplanted them among four seagrass beds within Bodega Harbor (California) at Campbell Cove ("CC", 38˚18'36"N, 123˚3'33"W), Mason's Marina ("MM", 38˚20'10"N, 123˚3'31"W), Westside Park ("WP", 38˚19'7"N, 123˚3'12"W), and Doran Beach ("DB", 38˚19'21"N, 123˚2'38"W). The sites represent discrete seagrass beds, but range in distance from each other from 0.9 km to 3.0 km. Plants at these sites have different phenotypic characteristics (e.g., nutrient uptake, morphological traits, growth traits, photosynthetic traits, and phenolics) when grown in common gardens (Abbott et al. 2018) and show a small degree of genetic differentiation using microsatellite loci (Kamel et al. 2012, Abbott et al. 2018).MM is the most distinct genetically and environmentally, potentially driven by finer sediment with higher organics as well as reduced water flow. CC is closest to the harbor mouth with high flow and sandy sediment and (along with WP) has the coolest water temperature of these sites. DB is our warmest site about 2˚C warmer in mean temperature than CC and WP and is also the site least impacted by human presence (all other sites are routinely visited by recreation clam fishers. In the summer of 2015, the mean temperature of these sites

ranged from 15.9˚C to 18.1˚C (instantaneous temperature across sites temperature ranged from 12.4˚C to 21.8˚C by HOBO loggers) (See Supplemental Table 2.S7 for temperature data by site).

We took collected plants to Bodega Marine lab, standardized shoot and rhizome length, and attached plants to vexar mesh blind to site of origin. Then we planted twelve vexar mesh screens with 16 plants at each of the four sites within an existing eelgrass bed with 1m in between screens (plants growing immediately below screens were removed). Two weeks before sampling for microbial samples, we marked plants to standardize the age of microbial samples.

We sampled plants destructively every month for three months during a pre-dawn low tide. When sampling, we randomly selected 3 screens at each site and measured and sampled from every (remaining, non-flowering) plant on those screens. Plants were rinsed in seawater on site before sampling to remove loose epiphytes and sediment. We collected approximately 10 roots along with a 2-3cm section of leaf from immediately distal to the marks made two weeks before punches from the oldest non-senescent leaf (resulting in all leaf tissue sampled being approximately the same age) from each plant and tissue that had not been exposed to the external environment at the time of transplant. We immediately froze all microbe samples on dry ice and stored at - 80˚C. Additionally, from each plot we took parallel microbial samples from four control plants (leaves and roots) of similar size that had not been transplanted from around the perimeter of the experimental plots.

Molecular Methods

We extracted DNA with the MoBio PowerSoil DNA kit from the surface of the leaves and roots and from scaled samples of samples. To get the surface of the leaves and roots only, we vortexed each frozen sample with 500ul of MilliQ water and then added that liquid to the bead

tubes and proceeded with the standard extraction protocol (full protocol available at github.mkardish/Transplants/Lab_Protocols). We lost DNA extractions for leaf samples transplanted to CC from MM and WP and have therefore not been included in further analyses that follow. At the Integrated Microbiome Resource at Dalhousie University, we amplified and sequenced the V4-V5 region of the 16S rRNA gene on an Illumina MiSeq on an Illumina MiSeq to identify bacteria present with primers 515F and 926R (Walters et al. 2016, Comeau et al. 2017).

Bioinformatic Analysis

We ran all bioinformatic and statistical analyses in R (version 3.6.1). We used a standard dada2 pipeline to error check our reads and to identify amplicon sequence variants (Callahan et al. 2016). We used only forward reads in our subsequent analyses (280 base pairs). We identified ASV taxonomy based on the SILVA database (Quast et al. 2013) and built a phylogeny of ASVs using alignments built with DECIPHER (Wright 2015) then a tree built with FastTree2 (Price et al. 2010) then converted to ultrametric (Britton et al. 2007). We then rooted the bacterial tree with an archeal outgroup (McMurdie and Holmes 2013, Paradis and Schliep 2019).

Sampling and sequencing success and results

We identified 43,118 bacterial ASVs across 681 leaf, root, sediment and water samples after quality filtering samples to 15,102,767 reads. Root samples contained between 239 and 1167 bacterial ASVs on their surface (we measured 330 root samples with read depth between 5,981 and 80,762 reads), and leaf samples between 118 and 1,010 bacterial ASVs (307 leaf samples with between 1,980 reads and 65,621 per sample).

Statistics

We determined differences among groups of samples based on euclidean distances after

phylogenetic isometric log transform described in (Silverman et al. 2017) in the R-package "philr" order to analyze the compositional changes in our dataset based on phylogenetic similarity. This analysis tests the differences in weighting of various regions of a phylogenetic tree rather than considering each ASV independently. We used PERMANOVA to determine differences among sample types (among sample types, sample timepoint, sample origin site and destination site) on ASVs present in at least 2 samples. We tested homogeneity of group dispersions with the betadispr function in 'vegan'. To measure bacterial richness, we rarified all samples to 1980 reads, calculated the number of "Observed ASVs", repeated this 200 times, and then used the average as our measure of bacterial richness in a sample (McMurdie and Holmes 2014). Pairwise-posthoc analyses were run to determine differences observed among groups.

We examined compositional differences among sites and treatments, by assessing phylogenetic clustering and overdispersion of groups relative to random draws from regional and local pools. We assume that many bacterial traits, especially those associated with major metabolic processes, are phylogenetically conserved, and thus conclude that phylogenetic clustering is associated with environmental filtering and dispersion with competitive forces, resource partitioning, or cross-feeding. We also examined the individual balances driving the differences in the communities we observed by identifying balances that made communities distinct from others.

We present data on the net relatedness index (NRI) of a community which is the negative of the standardized effect size of the calculated mean pairwise distance (MPD) compared to a null distribution. The NRI thus represents the average phylogenetic distance between all members of a community relative to an expected null value (Webb et al. 2008). We did this through the R package MicEco which implements a parallelized version of picante (Kembel et

al. 2010, Russel 2021). We used an independent swap null model in order to maintain sample richness and species occurrence frequency and compared MPD from our samples to 999 random draws. We only show data from abundance weighted models, but non-abundance weighted models show the same patterns. We tested for differences in clustering and dispersal among sites using ANOVAs or Kruskal Wallis tests when the residuals were not normal.

In addition to the clustering analysis, we also assessed which phylogenetic balances differed between groups of interest. This analysis uses multinomial logistic regression implemented in glmnet in order to identify which branches of the phylogeny differ in their representation among groups (Supplemental Figure 2.S1) (Friedman et al. 2010, Silverman et al. 2017). To select significant balances, we repeated cross validation procedures selecting the minimum lambda 100 times for each comparison to establish balances that best represented sites. We report how many iterations we found any balance shown across these trials. Finally, we summarized these balances, examining which families differed in leaves and roots across all time points. We also used a t-test to examine whether the placement of distinguishing nodes on the phylogenetic tree were different than we would have expected due to chance alone.

All data and code can be found at https://github.com/mkardish/Transplants and sequences have been deposited under the NCBI BioProject ID PRJNA731931.

Acknowledgements

We thank J. Eisen and E. Grosholz for their comments on this manuscript. We thank A. Alexiev for assistance with extractions and A. Firl for assistance in sequencing. We would like to thank the Stachowicz Lab for their expertise and assistance in field work. This work was funded by the UC Davis Center for Population Biology, the National Science Foundation Graduate Research

Fellowship (to M.Kardish), a grant from the Gordon and Betty Moore Foundation (to J. Eisen and JJS), and a grant from the NSF Biological Oceanography program (Grant# OCE 1829992 to JJS) . This work used the Extreme Science and Engineering Discovery Environment (XSEDE) on the Comet at SDSC through an allocation to M. Kardish TG-DEB160008.

References

Abbott, J. M., K. DuBois, R. K. Grosberg, S. L. Williams, and J. J. Stachowicz. 2018. Genetic distance predicts trait differentiation at the subpopulation but not the individual level in eelgrass, *Zostera marina*. Ecology and evolution:1–14.

Avena, C. V., L. W. Parfrey, J. W. Leff, H. M. Archer, W. F. Frick, K. E. Langwig, A. M. Kilpatrick, K. E. Powers, J. T. Foster, and V. J. McKenzie. 2016. Deconstructing the Bat Skin Microbiome: Influences of the Host and the Environment. Frontiers in microbiology 7:1753.

Bengtsson, M. M., A. Bühler, A. Brauer, S. Dahlke, H. Schubert, and I. Blindow. 2017. Eelgrass Leaf Surface Microbiomes Are Locally Variable and Highly Correlated with Epibiotic Eukaryotes. Frontiers in microbiology 8:1312.

Britton, T., C. L. Anderson, D. Jacquet, S. Lundqvist, and K. Bremer. 2007. Estimating divergence times in large phylogenetic trees. Systematic biology 56:741–752.

Callahan, B. J., P. J. McMurdie, M. J. Rosen, A. W. Han, A. J. A. Johnson, and S. P. Holmes. 2016. DADA2: High-resolution sample inference from Illumina amplicon data. Nature methods 13:581–583.

Cavender-Bares, J., D. D. Ackerly, D. A. Baum, and F. A. Bazzaz. 2004a. Phylogenetic overdispersion in Floridian oak communities. The American naturalist 163:823–843.

Cavender-Bares, J., K. Kitajima, and F. A. Bazzaz. 2004b. Multiple trait associations in relation to habitat differentiation among 17 Floridian oak species. Ecological monographs 74:635–662.

Christian, N., B. K. Whitaker, and K. Clay. 2015. Microbiomes: Unifying animal and plant systems through the lens of community ecology theory. Frontiers in microbiology 6:1–15.

Coleman-Derr, D., D. Desgarennes, C. Fonseca-Garcia, S. Gross, S. Clingenpeel, T. Woyke, G. North, A. Visel, L. P. Partida-Martinez, and S. G. Tringe. 2016. Plant compartment and biogeography affect microbiome composition in cultivated and native Agave species. The New phytologist 209:798–811.

Comeau, A. M., G. M. Douglas, and M. G. I. Langille. 2017. Microbiome Helper: a Custom and Streamlined Workflow for Microbiome Research. mSystems 2.

Copeland, J. K., L. Yuan, M. Layeghifard, P. W. Wang, and D. S. Guttman. 2015. Seasonal community succession of the phyllosphere microbiome. Molecular plant-microbe interactions: MPMI 28:274–285.

Cúcio, C., A. H. Engelen, R. Costa, and G. Muyzer. 2016. Rhizosphere Microbiomes of European + Seagrasses Are Selected by the Plant, But Are Not Species Specific. Frontiers in microbiology 7:1–15.

Duarte, C. M. 2002. The future of seagrass meadows. Environmental conservation 29:192–206.

Eriander, L., E. Infantes, M. Olofsson, J. L. Olsen, and P.-O. Moksnes. 2016. Assessing methods for restoration of eelgrass (Zostera marina L.) in a cold temperate region. Journal of experimental marine biology and ecology 479:76–88.

Fahimipour, A. K., M. R. Kardish, J. M. Lang, J. L. Green, J. A. Eisen, and J. J. Stachowicz.

2017. Globalscale structure of the eelgrass microbiome. Applied and environmental microbiology 83.

Fitzgerald, D. B., K. O. Winemiller, M. H. Sabaj Pérez, and L. M. Sousa. 2017. Seasonal changes in the assembly mechanisms structuring tropical fish communities. Ecology 98:21–31.

Fitzpatrick, C. R., J. Copeland, P. W. Wang, D. S. Guttman, P. M. Kotanen, and M. T. J. Johnson. 2018. Assembly and ecological function of the root microbiome across angiosperm plant species. Proceedings of the National Academy of Sciences of the United States of America 115:E1157–E1165.

Fonseca, M. S., J. S. Fisher, J. C. Zieman, and G. W. Thayer. 1982a. Influence of the seagrass, Zostera marina L., on current flow. Estuarine, coastal and shelf science 15:351–364.

Fonseca, M. S., W. J. Kenworthy, and G. W. Thayer. 1982b. A low cost transplanting procedure for sediment stabilization and habitat development using eelgrass (Zosteramarina). Wetlands 2:138–151.

Friedman, J., T. Hastie, and R. Tibshirani. 2010. Regularization paths for generalized linear models via coordinate descent. Journal of statistical software 33:1–22.

Fuhrman, J. A., J. A. Cram, and D. M. Needham. 2015. Marine microbial community dynamics and their ecological interpretation. Nature reviews. Microbiology 13:133–146.

Galushko, A., and J. Kuever. 2021, March 26. Desulfocapsaceae. Wiley.

Glasl, B., C. E. Smith, D. G. Bourne, and N. S. Webster. 2019. Disentangling the effect of host-genotype and environment on the microbiome of the coral Acropora tenuis. PeerJ 7:e6377.

Griffiths, S. M., R. E. Antwis, L. Lenzi, A. Lucaci, D. C. Behringer, M. J. Butler 4th, and R. F.

Preziosi. 2019. Host genetics and geography influence microbiome composition in the sponge Ircinia campana. The Journal of animal ecology 88:1684–1695.

Hammer, T. J., J. G. Sanders, and N. Fierer. 2019. Not all animals need a microbiome. FEMS microbiology letters 366.

Kardish, M. R., and J. J. Stachowicz. 2021, June 1. More than a stick in the mud: Eelgrass leaf and root bacterial communities are distinct from those on physical mimics.

Kembel, S. W., P. D. Cowan, M. R. Helmus, W. K. Cornwell, H. Morlon, D. D. Ackerly, S. P. Blomberg, and C. O. Webb. 2010. Picante: R tools for integrating phylogenies and ecology. Bioinformatics 26:1463–1464.

Kembel, S. W., T. K. O'Connor, H. K. Arnold, S. P. Hubbell, S. J. Wright, and J. L. Green. 2014. Relationships between phyllosphere bacterial communities and plant functional traits in a neotropical forest. Proceedings of the National Academy of Sciences of the United States of America 111:13715–13720.

Kraft, N. J. B., P. B. Adler, O. Godoy, E. C. James, S. Fuller, and J. M. Levine. 2015. Community assembly, coexistence and the environmental filtering metaphor. Functional ecology 29:592–599.

Marzinelli, E. M., A. H. Campbell, E. Zozaya Valdes, A. Vergés, S. Nielsen, T. Wernberg, T. de Bettignies, S. Bennett, J. G. Caporaso, T. Thomas, and P. D. Steinberg. 2015. Continental-scale variation in seaweed host-associated bacterial communities is a function of host condition, not geography. Environmental microbiology 17:4078–4088.

McFall-Ngai, M., M. G. Hadfield, T. C. G. Bosch, H. V. Carey, T. Domazet-Lošo, A. E. Douglas, N. Dubilier, G. Eberl, T. Fukami, S. F. Gilbert, U. Hentschel, N. King, S. Kjelleberg, A. H. Knoll, N. Kremer, S. K. Mazmanian, J. L. Metcalf, K. Nealson, N. E.

Pierce, J. F. Rawls, A. Reid, E. G. Ruby, M. Rumpho, J. G. Sanders, D. Tautz, and J. J. Wernegreen. 2013. Animals in a bacterial world, a new imperative for the life sciences. Proceedings of the National Academy of Sciences of the United States of America 110:3229–3236.

McMurdie, P. J., and S. Holmes. 2013. phyloseq: an R package for reproducible interactive analysis and graphics of microbiome census data. PloS one 8:e61217.

McMurdie, P. J., and S. Holmes. 2014. Waste not, want not: why rarefying microbiome data is inadmissible. PLoS computational biology 10:e1003531.

Miazaki, A. S., M. Gastauer, and J. A. A. Meira-Neto. 2015. Environmental severity promotes phylogenetic clustering in campo rupestre vegetation. Acta botanica Brasilica 29:561–566.

Moore, K. A., and F. T. Short. 2006. Zostera: Biology, Ecology, and Management. Pages 361–386 *in* A. W. D. Larkum, R. J. Orth, and C. M. Duarte, editors. SEAGRASSES: BIOLOGY, ECOLOGYAND CONSERVATION. Springer Netherlands, Dordrecht.

Paradis, E., and K. Schliep. 2019. ape 5.0: an environment for modern phylogenetics and evolutionary analyses in R. Bioinformatics 35:526–528.

Price, M. N., P. S. Dehal, and A. P. Arkin. 2010. FastTree 2--approximately maximum-likelihood trees for large alignments. PloS one 5:e9490.

Quast, C., E. Pruesse, P. Yilmaz, J. Gerken, T. Schweer, P. Yarza, J. Peplies, and F. O. Glöckner. 2013. The SILVA ribosomal RNA gene database project: improved data processing and web-based tools. Nucleic acids research 41:D590–6.

Rothschild, D., O. Weissbrod, E. Barkan, A. Kurilshikov, T. Korem, D. Zeevi, P. I. Costea, A. Godneva, I. N. Kalka, N. Bar, S. Shilo, D. Lador, A. V. Vila, N. Zmora, M. Pevsner-

Fischer, D. Israeli, N. Kosower, G. Malka, B. C. Wolf, T. Avnit-Sagi, M. Lotan-Pompan, A. Weinberger, Z. Halpern, S. Carmi, J. Fu, C. Wijmenga, A. Zhernakova, E. Elinav, and E. Segal. 2018. Environment dominates over host genetics in shaping human gut microbiota. Nature 555:210–215.

Rüger, L., K. Feng, K. Dumack, J. Freudenthal, Y. Chen, R. Sun, M. Wilson, P. Yu, B. Sun, Y. Deng, F. Hochholdinger, D. Vetterlein, and M. Bonkowski. 2021. Assembly Patterns of the Rhizosphere Microbiome Along the Longitudinal Root Axis of Maize (Zea mays L.). Frontiers in microbiology 12:614501.

Russel, J. 2021. Russel88/MicEco: v0.9.15.

Sand-Jensen, K. 1975. Biomass, net production and growth dynamics in an eelgrass (Zostera marina L.) population in Vellerup Vig, Denmark. Ophelia 14:185–201.

Schlechter, R. O., M. Miebach, and M. N. P. Remus-Emsermann. 2019. Driving factors of epiphytic bacterial communities: A review. Journal of advertising research 19:57–65.

Shade, A., P. S. McManus, and J. Handelsman. 2013. Unexpected diversity during community succession in the apple flower microbiome. mBio 4.

Shi, S., E. Nuccio, D. J. Herman, R. Rijkers, K. Estera, J. Li, U. N. da Rocha, Z. He, J. Pett-Ridge, E. L. Brodie, J. Zhou, and M. Firestone. 2015. Successional Trajectories of Rhizosphere Bacterial Communities over Consecutive Seasons. mBio 6:e00746.

Silverman, J. D., A. D. Washburne, S. Mukherjee, and L. A. David. 2017. A phylogenetic transform enhances analysis of compositional microbiota data. eLife 6:1–20.

Trevelline, B. K., S. S. Fontaine, B. K. Hartup, and K. D. Kohl. 2019. Conservation biology needs a microbial renaissance: a call for the consideration of host-associated microbiota in wildlife management practices. Proceedings. Biological sciences / The Royal Society

286:20182448.

Vacher, C., A. Hampe, A. J. Porté, U. Sauer, S. Compant, and C. E. Morris. 2016. The Phyllosphere: Microbial Jungle at the Plant–Climate Interface. Annual review of ecology, evolution, and systematics 47:1–24.

Vieira, S., J. Sikorski, S. Dietz, K. Herz, M. Schrumpf, H. Bruelheide, D. Scheel, M. W. Friedrich, and J. Overmann. 2020. Drivers of the composition of active rhizosphere bacterial communities in temperate grasslands. The ISME journal 14:463–475.

Wagner, M. R., D. S. Lundberg, T. G. Del Rio, S. G. Tringe, J. L. Dangl, and T. Mitchell-Olds. 2016. Host genotype and age shape the leaf and root microbiomes of a wild perennial plant. Nature communications 7:12151.

Walters, W., E. R. Hyde, D. Berg-Lyons, G. Ackermann, G. Humphrey, A. Parada, J. A. Gilbert, J. K. Jansson, J. G. Caporaso, J. A. Fuhrman, A. Apprill, and R. Knight. 2016. Improved Bacterial 16S rRNA Gene (V4 and V4-5) and Fungal Internal Transcribed Spacer Marker Gene Primers for Microbial Community Surveys. mSystems 1.

Wang, L., M. K. English, F. Tomas, and R. S. Mueller. 2020, April 23. Recovery and Community Succession of the Zostera marina Rhizobiome After Transplantation.

Webb, C. O. 2000. Exploring the Phylogenetic Structure of Ecological Communities: An Example for Rain Forest Trees. The American naturalist 156:145–155.

Webb, C. O., D. D. Ackerly, and S. W. Kembel. 2008. Phylocom: software for the analysis of phylogenetic community structure and trait evolution. Bioinformatics 24:2098–2100.

Webb, C. O., D. D. Ackerly, M. A. McPeek, and M. J. Donoghue. 2002. Phylogenies and Community Ecology. Annual review of ecology and systematics 33:475–505.

Weigel, B. L., and P. M. Erwin. 2017. Effects of reciprocal transplantation on the microbiome

and putative nitrogen cycling functions of the intertidal sponge, Hymeniacidon heliophila. Scientific reports 7:43247.

Weiher, E., and P. A. Keddy. 1995. The Assembly of Experimental Wetland Plant Communities. Oikos 73:323–335.

Whitman, T., R. Neurath, A. Perera, I. Chu-Jacoby, D. Ning, J. Zhou, P. Nico, J. Pett-Ridge, and M. Firestone. 2018. Microbial community assembly differs across minerals in a rhizosphere microcosm. Environmental microbiology 20:4444–4460.

Wright, E. S. 2015. DECIPHER: harnessing local sequence context to improve protein multiple sequence alignment. BMC bioinformatics 16:322.

Zhou, Y., P. Liu, B. Liu, X. Liu, X. Zhang, F. Wang, and H. Yang. 2014. Restoring eelgrass (Zostera marina L.) habitats using a simple and effective transplanting technique. PloS one 9:e92982.

Ziegler, M., C. G. B. Grupstra, M. M. Barreto, M. Eaton, J. BaOmar, K. Zubier, A. Al-Sofyani, A. J. Turki, R. Ormond, and C. R. Voolstra. 2019. Coral bacterial community structure responds to environmental change in a host-specific manner. Nature communications 10:3092.

Figures and Tables

Figure 2.1: Map of reciprocal transplant sites in Bodega Harbor, Bodega Bay, CA. All experimental eelgrass were transplanted existing eelgrass beds. Campbell Cove (CC) is the site closest to the mouth of the harbor and a mean temperature of 15.8˚C during our experiment. Doran Beach (DB) is the least impacted by human activities in the harbor (farther from clamming) and had a mean temperature of 15.9˚C during our experiment. Mason's Marina (MM) has finer grained sediment than other sites and is a restored site with patchier seagrass growth; in other experiments its temperature profile has been intermediate between the cooler sites and DB (HOBO logger at this site was lost). Westside Park (WP) had a mean temperature of 16.3˚C during our experiment and is used for many seagrass experiments within Bodega Harbor.

Figure 2.2: Here we show differences in leaf microbial communities among destination sites. Destination sites are indicated by different colors and ellipses; from darkest to lightest, they are Mason's Marina (MM), Campbell Cove (CC), Doran Beach (DB), and Westside Park (WP). (A-C) Ordination of leaf bacterial community structure based on principal coordinate analysis of phylogenetic-isometric log-ratio transformed distances. (A) shows differences among sites by destination site after one month, (B) after two months, and (C) after 3 months. All destination sites were distinct from others at all three timepoints (see Table 2.1). (D-F) Mean amplicon sequence variant (ASV) richness on leaves at each site by time point. Here, we plot means and standard errors. After one month (D), there were no differences in richness among destination sites, after two months (E), WP had the highest richness and DB the lowest, and after three months (F), WP had a higher richness than plants at each other destination site.

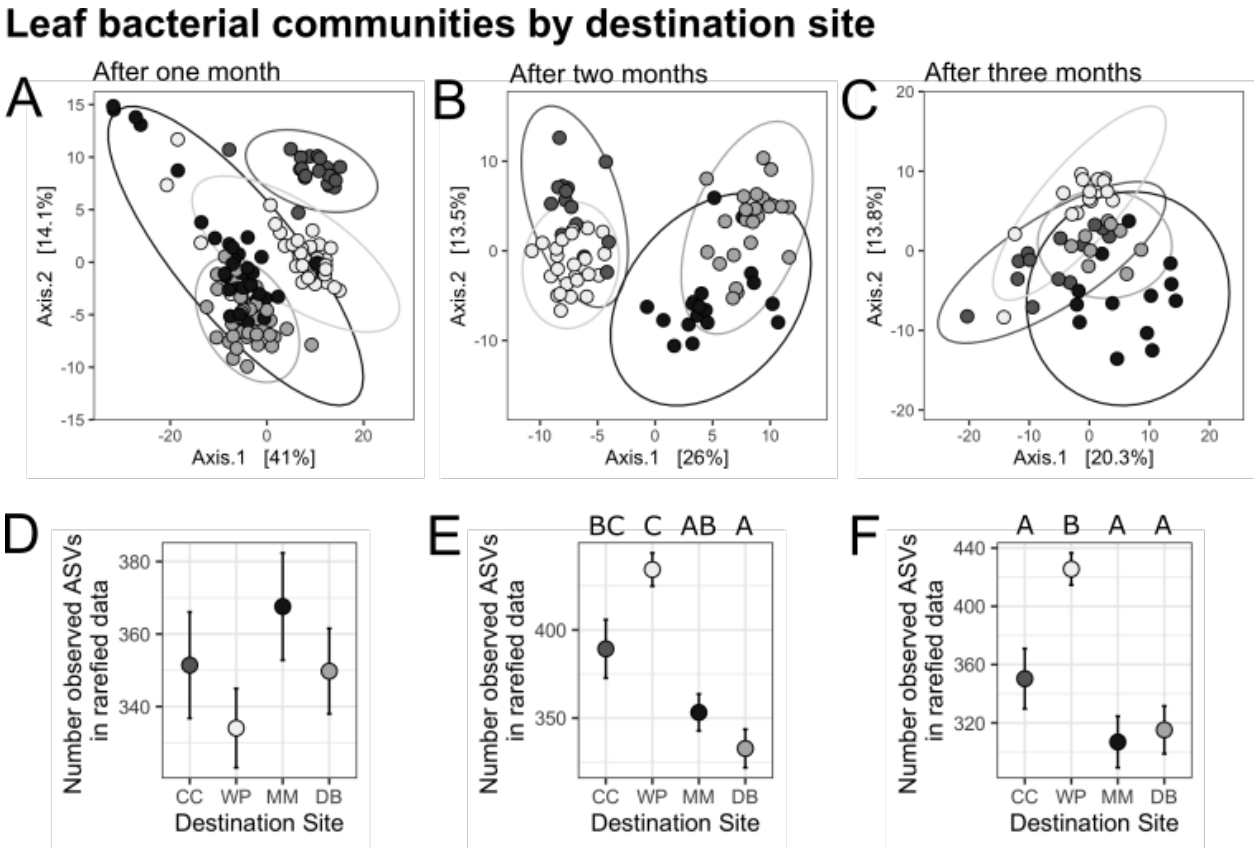

Figure 2.3: Here, we show differences in root microbial communities among destination sites. Destination sites are indicated by different colors and ellipses; from darkest to lightest, they are Mason's Marina (MM), Campbell Cove (CC), Doran Beach (DB), and Westside Park (WP). (A-C) 3-D ordination of root bacterial community structure based on principal coordinate analysis of phylogenetic-isometric log-ratio transformed distances. (A) shows differences among sites by destination site after one month, (B) after two months, and (C) after 3 months. All destination sites were distinct from others at all three timepoints (see Table 2.2). (D-F) Mean amplicon sequence variant (ASV) richness on roots at each site by time point. Here, we plot means and standard errors. After one month and three months (D & F), there were no differences in richness among destination sites, and after two months (E), WP had the highest richness, CC and MM the lowest, and DB was intermediate.

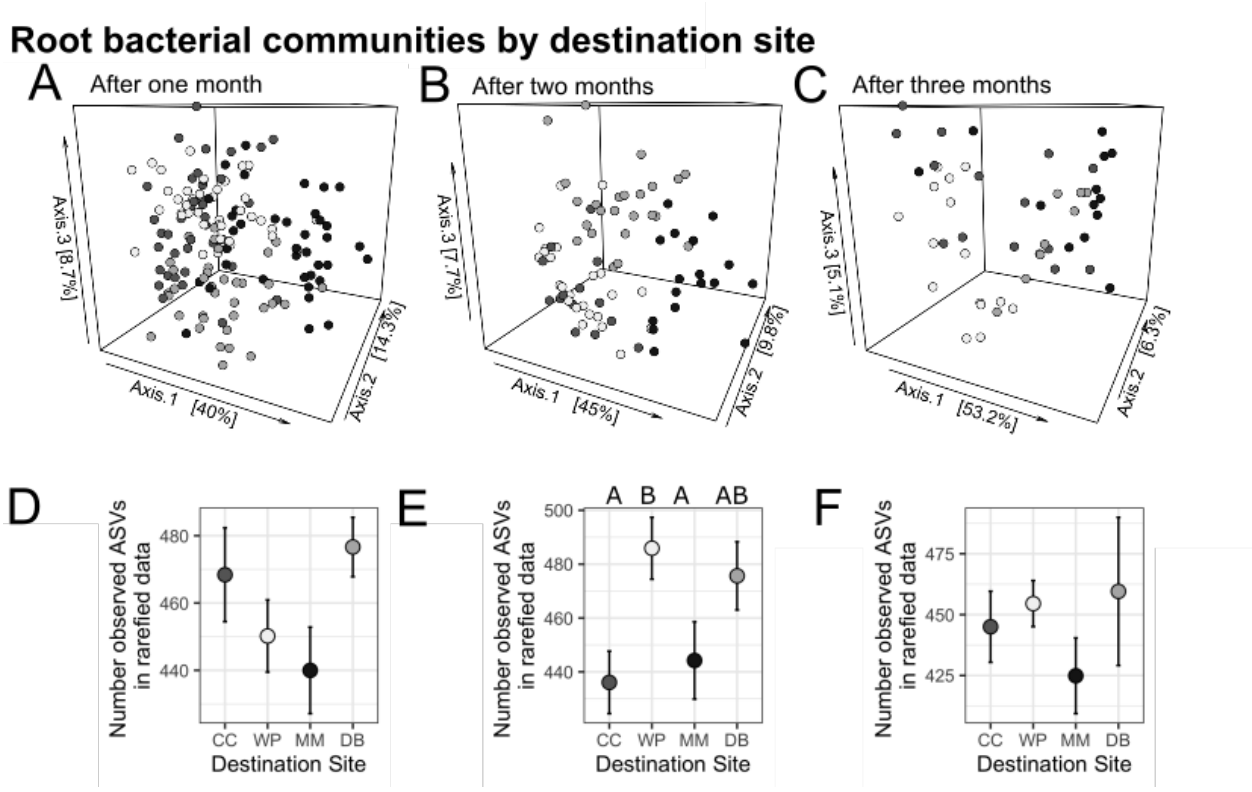

Figure 2.4: Across different months, we found different levels of leaf microbial community clustering by destination site across one (A), two (B), and three (C) months. Here, we plot the mean and standard error of the Net Relatedness Index (NRI) from each site. Destination sites are indicated by different colors and ellipses; from darkest to lightest, they are Mason's Marina (MM), Campbell Cove (CC), Doran Beach (DB), and Westside Park (WP). A positive NRI indicates that communities at a site are phylogenetically clustered, a negative NRI indicates that a community is phylogenetically overdispersed. If a communities NRI is significantly different from zero, we placed a box around the site name (see Supplemental Table 2.S5 for more detailed statistics). We found that different sites had different degrees of clustering in leaf microbial communities and that that varied across time.

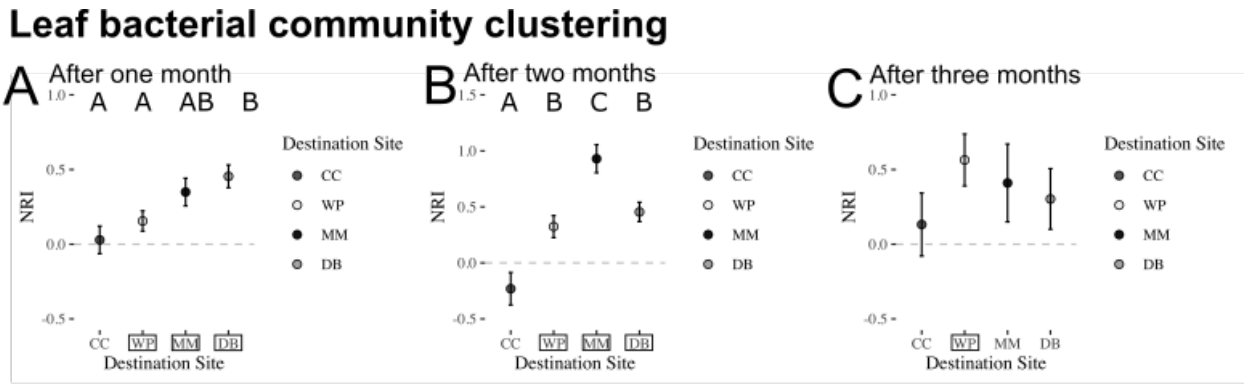

Figure 2.5: Across different months, we found similar patterns of community clustering in root microbial communities by destination site across one (A), two (B), and three (C) months. Here, we plot the mean and standard error of the Net Relatedness Index (NRI) from each site. Destination sites are indicated by different colors and ellipses; from darkest to lightest, they are Mason's Marina (MM), Campbell Cove (CC), Doran Beach (DB), and Westside Park (WP). A positive NRI indicates that communities at a site are phylogenetically clustered, a negative NRI indicates that a community is phylogenetically overdispersed. If a communities NRI is significantly different from zero, we placed a box around the site name (see Supplemental Table 2.S5 for more detailed statistics).

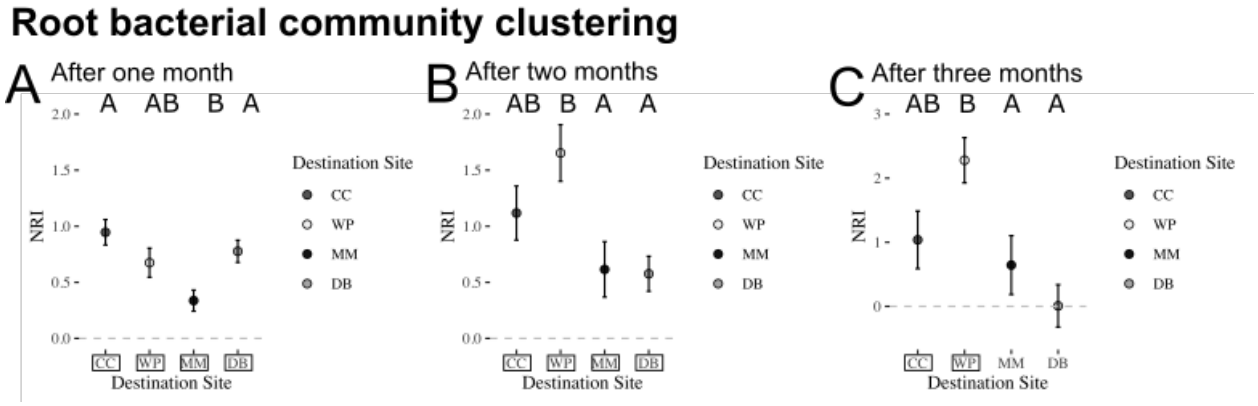

Figure 2.6: As our results indicated that microbial communities varied primarily at a family level or finer, we examined which families varied within plant compartments among sites. We then compared families that varied in leaves among sites to those among roots. We found the families that differed in leaves were different than those that varied in roots (Fisher's Exact Test $p<0.001$, Figure 2.6). There were a few families that varied among sites in both compartments, but most families that varied among sites were specific to leaves or roots.

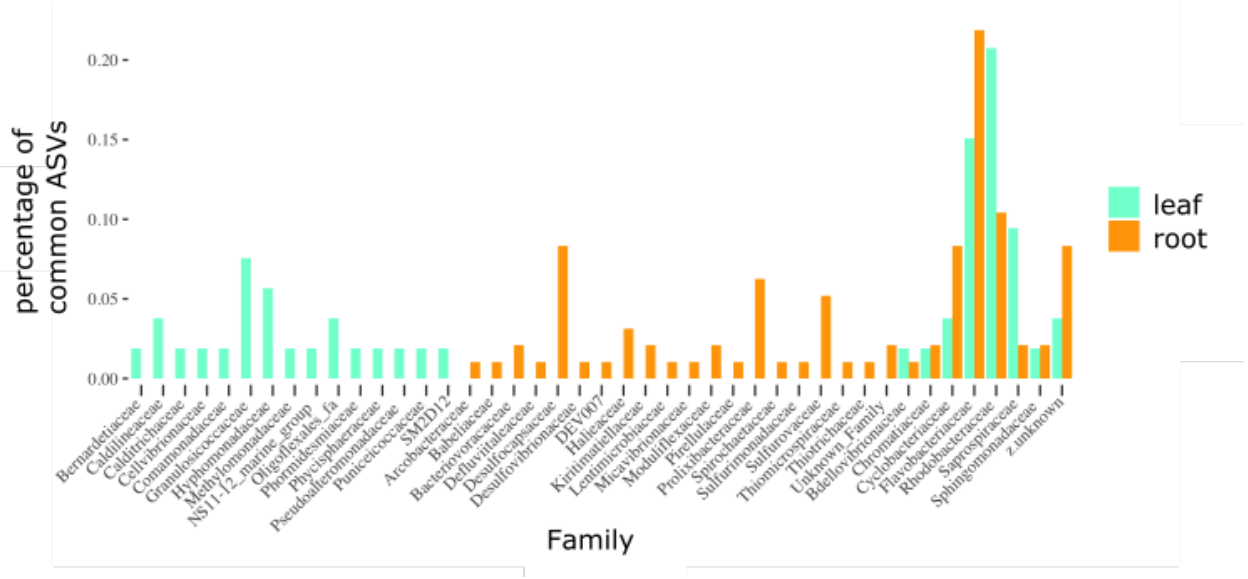

Figure 2.7: Leaf microbiomes were indistinguishable between transplant controls and undisturbed plants at any time point and retained the among-site differences described in Figure 2.2. Root microbiomes were distinct between transplant controls and undisturbed plants at all time points, while both transplanted and undisturbed root microbiomes demonstrated differences among sites. Undisturbed microbial communities are in light gray and transplanted microbial communities are in dark gray. Circles are microbial communities from Campbell Cove (CC), squares are microbial communities from Doran Beach (DB), triangles are microbial communities from Westside Park (WP), and diamonds are microbial communities from Mason's Marina (MM). (A-C) Ordination of leaf bacterial community structure based on principal coordinate analysis of phylogenetic-isometric log-ratio transformed distances. (A) shows differences among disturbed and undisturbed after one month, (B) after two months, and (C) after 3 months. (D-F) Ordination of root bacterial community structure based on principal coordinate analysis of phylogenetic-isometric log-ratio transformed distances. (D) shows differences among disturbed and undisturbed after one month, (E) after two months, and (F) after 3 months.

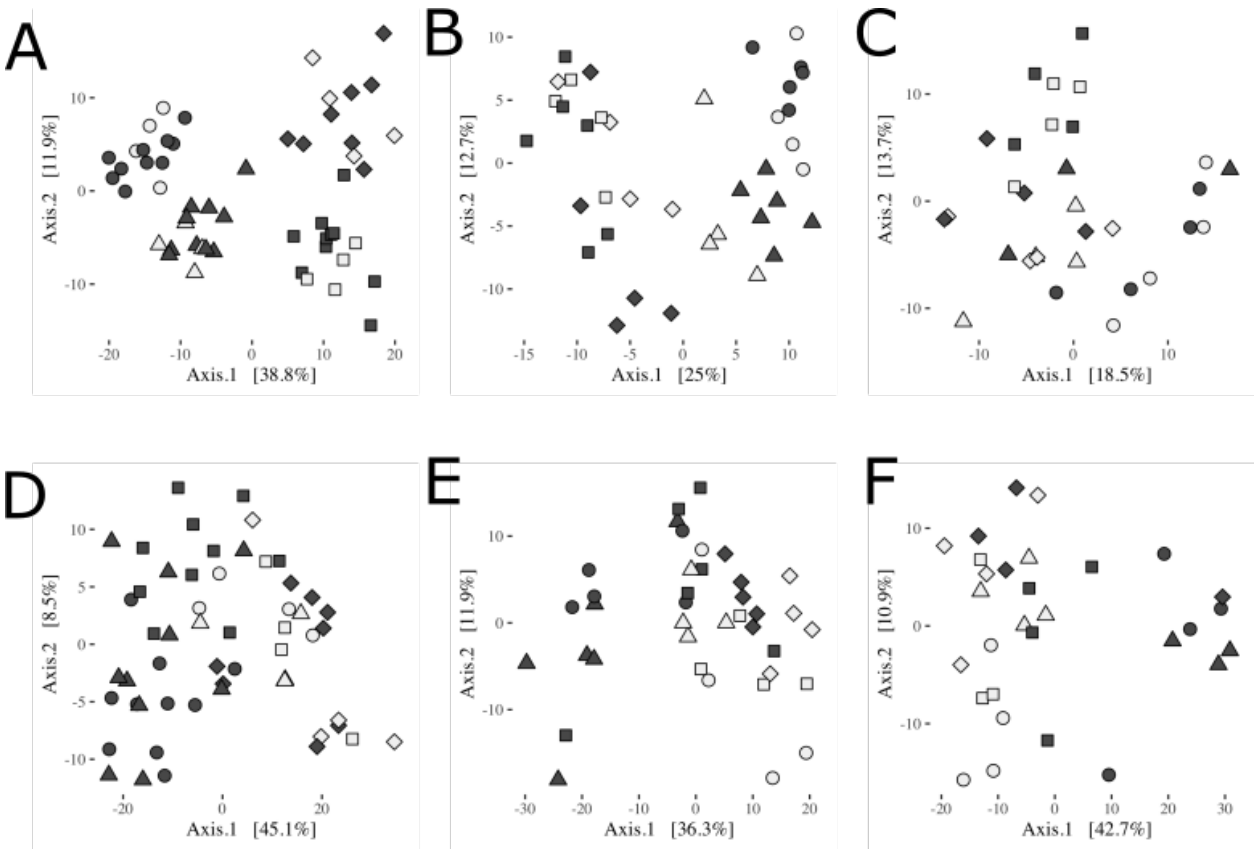
A
Axis.2 [11.9%]
Axis.1 [38.8%]
B
Axis.2 [12.7%]
Axis.1 [25%]
C
Axis.2 [13.7%]
Axis.1 [18.5%]
D
Axis.2 [8.5%]
Axis.1 [45.1%]
E
Axis.2 [11.9%]
Axis.1 [36.3%]
F
Axis.2 [10.9%]
Axis.1 [42.7%]

Table 2.1: Results of PERMANOVA indicating differences among transplanted leaf microbial communities.

		df	**Sum Of Squares**	**R^2**	**F-Statistic**	**Pr(>F)**
Timepoint 1	Destination Site	3	9433.009	0.312	20.302	**0.001**
	Origin Site	3	1050.953	0.035	2.262	**0.009**
	Destination : Origin	7	1760.358	0.058	1.624	**0.015**
	Residual	116	17966.060	0.595	NA	NA
	Total	129	30210.379	1	NA	NA
Timepoint 2	Destination Site	3	6100.417	0.371	14.782	**0.001**
	Origin Site	3	511.728	0.031	1.240	0.174
	Destination : Origin	9	1157.904	0.070	0.935	0.66
	Residual	63	8666.808	0.527	NA	NA
	Total	78	16436.857	1	NA	NA
Timepoint 3	Destination Site	3	3759.551	0.289	6.242	**0.001**
	Origin Site	3	652.923	0.050	1.084	0.301
	Destination : Origin	8	1573.425	0.121	0.980	0.547
	Residual	35	7026.486	0.540	NA	NA
	Total	49	13012.385	1	NA	NA

Table 2.2: Results of PERMANOVA showing differences among transplanted root microbial communities.

		df	Sum Of Squares	R^2	F-Statistic	Pr(>F)
Timepoint 1	Destination Site	3	12417.762	0.259	18.196	**0.001**
	Origin Site	3	1235.735	0.026	1.811	**0.036**
	Destination : Origin	9	3086.977	0.064	1.508	**0.016**
	Residual	137	31164.382	0.651	NA	NA
	Total	152	47904.856	1	NA	NA
Timepoint 2	Destination Site	3	11414.239	0.371	14.552	**0.001**
	Origin Site	3	600.808	0.020	0.766	0.704
	Destination : Origin	9	2295.097	0.075	0.975	0.49
	Residual	63	16472.277	0.535	NA	NA
	Total	78	30782.421	1	NA	NA
Timepoint 3	Destination Site	3	8991.433	0.360	8.760	**0.001**
	Origin Site	3	838.248	0.034	0.817	0.601
	Destination : Origin	8	2854.077	0.114	1.043	0.4
	Residual	36	12317.357	0.493	NA	NA
	Total	50	25001.115	1	NA	NA

Table 2.3: Results of PERMANOVA showing differences among based on variation in transplant status.

		df	Sum Of Squares	R^2	F-Statistic	Pr(>F)
Timepoint 1	Site	3	10979.408	0.511	18.072	**0.001**
	Transplant Status	1	370.765	0.017	1.831	0.091
	Destination Site:Transplant Status	3	819.616	0.038	1.349	0.145
	Residual	46	9315.596	0.434	NA	NA
	Total	53	21485.385	1	NA	NA
Timepoint 2	Site	3	4093.618	0.349	6.359	**0.001**
	Transplant Status	1	282.124	0.024	1.315	0.158
	Site:Transplant Status	3	930.523	0.079	1.446	0.052
	Residual	30	6437.063	0.548	NA	NA
	Total	37	11743.328	1	NA	NA
Timepoint 3	Site	3	2938.888	0.279	3.559	**0.001**
	Transplant Status	1	413.074	0.039	1.501	0.08
	Site:Transplant Status	3	848.899	0.081	1.028	0.407
	Residual	23	6331.219	0.601	NA	NA
	Total	30	10532.080	1	NA	NA

Table 2.4: Results of PERMANOVA showing differences among based on variation in transplant status in roots.

		df	Sum Of Squares	R^2	F-Statistic	Pr(>F)
Timepoint 1	Site	3	7249.876	0.261	7.602	**0.001**
	Transplant Status	1	4336.789	0.156	13.643	**0.001**
	Site : Transplant Status	3	1605.829	0.058	1.684	0.056
	Residual	46	14622.473	0.526	NA	NA
	Total	53	27814.967	1	NA	NA
Timepoint 2	Site	3	4772.688	0.245	4.608	**0.001**
	Transplant Status	1	2723.638	0.140	7.888	**0.001**
	Site : Transplant Status	3	1596.102	0.082	1.541	0.081
	Residual	30	10358.056	0.533	NA	NA
	Total	37	19450.484	1	NA	NA
Timepoint 3	Site	3	3191.330	0.183	2.797	**0.003**
	Transplant Status	1	4062.769	0.233	10.682	**0.001**
	Site : Transplant Status	3	1788.470	0.103	1.567	0.08
	Residual	22	8367.592	0.481	NA	NA
	Total	29	17410.161	1	NA	NA

Supplemental Table 2.S1A: P-values from pairwise PERMANOVA of leaf samples at T1 testing the effects of destination site at particular destination sites. All values are fdr-correct and bold values are significant at 0.05 after a correction.

	from CC	from DB	from MM	from WP
CC and DB	**0.0018**	**0.0018**	NA	NA
CC and MM	**0.0018**	**0.0018**	NA	NA
CC and WP	**0.0018**	**0.0018**	NA	NA
DB and MM	**0.0018**	**0.0018**	**0.0018**	**0.0245**
DB and WP	**0.0018**	**0.0018**	**0.0018**	**0.0018**
MM and WP	**0.0018**	**0.0018**	**0.026**	**0.0267**

Supplemental Table 2.S1B: R^2 from pairwise PERMANOVA of leaf samples at T1 testing the effects of destination site at particular origin sites. Bold values were significant after fdr-correction (see Supplemental Table 2.S1A for p-values)

	from CC	from DB	from MM	from WP
CC and DB	**0.607**	**0.452**	NA	NA
CC and MM	**0.521**	**0.406**	NA	NA
CC and WP	**0.339**	**0.215**	NA	NA
DB and MM	**0.214**	**0.231**	**0.278**	**0.123**
DB and WP	**0.484**	**0.334**	**0.201**	**0.348**
MM and WP	**0.416**	**0.31**	**0.174**	**0.139**

Supplemental Table 2.S2A: P-values from pairwise PERMANOVA of leaf samples at T1 testing the effects of origin site at particular destination sites. All values are fdr-correct and bold values are significant at 0.05 after a correction.

	to CC	to DB	to MM	to WP
CC and DB	0.0944	0.1356	0.4216	0.3628
CC and MM	NA	**0.0035**	**0.026**	0.0519
CC and WP	NA	0.2027	0.0829	0.2493
DB and MM	NA	**0.0068**	0.0546	0.0931
DB and WP	NA	0.856	0.0735	0.1003
MM and WP	NA	0.22	0.0787	0.0768

Supplemental Table 2.S2B: R^2 from pairwise PERMANOVA of leaf samples at T1 testing the effects of origin site at particular destination sites. Bold values were significant after fdr-correction (see Supplemental Table 2.S1A for p-values)

	to CC	to DB	to MM	to WP
CC and DB	0.083	0.067	0.051	0.06
CC and MM	NA	**0.131**	**0.097**	0.163
CC and WP	NA	0.07	0.102	0.066
DB and MM	NA	**0.098**	0.137	0.122
DB and WP	NA	0.038	0.129	0.078
MM and WP	NA	0.067	0.107	0.139

Supplemental Table 2.S3A: P-values from pairwise PERMANOVA of root samples at T1 testing the effects of destination site at particular origin sites. All values are fdr-correct and bold values are significant at 0.05 after a correction.

	from CC	from DB	from MM	from WP
CC and DB	**0.0027**	**0.0027**	**0.0094**	**0.006**
CC and MM	**0.0027**	**0.0027**	**0.0027**	**0.0027**
CC and WP	**0.006**	**0.006**	**0.0048**	**0.0162**
DB and MM	**0.0027**	**0.0027**	**0.0048**	**0.0103**
DB and WP	**0.0048**	**0.0027**	**0.0103**	**0.0027**
MM and WP	**0.0027**	**0.0103**	**0.0027**	**0.0027**

Supplemental Table 2.S3B: R^2 from pairwise PERMANOVA of root samples at T1 testing the effects of destination site at particular origin sites. Bold values were significant after fdr-correction (see Supplemental Table 2.S3A for p-values)

	from CC	from DB	from MM	from WP
CC and DB	**0.287**	**0.208**	**0.175**	**0.254**
CC and MM	**0.42**	**0.295**	**0.43**	**0.376**
CC and WP	**0.187**	**0.172**	**0.135**	**0.137**
DB and MM	**0.352**	**0.26**	**0.291**	**0.218**
DB and WP	**0.213**	**0.195**	**0.188**	**0.282**
MM and WP	**0.213**	**0.173**	**0.418**	**0.375**

Supplemental Table 2.S4A: P-values from pairwise PERMANOVA of root samples at T1 testing the effects of origin site at particular destination sites. All values are fdr-correct and bold values are significant at 0.05 after a correction.

	to CC	to DB	to MM	to WP
CC and DB	0.4189	0.3727	0.5369	0.456
CC and MM	*0.0747*	0.2437	**0.0385**	0.1404
CC and WP	**0.0189**	0.3826	0.2808	**0.042**
DB and MM	**0.046**	0.759	**0.046**	0.2175
DB and WP	*0.0518*	0.6071	0.3353	**0.015**
MM and WP	0.4757	0.5126	**0.0077**	**0.046**

* Note: Many of the p-values varied slightly between different permutations of data. We've highlighted sets here that were close to significance after correction as their variance allows us to best understand the community patterns.

Supplemental Table 2.S4B: R^2 from pairwise PERMANOVA of root samples at T1 testing the effects of origin site at particular destination sites. Bold values were significant after fdr-correction (see Supplemental Table 4A for p-values)

	to CC	to DB	to MM	to WP
CC and DB	0.287	0.208	0.175	0.254
CC and MM	*0.42*	0.295	**0.43**	0.376
CC and WP	**0.187**	0.172	0.135	**0.137**
DB and MM	**0.352**	0.26	**0.291**	0.218
DB and WP	*0.213*	0.195	0.188	**0.282**
MM and WP	0.213	0.173	**0.418**	**0.375**

Supplemental Table 2.S5: Do the calculated Net Relatedness Index (NRI) values differ from zero by time point and site? Here a significant p-value indicates that a site has an NRI are significantly different from zero. In our case, all of these indicate clustered communities at a site (see Figures 2.4 and 2.5).

Sample Type	Time	Site	p-value NRI
Leaf	1	CC	0.762
		DB	**<0.001**
		MM	**0.001**
		WP	**0.028**
	2	CC	0.135
		DB	**<0.001**
		MM	**<0.001**
		WP	**0.003**
	3	CC	0.544
		DB	0.174
		MM	0.142
		WP	**0.006**
Root	1	CC	**<0.001**
		DB	**<0.001**
		MM	**0.001**
		WP	**<0.001**
	2	CC	**<0.001**
		DB	**0.001**
		MM	**0.024**
		WP	**<0.001**
	3	CC	**0.038****
		DB	0.984
		MM	0.186
		WP	**<0.001**

** ns after fdr correction

Supplemental Table 2.S7: Temperature and other notes about site characteristics.

	Campbell Cove (CC)	**Westside Park (WP)**	**Mason's Marina (MM)**	**Doran Beach (DB)**
Temperature summer 2015 (7/8 -9/23) ˚C mean +/- SD range *Measured in this study*	15.86 +/- 1.21 12.5 - 19.66	16.27 +/- 1.24 12.4 - 20.62	N/A (HOBO data collector lost)	18.07 +/- 1.38 14.42 - 21.76
Temperature summer 2019 (7/17 - 8/30) ˚C mean +/- SD range *Stachowicz unpublished data*	14.86 +/- 1.57 10.59 - 18.83	15.34 +/- 1.56 10.34 - 21.11	15.81 +/- 1.48 12.44 - 18.83	N/A (not measured in this study)
Other site notes	Closest to mouth of the harbor, high flow, sandy sediment	Site of many eelgrass experiments at Bodega Bay	Restored site, finer sediment grain size	Furthest from clamming activity

Supplemental Table 2.S6: Are nodes that are significantly different among sites more or less phylogenetically shallow than expected by chance? Red is the observed distribution of tip placement as shown in Figures 2.S2-2.S7, black is the null distribution based on all nodes present in samples at those time points. Only roots at T2 and T3 show slightly less than expected. All distances are log-normalized.

Sample Type	Time		t-test
Leaf	1	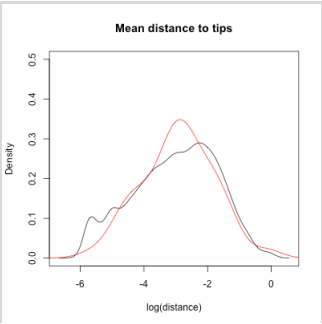	t = - 0.81862, df = 88.148, p-value = 0.415
	2	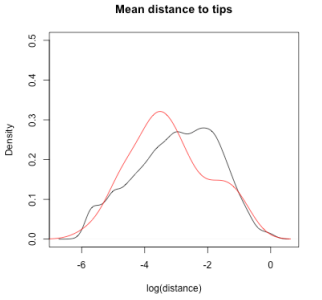	t = 1.2126, df = 39.488, p-value = 0.2325
	3	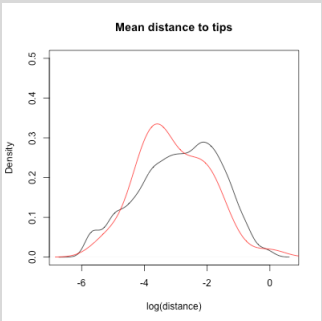	t = 1.1535, df = 46.008, p-value = 0.2547
Root	1	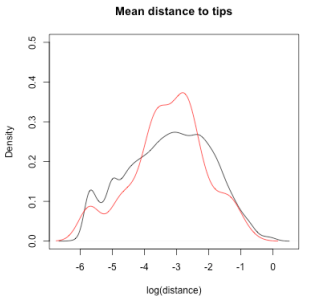	t = 0.18297, df = 68.81, p-value = 0.8554

	2	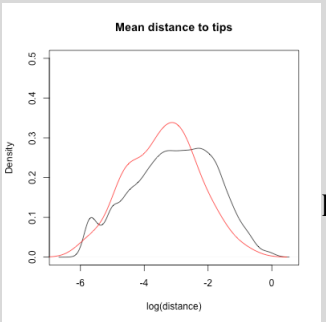	**t = 2.2451, df = 54.835, p-value = 0.02881**
	3	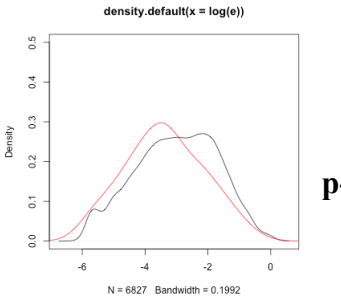	**t = 2.3334, df = 45.165, p-value = 0.02414**

Supplemental information on balances

Leaf microbial balances contained between 2 and 9241 ASVs; Root balances contained between 2 and 478 ASVs.

Supplemental Figure 2.S1 Each balance identified here is a single node in the tree of microbial communities where one site was differentially weighted compared to all other sites. Here for this node within the bacterial family Cyclobacteriaceae, CC has two ASVs in this family upweighted compared to the seven ASVs on the other side of the node. All other sites had higher relative abundance of the ASVs on the other side of the node.

Supplemental Figure 2.S2: After one month, we identified 14 balances distinguishing leaf bacterial communities at CC, 15 balances at DB, 35 at MM and 27 at WP.

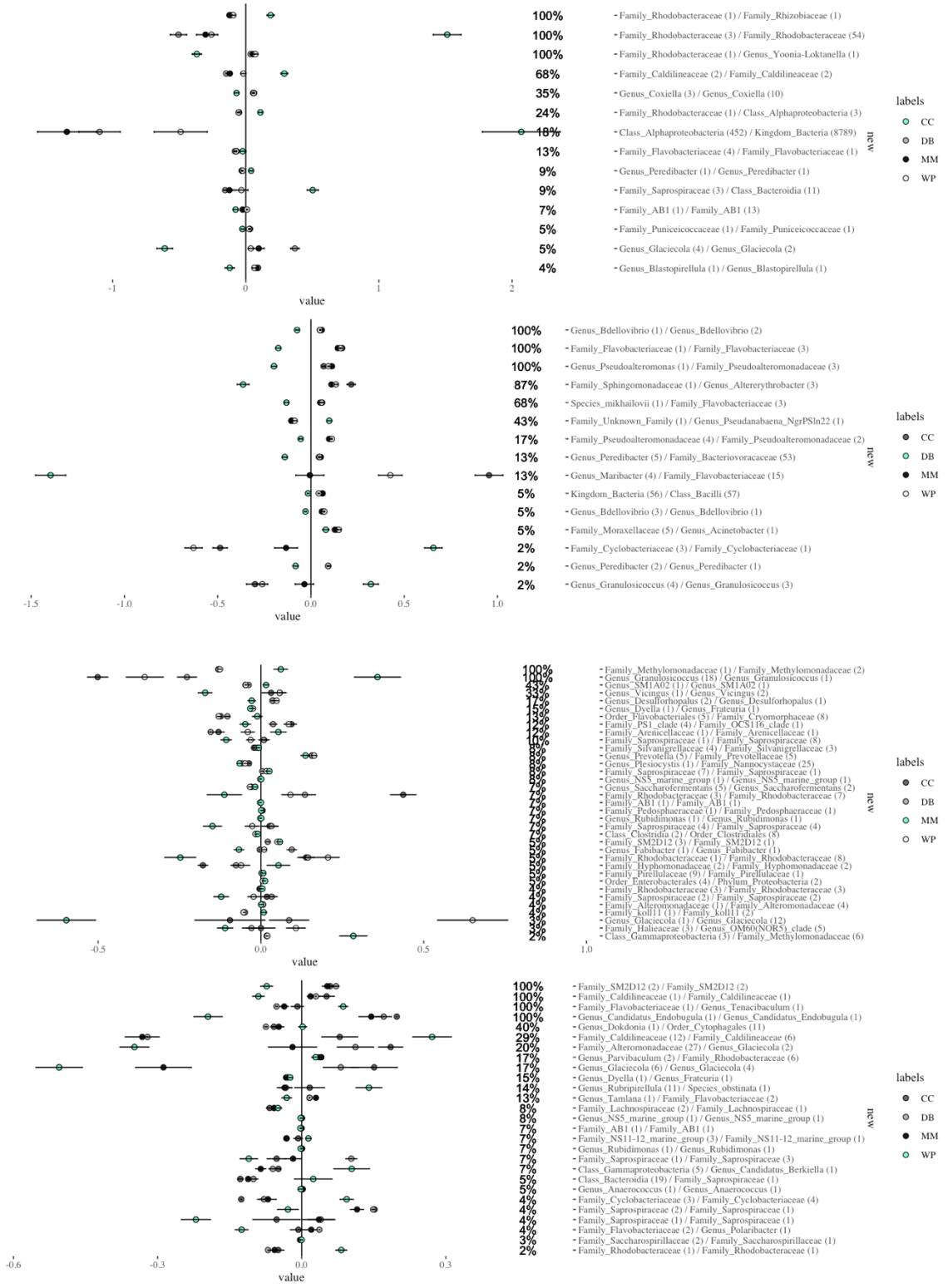

Supplemental Figure 2.S3: After two months, we identified 9 balances distinguishing leaf bacterial communities at CC, 11 balances at DB, 11 at MM and 9 at WP.

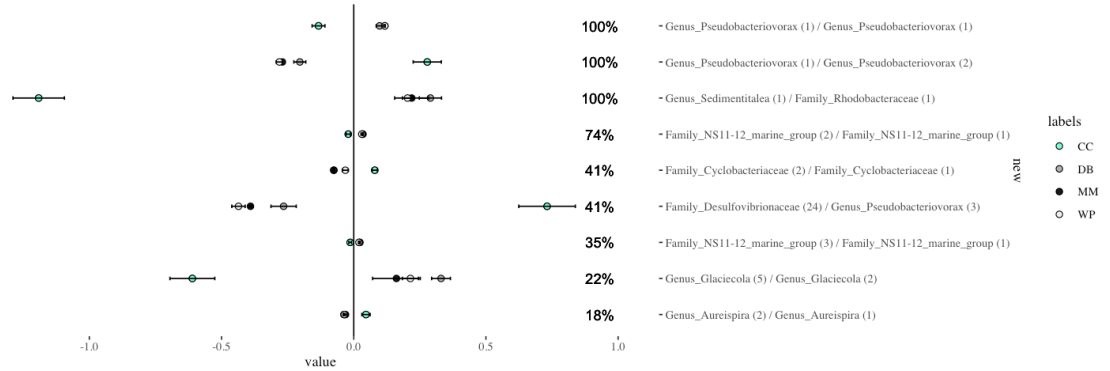

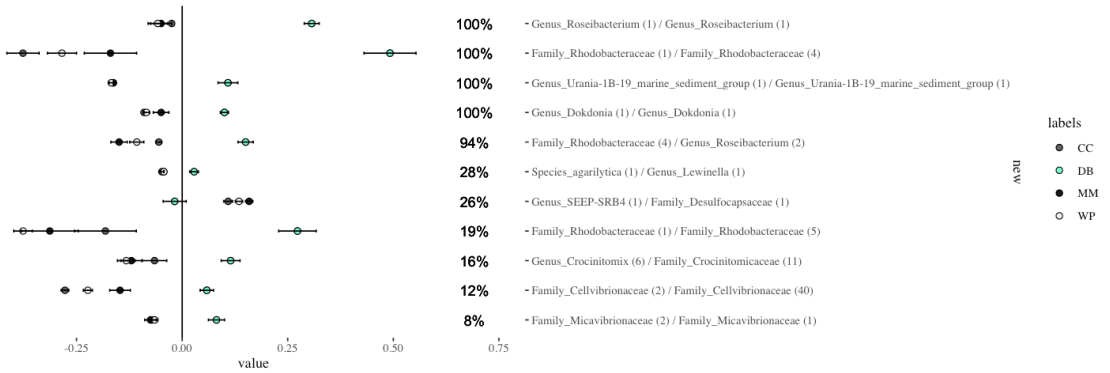

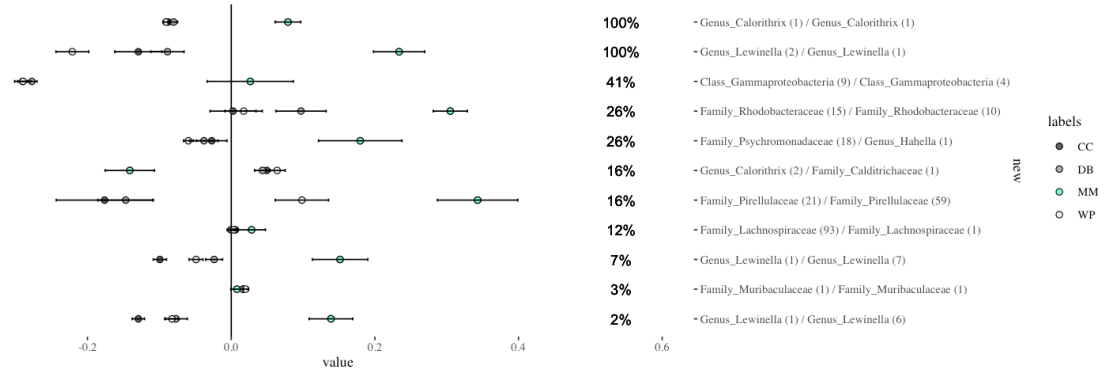

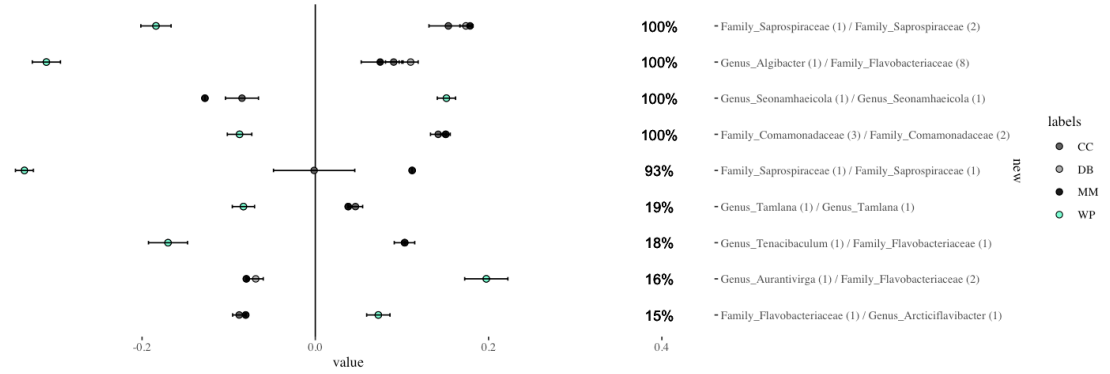

Supplemental Figure 2.S4: After three months, we identified 8 balances distinguishing leaf bacterial communities at CC, 11 balances at DB, 16 at MM and 11 at WP.

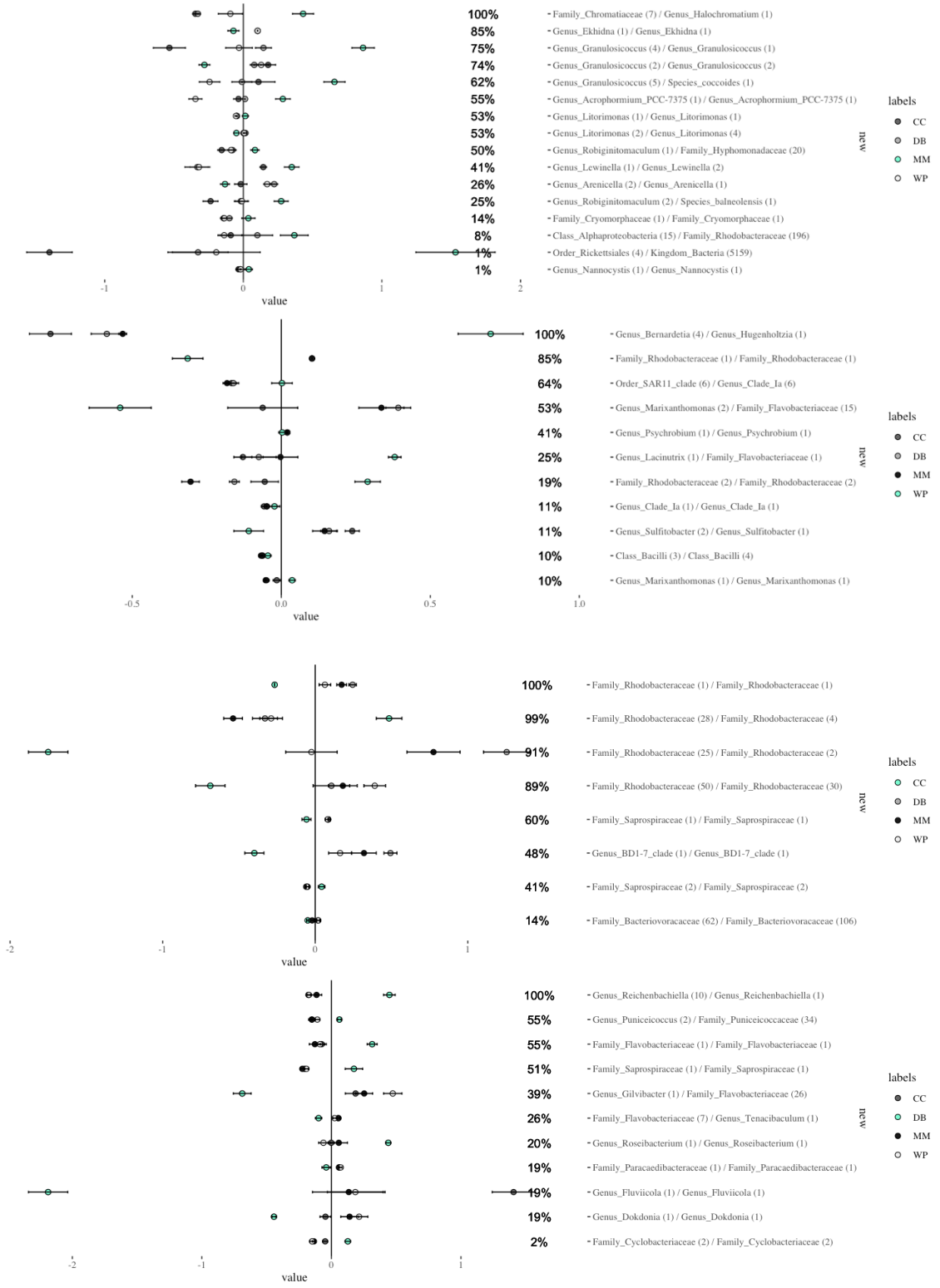

Supplemental Figure 2.S5: In roots, after one month, we identified 17 balances distinguishing root bacterial communities at CC, 10 balances at DB, 23 at MM and 20 at WP.

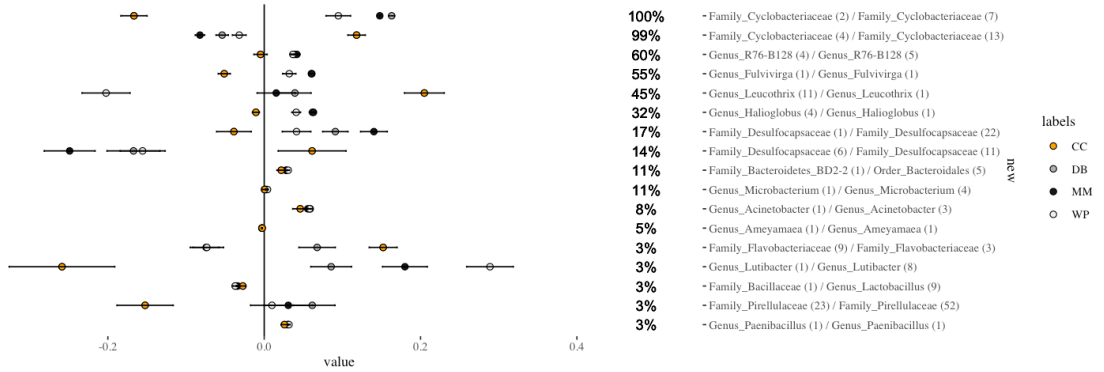

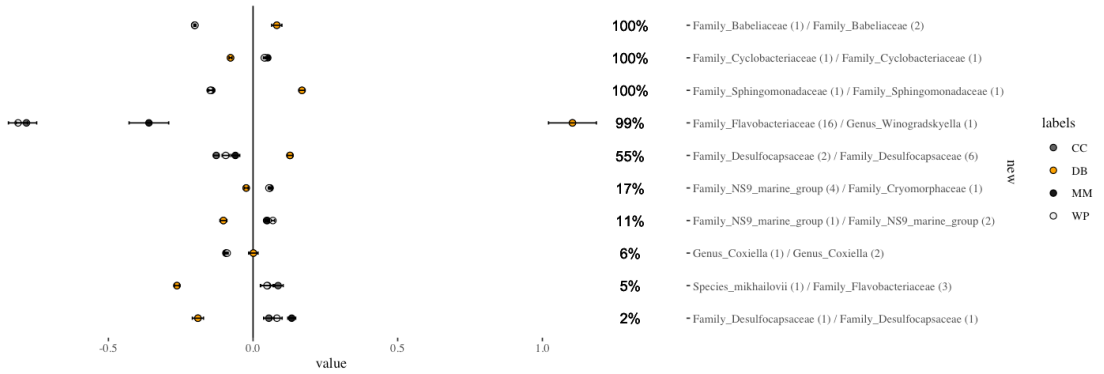

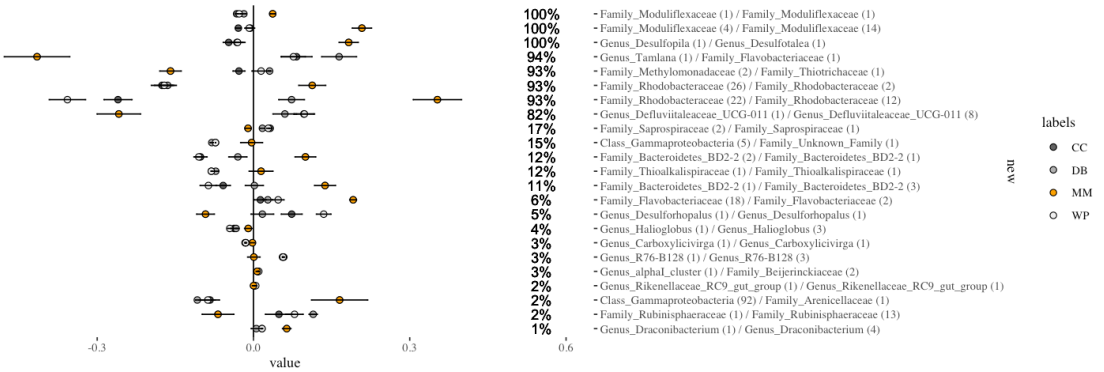

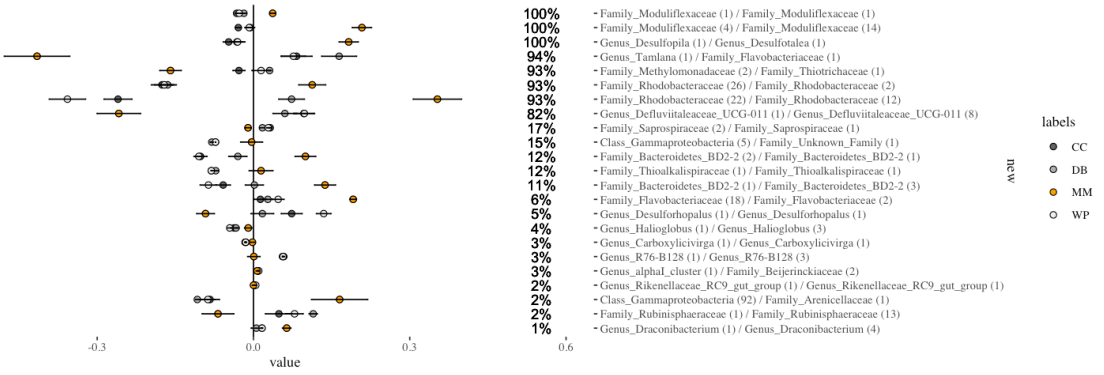

Supplemental Figure 2.S6: After two months, we identified 21 balances distinguishing leaf bacterial communities at CC, 10 balances at DB, 18 at MM and 6 at WP.

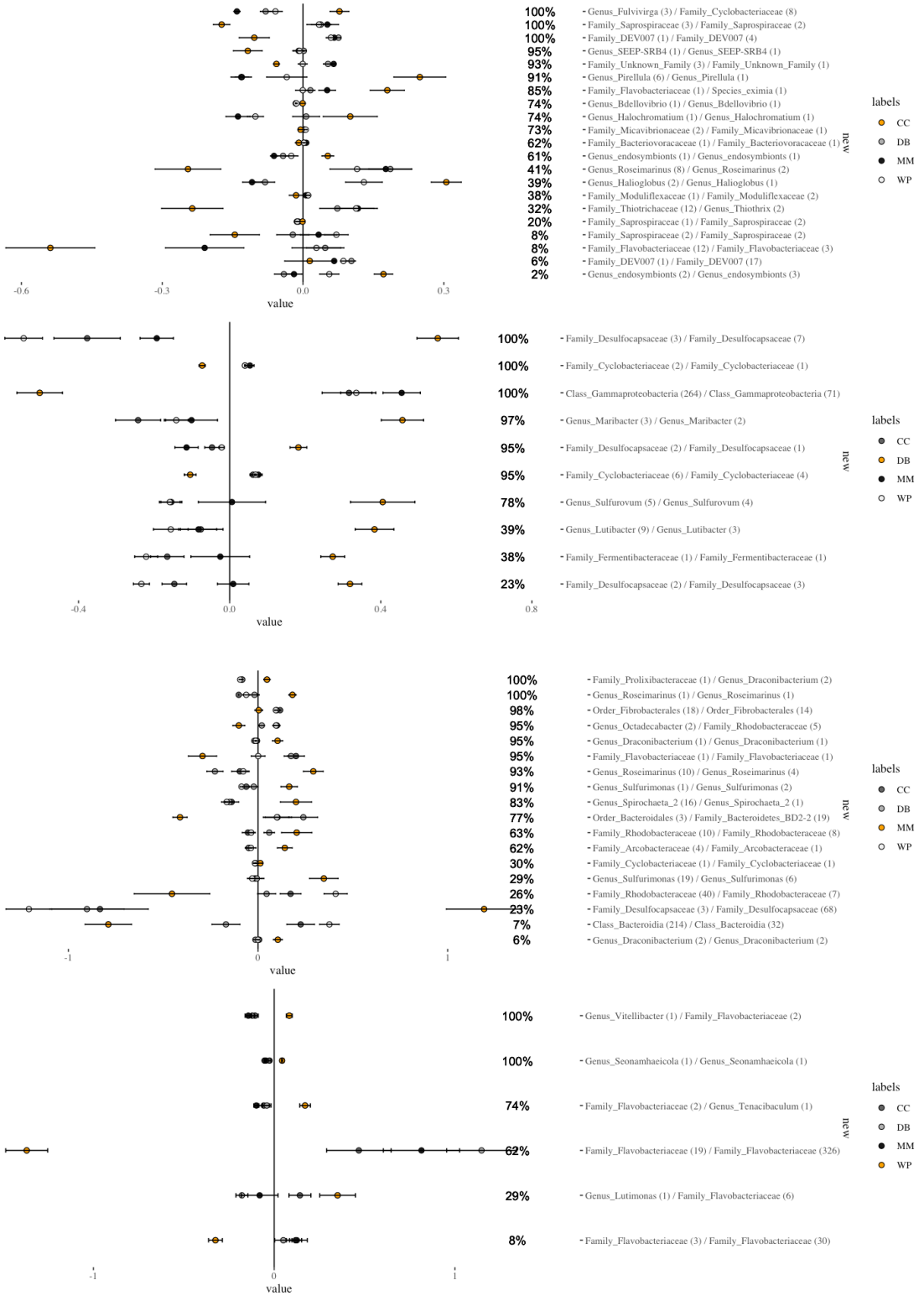

Supplemental Figure 2.S7: After three months, we identified 12 balances distinguishing leaf bacterial communities at CC, 5 balances at DB, 15 at MM and 13 at WP.

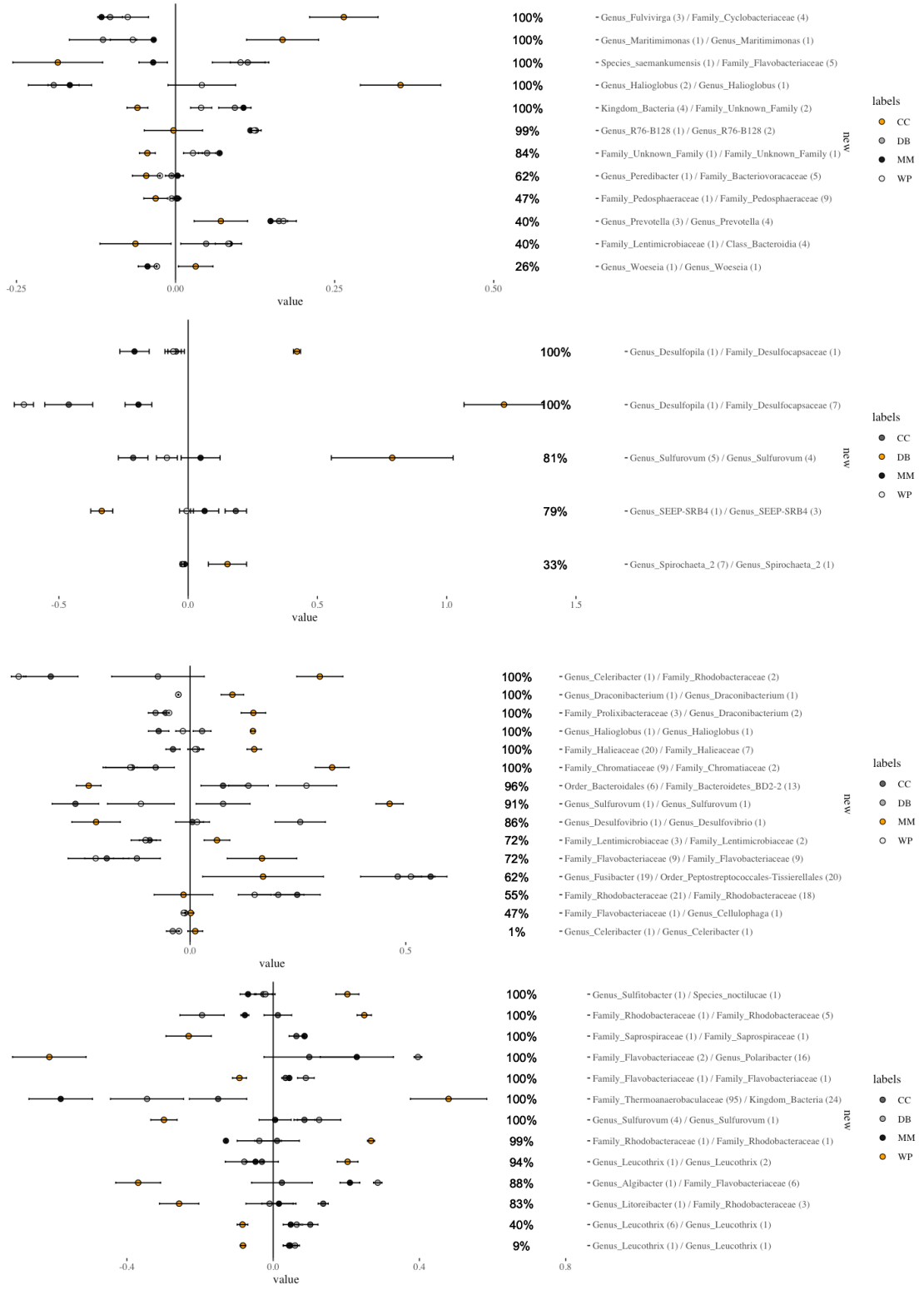

Supplemental Figure 2.S8: Mean amplicon sequence variant (ASV) richness on leaves (left column) and roots (right column by transplant status. Here, we plot means and standard errors by time point; the first row is after one month, the second after two, and the third after three months. Only leaves at T3 showed a significant difference in microbial community richness.

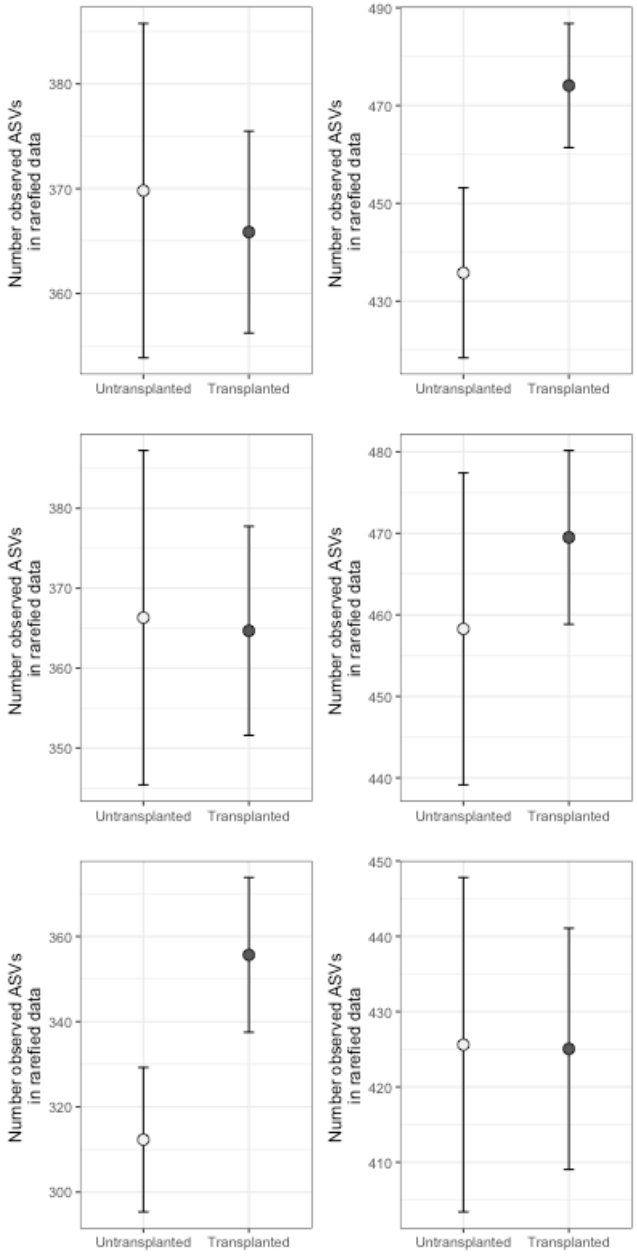

Supplemental Figure 2.S9: Ordination of leaf bacterial community structure based on principal coordinate analysis of phylogenetic-isometric log-ratio transformed distances. Though there is a transplantation effect in root microbiome, this was not due to them changing to resemble leaves. Here brown/yellow points are root communities and green points are leaf communities. Brighter triangles indicate undisturbed controls and darker circles are transplanted plants. While transplanted microbial communities were distinct from undisturbed microbial communities in roots, they still strongly resemble control root microbial communities rather than leaf microbial communities.

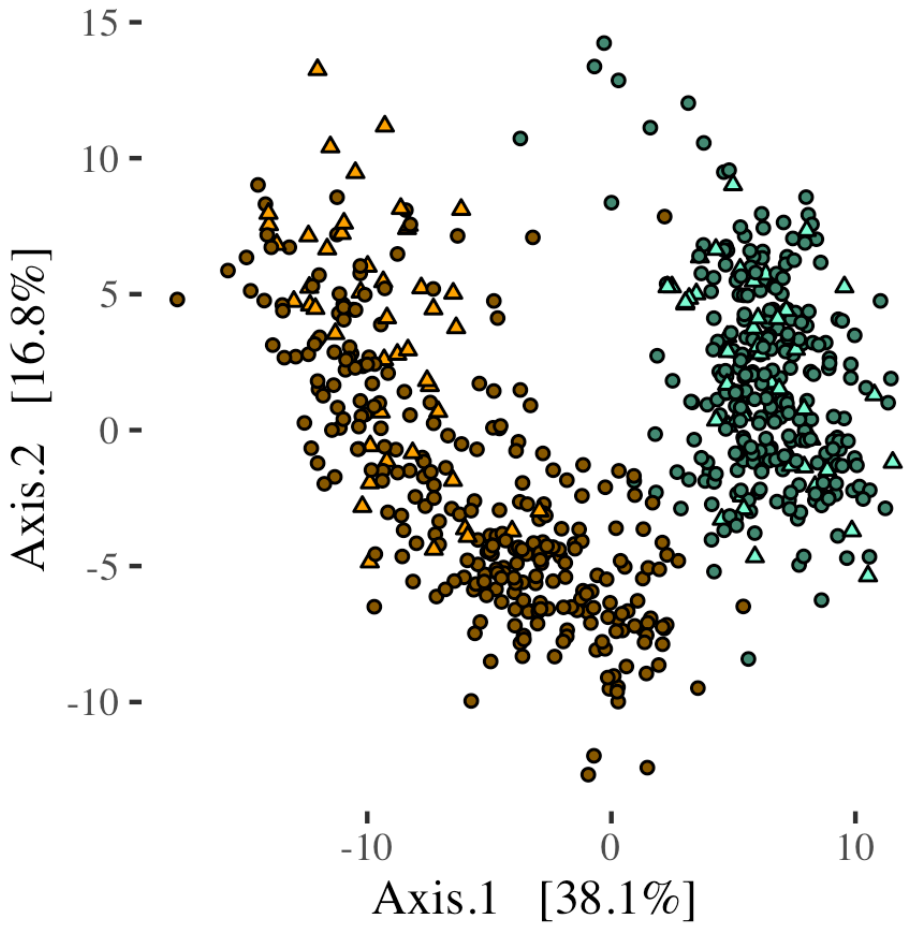

Seagrass root microbial communities are dependent on environmental inputs and not initial community

Authors: Melissa R. Kardish, Mackenzie A. Kawahara, Elizabeth A. Allen, and John. J. Stachowicz

Introduction

With increasing emphasis on both the ubiquity and variability in the importance of host-associated microbial communities, understanding how these communities assemble is key to understanding their operation and function (Christian et al. 2015, Coyte et al. 2015, 2021, Trivedi et al. 2020). Especially when on the surfaces of hosts, microbial communities influence interactions with other organisms and the environment (Laforest-Lapointe and Whitaker 2019). With a fuller understanding of how communities assemble, we can assess how microbes mediate interactions between environments and hosts (Kembel et al. 2014, Wagner et al. 2016, Aleman and Valenzano 2019, Kim and Benayoun 2020).

Environmental manipulations have been widely shown to alter host microbiomes (Greenspan et al. 2020, Ahn and Hayes 2021), but are limited in their ability to attribute change in host performance directly to microbial shifts. Deletion or addition of particular taxa of interest remain challenging with the high-diversity microbiomes typical of many non-model hosts. Associational and metagenomic studies can help in this regard (Antwis et al. 2017, Leray et al. 2021), but supplementing these approaches with direct manipulations is needed to advance our understanding of microbiome assembly and function. As a step toward deepening understanding of host-microbe interactions, experiments that create reduced-diversity environments have enabled better understanding of specific interactions, effects of probiotics, and even population metrics like increasing crop yields (Kutschera and Khanna 2016, Uzbay 2019). This approach has been applied to select communities as a whole (Mueller et al. 2016) or to help identify key taxa that may be altered in a dysbiotic setting (Tudela et al. 2021). These coarse level manipulations of plant microbiomes can involve either removing the extant microbiome or altering the source pool from which microbiomes are drawn, and the relative size of these effects

can inform us about the importance of different processes in microbiome assembly such as priority effects, host, and environmental control.

Seagrass root microbial communities occur in unusual environments for vascular plants: on the surface of angiosperm roots in fully water-logged and largely or hypoxic or even anoxic sediments (Hasler-Sheetal and Holmer 2015). Anoxic sediments play host to a distinct community of bacteria relying on energy sources capitalizing on sulfur metabolism (Hasler-Sheetal and Holmer 2015, Fahimipour et al. 2017). However, seagrass roots exude oxygen (Terrados et al. 1999) which can result in microzones of oxic environments around the roots, although the extent and stability of these zones may depend on conditions in the surrounding sediments. Seagrass has a diversity of mechanisms across species to deal with these anoxic sediments and the toxic sulfides generated within them, including this radial oxygen loss (Pedersen et al. 2004), partnership with lucinid clams hosting sulfur oxidizing bacteria (van der Heide et al. 2012, De Fouw et al. 2016), and direct partnerships with sulfur-oxidizing bacteria (Smith et al. 2004). Previously, we have found evidence that although seagrass root microbiomes consistently associate with taxa likely involved in sulfate and sulfide metabolism (Fahimipour et al. 2017, Chapter 1, 2). However we also have shown that the microbiome on these roots does vary as a function of local environmental conditions (Chapter 2). In a transplant experiment, despite initial differences among local sites, plants reflected microbial communities from the site they were transplanted within one to two months (Chapter 2), showing some adaptability and suggesting the potential for relatively rapid turnover.

In this study, we ask how seagrasses and their microbiomes are affected by direct removal of microbes vs altering the source pool in the sediments. In a laboratory setting, we grew plants from known genotypes in autoclaved and non-sterile field-collected sediments to

assess the effects of a reduced pool on bacterial community assembly. Additionally, we investigate the role of priority effects in driving seagrass bacterial community structure by assessing the relative importance of source pool vs direct removal of resident microbiota in determining microbiome composition. We also evaluate the effects of these changes on plant growth.

Methods:

Experiment 1: Manipulating source pool of microbes via autoclaving sediments

In January 2018, we collected eelgrass shoots for planting from known genotypes grown in outdoor culture (Hughes et al. 2009). We used the eight genotypes from (Hughes et al. 2009) that have been growing in outdoor tanks at Bodega Marine Lab since 2004, plus a single additional genotype described in (Abbott et al. 2018) (MMS08, here MM) that had been propagated since 2012. We then planted individual plants in treated sediment that sat in pots between 2 and 3 days before planting. We collected 12 terminal shoots from each genotype, standardized shoots to 5cm of rhizome length and 30cm of leaf length and marked shoots for growth. The next day, we collected 5 roots from each replicate for microbial sequencing.

We then planted plants in autoclaved and not-autoclaved sediments that had acclimated for 2 days in 82L aquaria in a cold room at 18˚C at University of California, Davis. These tanks had been bleached-sterilized and then filled with filtered seawater before adding plants. We placed an airstone in each tank for oxygenation and lit tanks with fluorescent bulbs (Gribben et al. 2017). All sediments for this experiment were collected from Westside Park, Bodega Bay, California, USA (38˚19’7”N, 123˚3’12”W). Sediments were collected from the top ~5cm of field

sediment from gaps within seagrass beds, homogenized, passed through a 1cm sieve to remove large particles and infauna, and transported to University of California, Davis. Sediment was autoclaved in a one-hour liquid cycle in 500ml volumes. We then filled 90mL autoclaved glass jars with either autoclaved or not-autoclaved sediment and submerged jars in seawater.

To confirm that autoclave treatment substantially altered microbial community composition we measured community composition immediately after autoclaving compared to a control in November 2017. We took 15 ~50 mg samples of sediments that had been autoclaved and compared to 15 samples that had not and were not to establish the effect of autoclaving on treatment. These samples were preserved at -80˚C until extraction. We verified that autoclaving changed neither the grain size or the organic content in the sediments. While we assess and analyze the community present in these autoclaved sediments, these are not a measure of surviving bacteria, but of surviving DNA of bacteria.

We measured plant growth every other week using the standard hole-punch method (Zieman 1980, Dennison 1990). After 7.5 weeks, we ended the experiment, and we took microbial samples by selecting ~10 roots and ~0.25g adjacent sediments from each replicate and freezing at -80˚C promptly after collection until extraction. We froze remaining plant tissue at -20˚C and measured growth in the final period from cut frozen plant samples. During the experiment, we were blind to the experimental treatment and genotype of each plant.

Experiment 2: Manipulating host microbiome directly via bleaching surface tissues

To investigate the role of initial root microbiome on final community structure, we compared microbiomes on plants that had extant microbiomes removed via bleaching versus

those on control plants after four weeks of growth. We collected 56 eelgrass terminal shoots and associated rhizome and root material from Westside Park in October 2019. We did not control for genotype, but the distance among plants was > 2m suggesting that each plant was likely a unique genotype (Kamel et al. 2012, Abbott et al. 2018). We cut leaves to a standardized length of 30 cm and rhizomes to 3 cm then individually submerged the roots and rhizomes of half the plants in a 1% bleach solution for 1 minute, and then twice in deionized water for one minute. We submerged the roots and rhizomes of the other 28 plants in two deionized water rinses. We collected ~10 roots from each of 8 plants from each treatment and froze at -80˚C until extraction to quantify community composition by bacterial 16S rRNA sequencing (see below). We also verified that bleach treatment reduced the abundance of microbes on the surfaces of roots by DAPI staining surfaces (revealing fewer microbes on root surfaces on bleach vs. unbleached surfaces and by comparing DNA concentrations from extracted root surfaces measured by Qubit. We then potted plants with bleached and non-bleached roots into autoclaved and non-autoclaved sediments prepared as described in Experiment 1 (see Supplemental Table 3.1 for replication numbers). After four weeks, we sampled root and sediment microbiomes as in Experiment 1. We blinded ourselves to experimental treatment immediately after bleaching plants.

Molecular Methods and Bioinformatic analysis

We extracted DNA with the MoBio PowerSoil DNA kit from roots and sediments. To get the surface of roots only, we vortexed each frozen sample of ~10 roots with 500ul of MilliQ water and then added that liquid to the bead tubes and proceeded with the standard extraction protocol (full protocol available at github.mkardish/Transplants/Lab_Protocols). For sediments, we added a small amount of sediment (approximately 0.25 mg) directly to the bead tube. We amplified and sequenced the V4-V5 region of the 16S rRNA gene on an Illumina MiSeq to

identify bacteria present at the Integrated Microbiome Resource at Dalhousie University with primers 515F and 926R (Walters et al. 2016, Comeau et al. 2017).

Bioinformatic Analysis

We ran all bioinformatic and statistical analyses in R (version 4.0.5). We trimmed primer sequences with cutadapt (Martin 2011). We used a standard dada2 pipeline to error check our reads and to identify amplicon sequence variants of merged sequences (Callahan et al. 2016). We identified ASV taxonomy based on the SILVA database (Quast et al. 2013) and built a phylogeny of ASVs using alignments built with DECIPHER (Wright 2015) then a tree built with FastTree2 (Price et al. 2010) then converted to ultrametric (Britton et al. 2007). We then rooted the bacterial tree with an archaeal outgroup (Callahan et al. 2016).

Sampling and sequencing success

For information on sequencing depth, ASVs per sample, and sample numbers split by experiment and sample type, see Supplemental Table 3.S1.

Statistical analysis

For plant growth data, we analyzed data using a mixed effect model in generalized linear model : Plant Growth ~ Treatment + Days since planting + Treatment:Days since planting.

We analyzed the compositional changes in our microbial dataset based on phylogenetic similarity among samples by normalizing samples via a phylogenetic isometric log transform described in (Silverman et al. 2017) and implemented in the R-package “philr”. This allows a compositional transformation of the phylogenetic data -- comparing differential weights at nodes throughout the bacterial tree as opposed to just ASVs. We then calculated the Euclidean distance

among samples before using PERMANOVA to determine differences among treatments and genotypes (when applicable) controlling for tank by constraining permutations. We tested homogeneity of group dispersions with the betadispr function in 'vegan'.

To measure bacterial richness, we rarified all samples to 6542 reads samples which we repeated 200 times (McMurdie and Holmes 2014) and used each sample's average "Observed ASVs" in our analysis as our measure of bacterial richness in a sample. We separately rarefied to 1384 reads in comparisons of initially autoclaved sediments or initially bleached roots as some of these samples had very low read counts due to bacterial removal. We tested differences in Observed ASVs using the negative binomial mixed model with random effects implemented in lme4 : Observed ASVs ~ Treatment + Genotype + Genotype:Treatment + (1 | Tank) (Bates et al. 2015). We also visualized overlap in observed ASVs to identify the numbers of overlapping and non-overlapping ASVs between autoclaved and non-sterile treatments (Conway et al. 2017).

To identify which ASVs significantly varied between treatments we used the Wald test in DESeq2 to contrast autoclaved and not autoclaved sequences after geometric mean centering raw ASV abundances (Love et al. 2014). We also contrasted individual genotypes versus other genotypes to determine specific ASVs that were specifically variable in their relative abundance on certain genotypes.

Results

Experiment 1: Manipulation of source pools via autoclaving results in bacterial community differences on roots and sediments

Plants in autoclaved sediments showed reduced growth over time

Initially, plants in autoclaved sediments showed equivalent growth to plants in non-sterile sediments (GLM $p_{10\ days} = 0.649$, $p_{24\ days} = 0.199$) , however by 38 days after planting, plant growth in autoclaved sediments began to diverge from plant growth in autoclaved sediments and (Figure 3.1, $p_{38\ days} = 0.046$, p_{51} days = 0.009, for full generalized linear model results see Supplemental Table 3.S2). This indicated potential important roles in bacterial or other microbial or meiofaunal communities in affecting plant growth.

Root microbial communities in autoclaved sediments were more variable and more diverse than in non-sterile sediments

After 7.5 weeks, we found compositional differences among root microbial communities in autoclaved and not-autoclaved sediments that grew in (Figure 3.2A, for PERMANOVA blocked by tank see Table 3.1), greater dispersion in samples from roots in autoclaved sediments (Figure 3.2A, ANOVA betadisper $p < 0.001$), higher ASV richness in roots in autoclaved sediments (Figure 3.2B, ANOVA negative binomial glm $p_{treatment} = 0.033$, $p_{genotype} = 0.236$, $p_{genotype:treatment} = 0.629$), and fewer shared ASVs across samples (~30% of core ASVs shared, ~50% of all ASVs shared). Roots growth in autoclaved sediments contained relatively fewer bacteria in Deltaproteobacteria, Bacteroidiia, Spirochaetes, and Clostridia, and relatively more bacteria in Gammaproteobacteria, Flavobacteria, and Sphingobacteriia. A full list of individual root microbial taxa that varied by treatment can be found in Supplemental Table 3.S3. Additionally, we confirmed that initially there had been no differences in richness, identity, or community structure between roots planted when they were planted in autoclaved and non-autoclaved sediments (Appendix 3.A; Figure 3.A2), while there was still an effect of genotype, so these resulting differences are due to differences in the source community plants had been exposed to over the course of the experiment.

We were further interested in how communities on individual plants changed over the course of the experiment by assessing the distance between initial and final communities. Final bacterial communities in autoclaved sediments were more distinct from the starting community than root communities in not-autoclaved sediments (Figure 3.3A, LMER ~ treatment + genotype + treatment:genotype+(1|tank) ANOVA treatment $p < 0.001$, Genotype $p = 0.015$, genotype:treatment $p = 0.808$). There was no difference between the change in richness from the start to the end of the experiment in either treatment (Figure 3.3B, $p > 0.05$). Communities on roots in sediments that were less microbially rich were more distinct from their initial composition than those in more microbially complex sediment. We also compared community structure among sediments and the roots in them and found that roots from sediments in autoclaved were not more similar to adjacent sediments than and roots in non-autoclaved sediments and the adjacent sediment (Figure 3.3C). For an ordination and other direct comparisons of plant samples before and after Experiment 1 see Supplemental Figure 3.S1.

Autoclaving sediment reduces sediment microbial diversity and richness and alters sediment microbial composition

Autoclaving sediment caused dramatically reduced alpha and gamma diversity of bacteria in sediments (Appendix 3.A, Figure 3.A1) at the start of the experiment as measured by relative abundance in DNA extraction. Importantly is not a measure of surviving bacteria but of surviving DNA of bacteria. Two thirds of ASVs autoclaved sediments were Gammaproteobacteria.

In sediments at the end of the experiment, we found that differences among sediment treatments persisted (Figure 3.4). Autoclaved sediments were distinct from (PERMANOVA, $F = 69.35$, $p = 0.001$, $r = 0.77$) and more variable than (betadisper, permtest, $p = 0.001$) not-

autoclaved sediments (Figure 3.4A). There was still lower ASV richness in autoclaved sediments (mean = 194) vs. not-autoclaved sediments (mean = 637) (negative binomial glm, estimate = 1.18675, standard error = 0.08139, z-value 14.58, $p < 0.001$). When we examined overlapping ASVs, we found that there were 6 shared core ASVs (shared by by at least 50% of samples at at least a 1% detection rate) between autoclaved and non autoclaved sediments (autoclaved sediments had 53 core ASVs and not-autoclaved had 272). When we compared all ASVs in autoclaved and not-autoclaved sediments, we found 53 shared ASVs, 392 ASVs unique to autoclaved sediments, and 1074 ASVs unique to not-autoclaved sediments. When we examined which ASVs were at significantly higher or lower abundance, we found 559 ASVs at higher abundance in not-autoclaved sediments and 114 ASVs were higher in autoclaved sediments. Autoclaved sediments showed relatively higher abundance of Gammaproteobacteria though less than they had immediately after treatment (Figure 3.4E). A full list of individual taxa that significantly varied by treatment can be found in Supplemental Table 3.S4.

Different genotypes harbored different microbial communities

In addition to the effects of growing in treated or untreated sediments, we found small effects of genotypic differences among plants that did not interact with autoclave treatment (Figure 3.5 for samples after 7.5 weeks, Appendix 3.A Figure 3.A3 for initial samples). Upon closer investigation, we found that initially all genotypes were distinct from each other except Orange & Yellow and White & MM (each pair was indistinguishable) (pairwise PERMANOVA with fdr corrected p-values < 0.05). At the end of the experiment, most genotypes looked similar (pairwise PERMANOVA with fdr correct p-values > 0.05) except Red & Green ($p = 0.036$), Purple & Blue ($p = 0.018$) and Grey and White ($p = 0.018$) which remained distinct.

We again tested with DESeq2 to identify specific ASVs that distinguished genotypes. We summarize these results in Figure 3.6 to highlight the genotypes that are most distinct from each other. Supplemental Figures S2-S10 show ASVs that varied before the experiment by genotype including the log2-fold change ratio of each significant comparison. Appendix 3.A Figures 3.A4-A12 show ASVs that varied by genotype before our experiment compared to each other genotype.

Experiment 2: Direct manipulation of root microbiota.

Changing initial root bacterial composition by bleaching did not alter final community structure

We confirmed that bleaching eliminated most bacteria on the surface of roots via microscopy and through reduction in bacterial DNA concentration (mean 1.43 ng/µl in bleached samples (max 2.96ng/µl)), mean on rinsed roots 19.46 ng/µl (min 6.77 ng/µl). Immediately after bleaching, compared to control roots, bleached roots had different composition (Figure 3.7A, PERMANOVA : $r^2 = 0.151$, $F = 6.743$, $p = 0.001$), lower ASV richness (Figure 3.7B, mean of 61.68 vs 506.79 in non-autoclaved sediments, negative binomial glm, estimate = 2.106, standard error = 0.062, z-value = 33.87, $p < 0.001$), and equivalent variance (ANOVA betadisper $p = 0.626$).

However, after 4 weeks of growth, there was no effect of initial bleaching treatment on root microbiome (Figure 3.7). There were compositional differences among roots grown in different sediment treatments (autoclaving) but not root treatments (bleaching) (Figure 3.7 C & D, Table 3.2 for results from PERMANOVA). We found lower ASV richness on roots in autoclaved sediments, but no difference among bleached vs unbleached roots (Figure 3.7B,

ANOVA negative binomial glm $p_{autoclaved} < 0.001$, $p_{bleached} = 0.731$, $p_{autoclaved:bleached} = 0.630$) and no difference in dispersion among treatments (Figure 3.7C&D, ANOVA betadisper $p = 0.639$). Additionally, when we examined composition, there were few differences among bleached and not-bleached roots at the end of the experiment, though there were a few bacterial ASVs that significantly varied among bleached and not-bleached roots (Supplemental Table 3.S5). Thus although bleaching treatment did alter root microbiomes, effects of sediment microbiota rapidly overwhelmed these effects and was the dominant driver of host root microbiome composition.

Discussion

We demonstrate reducing the diversity and abundance of the bacterial source pool in sediments results in eelgrass root microbial communities that were more varied, more rich, and distinct from those in control sediments. Disruption of the sediment microbiome results in root assemblages that are less consistent and with a higher richness highlighting the role of dominant community members in structuring stable communities in eelgrass root microbiomes. Additionally, this disruption to the bacterial community is associated with reduced plant growth. Further, we show that effects of direct manipulation of microbiome on roots by bleaching are rapidly overwhelmed by sediment source effects. This suggests that source pools play a dominant role in determining seagrass microbiome composition, consistent with prior results from field transplants that showed that transplanted eelgrass rapidly assumed a microbiome indistinguishable from other plants at that site (Chapter 2). However, we did find that eelgrass genotypes vary in their microbiome even when placed in common sediment types, suggesting that plant traits mediate the final community assembled from the environment.

Zaneveld et al. 2017 proposed that animal microbiomes follow the Anna Karenina hypothesis: “all happy microbiomes are alike and each unhappy microbiome is unhappy in its own way” (Zaneveld et al. 2017), where when faced with disease or stress, a host associated microbiome will reach a state of dysbiosis where microbiomes diverge from a ‘normal’ state when faced with disease. This hypothesis has generated mixed support depending on the dynamics of the disease and host system involved. For example, studies show no support in slow spreading coral disease (Sweet et al. 2019), no evidence in voles after radioactive exposure (Lavrinienko et al. 2020), mixed results depending on pathogen in rice (Bez et al. 2021), and suggestions that domestications may lead to similarly dysbiotic communities (Özkurt et al. 2020). We extend this investigation of divergence under stress here by placing hosts dependent on their environments for microbial communities in reduced microbial environments (the first explicit test of the Anna Karenina microbiome hypothesis in reduced diversity environments to our knowledge). Not only did we find less consistent core microbiome community membership, more variable communities on roots in autoclaved sediments, these communities had higher microbial richness although we found decreased community richness in Experiment 2. This suggests to us that assembly on seagrass roots may be dependent on a competitive lottery system from surrounding sediments (Sale 1979); in this environment, as recruitment from the environment is limited, the microbial community assembled appears more random. We suggest that manipulation of these bacterial communities is best done by changing the membership and composition of the sediment communities rather than by direct removal and manipulation which can lead to variable outcomes.

When considering increased variability in a community, instead of indications that these microbial communities have assembled unique “stress” communities, it could indicate that the

community is in an interim state and eventually will assemble a more stable community losing some of the faster colonizers (Zaneveld et al. 2017). This could be supported by the increased richness in these communities compared to natural communities. Regardless, these communities are more divergent so if in an interim state to a similar climax community are following different paths. We think that this is less likely, however, because we saw when we eliminated eelgrass microbial communities, they followed the same assembly patterns as bleached and not-bleached communities; this indicates that there do not seem to be priority effects in these communities, or rather that any priority effects are based on current environmental inputs and matching rather than anything that may be directly grown on plants. It could, however, be that the sediment communities are reassembling their own structure following the autoclaving disturbance and the roots themselves are reflecting a source community in transition. Incremental measurements over time would be needed to test this pattern and the pace of reassembly of these communities directly, though our best indications are that this takes between 4 and 6 weeks (Chapter 2).

In terrestrial plant microbiomes, rhizosphere microbiomes have been shown to generally have less genotype-specific community membership than parallel phyllosphere microbiomes (Wagner et al. 2016). When there are effects of genotype on microbiome, there is often an interaction between soil and genotype (Wagner et al. 2016, Brown et al. 2020), and soil is often the sole or dominant driver of rhizosphere microbiome structure (Hartman et al. 2018, Prudence et al. 2021). Here we found support that there are some genotypic differences in root microbiomes (both before and after our experimental manipulation) and consistent with terrestrial plants these effects are smaller than dominant drivers of source community structure. This suggests that these aquatic angiosperm rhizosphere microbiomes assemble similarly, with the microbial community surrounding the roots responding to specific environmental

modifications by the plant (Bulgarelli et al. 2015, Edwards et al. 2015), and more specific endophytic differences may vary by plant genotype. Given preliminary evidence of some genotypic differences we suggest future work investigate if there are endophytic differences in bacterial communities that vary by genotype. These genotypes were harvested from different mesocosms that may have harbored distinct microbiomes, which could explain initial differences among microbiomes. However, at the end of this experiment we saw a continued genotype effect among several genotype pairs. This suggests that there are specific effects of some genotypes in how they affect the structure of their rhizosphere communities. As these genotypes are known to have a diversity of phenotypic characteristics and responses including differences in growth, shoot production, nutrient uptake rates, and photosynthetic rates (Hughes et al. 2009), we suspect that these microbial assemblages may be capitalizing on subtle genotype-based differences in the rhizosphere communities; though as there are no clear indications comparing genotypes with distinct traits to those with distinct microbial communities, we suspect these are results of measured and unmeasured phenotype interactions.

Understanding the assembly of host microbiomes is critical to understanding the importance of these relationships and their ability to respond to novel environments. An important consideration in understanding microbial assembly involves employing reduced diversity environments to better understand specific interactions or suites of interactions among hosts, microbiomes, and their environments (Gould et al. 2018, Steven et al. 2021). We demonstrate here that these interactions may function differently both among genetically different individuals, but, more importantly, that these communities may structure in more divergent ways under reduced diversity conditions, a critical link to consider when connecting natural and experimental microbial experiments.

Acknowledgements

We would like to thank J. Eisen and E. Grosholz for their comments on this manuscript. We would like to thank T. Burns, E. Diaz, T. Nguyen, F. Pham, H. Sui, and other members of the Stachowicz lab for their assistance in data collection and monitoring of these experiments. This work was funded by the UC Davis Center for Population Biology, the National Science Foundation Graduate Research Fellowship (to MRK) and a grant from the Gordon and Betty Moore Foundation (to JJS and J. Eisen). This work used the Extreme Science and Engineering Discovery Environment (XSEDE) on the Comet at SDSC through an allocation to MRK (TG-DEB160008).

References

Abbott, J. M., K. DuBois, R. K. Grosberg, S. L. Williams, and J. J. Stachowicz. 2018. Genetic distance predicts trait differentiation at the subpopulation but not the individual level in eelgrass, *Zostera marina*. Ecology and evolution:1–14.

Ahn, J., and R. B. Hayes. 2021. Environmental Influences on the Human Microbiome and Implications for Noncommunicable Disease. Annual review of public health 42:277–292.

Aleman, F. D. D., and D. R. Valenzano. 2019. Microbiome evolution during host aging. PLoS pathogens 15:e1007727.

Antwis, R. E., S. M. Griffiths, X. A. Harrison, P. Aranega-Bou, A. Arce, A. S. Bettridge, F. L. Brailsford, A. de Menezes, A. Devaynes, K. M. Forbes, E. L. Fry, I. Goodhead, E.

Haskell, C. Heys, C. James, S. R. Johnston, G. R. Lewis, Z. Lewis, M. C. Macey, A. McCarthy, J. E. McDonald, N. L. Mejia-Florez, D. O'Brien, C. Orland, M. Pautasso, W. D. K. Reid, H. A. Robinson, K. Wilson, and W. J. Sutherland. 2017. Fifty important research questions in microbial ecology.

Bates, D., M. Mächler, B. Bolker, and S. Walker. 2015. Fitting Linear Mixed-Effects Models Using lme4. Journal of Statistical Software, Articles 67:1–48.

Bez, C., A. Esposito, H. D. Thuy, M. Nguyen Hong, G. Valè, D. Licastro, I. Bertani, S. Piazza, and V. Venturi. 2021. The rice foot rot pathogen Dickeya zeae alters the in-field plant microbiome. Environmental microbiology.

Britton, T., C. L. Anderson, D. Jacquet, S. Lundqvist, and K. Bremer. 2007. Estimating divergence times in large phylogenetic trees. Systematic biology 56:741–752.

Brown, S. P., M. A. Grillo, J. C. Podowski, and K. D. Heath. 2020. Soil origin and plant genotype structure distinct microbiome compartments in the model legume Medicago truncatula. Microbiome 8:139.

Bulgarelli, D., R. Garrido-oter, A. C. Mchardy, and P. Schulze-lefert. 2015. Structure and Function of the Bacterial Root Microbiota in Wild and Domesticated Barley Resource Structure and Function of the Bacterial Root Microbiota in Wild and Domesticated Barley. Cell host & microbe 17:392–403.

Callahan, B. J., P. J. McMurdie, M. J. Rosen, A. W. Han, A. J. A. Johnson, and S. P. Holmes. 2016. DADA2: High-resolution sample inference from Illumina amplicon data. Nature methods 13:581–583.

Christian, N., B. K. Whitaker, and K. Clay. 2015. Microbiomes: Unifying animal and plant systems through the lens of community ecology theory. Frontiers in microbiology 6:1–15.

Comeau, A. M., G. M. Douglas, and M. G. I. Langille. 2017. Microbiome Helper: a Custom and Streamlined Workflow for Microbiome Research. mSystems 2.

Conway, J. R., A. Lex, and N. Gehlenborg. 2017. UpSetR: an R package for the visualization of intersecting sets and their properties. Bioinformatics 33:2938–2940.

Coyte, K. Z., C. Rao, S. Rakoff-Nahoum, and K. R. Foster. 2021. Ecological rules for the assembly of microbiome communities. PLoS biology 19:e3001116.

Coyte, K. Z., J. Schluter, and K. R. Foster. 2015. The ecology of the microbiome: Networks, competition, and stability. Science 350.

De Fouw, J., L. L. Govers, J. Van De Koppel, J. Van Belzen, W. Dorigo, M. A. Sidi Cheikh, M. J. A. Christianen, K. J. Van Der Reijden, M. Van Der Geest, T. Piersma, A. J. P. Smolders, H. Olff, L. P. M. Lamers, J. A. Van Gils, and T. Van Der Heide. 2016. Drought, Mutualism Breakdown, and Landscape-Scale Degradation of Seagrass Beds. Current biology: CB 26:1051–1056.

Dennison, W. C. 1990. Leaf production. Seagrass research methods, UNESCO, Paris:77–79.

Edwards, J., C. Johnson, C. Santos-Medellín, E. Lurie, N. K. Podishetty, S. Bhatnagar, J. A. Eisen, and V. Sundaresan. 2015. Structure, variation, and assembly of the root-associated microbiomes of rice. Proceedings of the National Academy of Sciences of the United States of America 112:E911–20.

Fahimipour, A. K., M. R. Kardish, J. M. Lang, J. L. Green, J. A. Eisen, and J. J. Stachowicz. 2017. Globalscale structure of the eelgrass microbiome. Applied and environmental microbiology 83.

Gould, A. L., V. Zhang, L. Lamberti, E. W. Jones, B. Obadia, N. Korasidis, A. Gavryushkin, J. M. Carlson, N. Beerenwinkel, and W. B. Ludington. 2018. Microbiome interactions shape host fitness. Proceedings of the National Academy of Sciences of the United States of America 115:E11951–E11960.

Greenspan, S. E., G. H. Migliorini, M. L. Lyra, M. R. Pontes, T. Carvalho, L. P. Ribeiro, D. Moura-Campos, C. F. B. Haddad, L. F. Toledo, G. Q. Romero, and C. G. Becker. 2020. Warming drives ecological community changes linked to host-associated microbiome dysbiosis. Nature climate change 10:1057–1061.

Gribben, P. E., S. Nielsen, J. R. Seymour, D. J. Bradley, M. N. West, and T. Thomas. 2017. Microbial communities in marine sediments modify success of an invasive macrophyte. Scientific reports 7:1–8.

Hartman, K., M. G. A. van der Heijden, R. A. Wittwer, S. Banerjee, J.-C. Walser, and K. Schlaeppi. 2018. Cropping practices manipulate abundance patterns of root and soil microbiome members paving the way to smart farming. Microbiome 6:14.

Hasler-Sheetal, H., and M. Holmer. 2015. Sulfide intrusion and detoxification in the seagrass zostera marina. PloS one 10:1–19.

van der Heide, T., L. L. Govers, J. de Fouw, H. Olff, M. van der Geest, M. M. van Katwijk, T. Piersma, J. van de Koppel, B. R. Silliman, A. J. P. Smolders, and J. A. van Gils. 2012. A

Three-Stage Symbiosis Forms the Foundation of Seagrass Ecosystems. Science 336:1432–1434.

Hughes, A. R., J. J. Stachowicz, and S. L. Williams. 2009. Morphological and physiological variation among seagrass (Zostera marina) genotypes. Oecologia 159:725–733.

Kamel, S., A. Hughes, R. Grosberg, and J. Stachowicz. 2012. Fine-scale genetic structure and relatedness in the eelgrass Zostera marina. Marine ecology progress series 447:127–137.

Kembel, S. W., T. K. O'Connor, H. K. Arnold, S. P. Hubbell, S. J. Wright, and J. L. Green. 2014. Relationships between phyllosphere bacterial communities and plant functional traits in a neotropical forest. Proceedings of the National Academy of Sciences of the United States of America 111:13715–13720.

Kim, M., and B. A. Benayoun. 2020. The microbiome: an emerging key player in aging and longevity. Translational medicine of aging 4:103–116.

Kutschera, U., and R. Khanna. 2016. Plant gnotobiology: Epiphytic microbes and sustainable agriculture. Plant signaling & behavior 11:e1256529.

Laforest-Lapointe, I., and B. K. Whitaker. 2019. Decrypting the phyllosphere microbiota: progress and challenges. American journal of botany 106:171–173.

Lavrinienko, A., E. Tukalenko, J. Kesäniemi, K. Kivisaari, S. Masiuk, Z. Boratyński, T. A. Mousseau, G. Milinevsky, T. Mappes, and P. C. Watts. 2020. Applying the Anna Karenina principle for wild animal gut microbiota: Temporal stability of the bank vole gut microbiota in a disturbed environment. The Journal of animal ecology 89:2617–2630.

Leray, M., L. G. E. Wilkins, A. Apprill, H. M. Bik, F. Clever, S. R. Connolly, M. E. De León, J. Emmett Duffy, L. Ezzat, S. Gignoux-Wolfsohn, E. A. Herre, J. Z. Kaye, D. I. Kline, J. G. Kueneman, M. K. McCormick, W. Owen McMillan, A. O'Dea, T. J. Pereira, J. M. Petersen, D. F. Petticord, M. E. Torchin, R. V. Thurber, E. Videvall, W. T. Wcislo, B. Yuen, and J. A. Eisen. 2021. Natural experiments and long-term monitoring are critical to understand and predict marine host–microbe ecology and evolution. PLoS biology 19:e3001322.

Love, M. I., W. Huber, and S. Anders. 2014. Moderated estimation of fold change and dispersion for RNA-seq data with DESeq2. Genome biology 15:550.

McMurdie, P. J., and S. Holmes. 2014. Waste not, want not: why rarefying microbiome data is inadmissible. PLoS computational biology 10:e1003531.

Mueller, U. G., T. E. Juenger, M. R. Kardish, A. L. Carlson, K. Burns, C. C. Smith, and D. L. De Marais. 2016. Artificial Microbiome-Selection to Engineer Microbiomes That Confer Salt-Tolerance to Plants. bioRxiv.

Özkurt, E., M. Amine Hassani, U. Sesiz, S. Künzel, T. Dagan, H. Özkan, and E. H. Stukenbrock. 2020. Seed-Derived Microbial Colonization of Wild Emmer and Domesticated Bread Wheat (Triticum dicoccoides and T. aestivum) Seedlings Shows Pronounced Differences in Overall Diversity and Composition.

Pedersen, O., T. Binzer, and J. Borum. 2004. Sulphide intrusion in eelgrass (Zostera marina L.). Plant, cell & environment 27:595–602.

Price, M. N., P. S. Dehal, and A. P. Arkin. 2010. FastTree 2--approximately maximum-likelihood trees for large alignments. PloS one 5:e9490.

Prudence, S. M., J. T. Newitt, S. F. Worsley, M. C. Macey, J. C. Murrell, L. E. Lehtovirta-Morley, and M. I. Hutchings. 2021. Soil, senescence and exudate utilisation: characterisation of the Paragon var. spring bread wheat root microbiome. Environmental microbiome 16:12.

Quast, C., E. Pruesse, P. Yilmaz, J. Gerken, T. Schweer, P. Yarza, J. Peplies, and F. O. Glöckner. 2013. The SILVA ribosomal RNA gene database project: improved data processing and web-based tools. Nucleic acids research 41:D590–6.

Sale, P. F. 1979. Recruitment, loss and coexistence in a guild of territorial coral reef fishes. Oecologia 42:159–177.

Silverman, J. D., A. D. Washburne, S. Mukherjee, and L. A. David. 2017. A phylogenetic transform enhances analysis of compositional microbiota data. eLife 6:1–20.

Smith, A. C., J. E. Kostka, R. Devereux, and D. F. Yates. 2004. Seasonal composition and activity of sulfate-reducing prokaryotic communities in seagrass bed sediments. Aquatic microbial ecology: international journal 37:183–195.

Steven, B., J. Hyde, J. C. LaReau, and D. E. Brackney. 2021. The Axenic and Gnotobiotic Mosquito: Emerging Models for Microbiome Host Interactions. Frontiers in microbiology 12:714222.

Sweet, M., A. Burian, J. Fifer, M. Bulling, D. Elliott, and L. Raymundo. 2019. Compositional homogeneity in the pathobiome of a new, slow-spreading coral disease. Microbiome 7:139.

Terrados, J., C. M. Duarte, L. Kamp-Nielsen, N. S. R. Agawin, E. Gacia, D. Lacap, M. D. Fortes, J. Borum, M. Lubanski, and T. Greve. 1999. Are seagrass growth and survival constrained by the reducing conditions of the sediment? Aquatic botany 65:175–197.

Trivedi, P., J. E. Leach, S. G. Tringe, T. Sa, and B. K. Singh. 2020. Plant-microbiome interactions: from community assembly to plant health. Nature reviews. Microbiology 18:607–621.

Tudela, H., S. P. Claus, and M. Saleh. 2021. Next Generation Microbiome Research: Identification of Keystone Species in the Metabolic Regulation of Host-Gut Microbiota Interplay. Frontiers in cell and developmental biology 9:719072.

Uzbay, T. 2019. Germ-free animal experiments in the gut microbiota studies. Current opinion in pharmacology 49:6–10.

Wagner, M. R., D. S. Lundberg, T. G. Del Rio, S. G. Tringe, J. L. Dangl, and T. Mitchell-Olds. 2016. Host genotype and age shape the leaf and root microbiomes of a wild perennial plant. Nature communications 7:12151.

Walters, W., E. R. Hyde, D. Berg-Lyons, G. Ackermann, G. Humphrey, A. Parada, J. A. Gilbert, J. K. Jansson, J. G. Caporaso, J. A. Fuhrman, A. Apprill, and R. Knight. 2016. Improved Bacterial 16S rRNA Gene (V4 and V4-5) and Fungal Internal Transcribed Spacer Marker Gene Primers for Microbial Community Surveys. mSystems 1.

Wright, E. S. 2015. DECIPHER: harnessing local sequence context to improve protein multiple sequence alignment. BMC bioinformatics 16:322.

Zaneveld, J. R., R. McMinds, and R. Vega Thurber. 2017. Stress and stability: applying the Anna Karenina principle to animal microbiomes. Nature microbiology 2:17121.

Zieman, J. C. 1980. Productivity in seagrasses: methods and rates. Pages 87–116 *in* R. C. Phillips and C. P. McRoy, editors. Handbook of Seagrass Biology: an ecosystem perspective. Garland STPM Press.

Figures and Tables

Figure 3.1: After planting in autoclaved and non-autoclaved sediment, we saw that over the course of 7.5 weeks, plant growth rate diverged between plants in autoclaved and not-autoclaved sediments. Autoclaved and not-autoclaved sediments were significantly different after 38 & 51 days. Here we plot the average growth area per day for the previous week measured through the hole-punch method. Means and standard errors are plotted in light purple for plants in autoclaved sediments and dark purple for not-autoclaved sediments. Model coefficients can be found in Supplemental Table 3.S2.

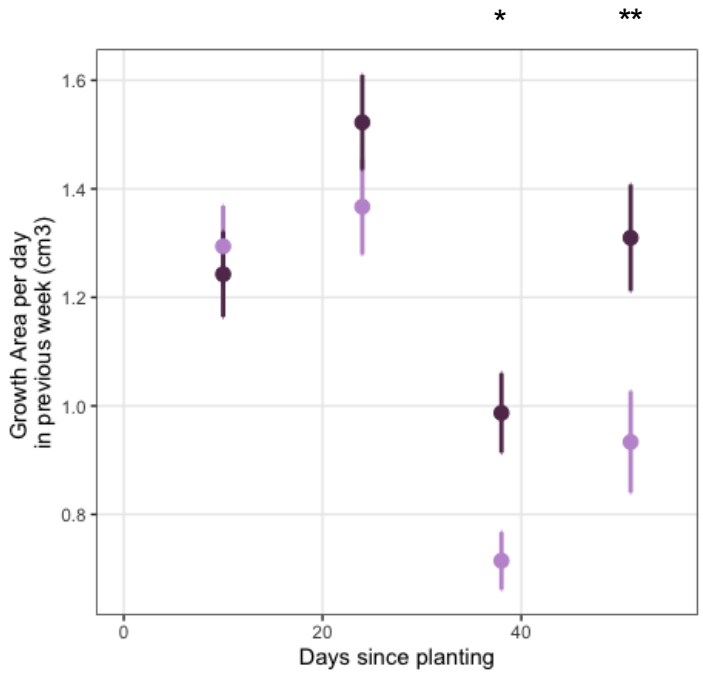

Figure 3.2: After 7.5 weeks, roots in autoclaved (light purple) and not autoclaved sediments (dark purple) developed distinct bacterial profiles. A) Principal coordinate representation of phylogenetic isometric log-ratio transformed abundances show differences between microbial communities on roots in autoclaved and not-autoclaved sediments. (B) Per sample community richness by sample type. All samples are shown in jittered and means and standard errors are plotted in light purple for roots in autoclaved sediments and dark purple for not-autoclaved sediments. Roots in autoclaved sediments had a slightly higher number of observed ASVs. (C) Pooled community richness by sample type. Here all bacteria that occurred in at least 50% of samples at at least a 0.5% detection rate pooled by sample type. Hashed bars indicate ASVs that were shared across sample types. (D) Pooled community richness including all bacteria in a sample type. Hashed bars indicate ASVs that were shared across sample types. (E) On a rough class level, the composition of root microbial communities in autoclaved vs. not autoclaved sediments varied substantially. This bar graph represents the mean abundance of different bacterial classes within sample types. See Supplemental Table 3.S3 for individual ASVs that significantly varied among treatments.

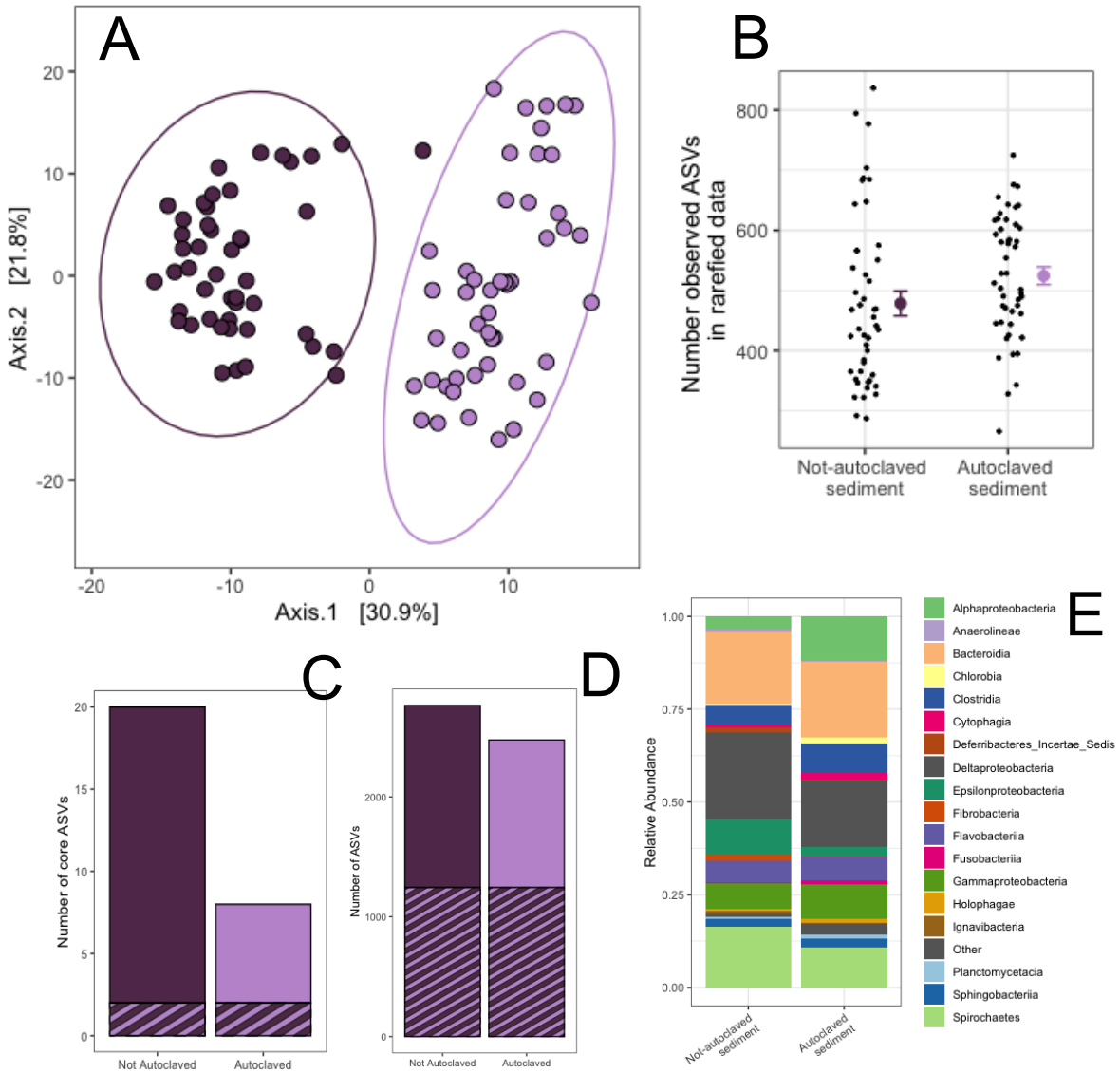
A
Axis.2 [21.8%]
Axis.1 [30.9%]
B
Number observed ASVs in rarefied data
Not-autoclaved sediment
Autoclaved sediment
C
Number of core ASVs
Not Autoclaved
Autoclaved
D
Number of ASVs
Not Autoclaved
Autoclaved
E
Relative Abundance
Not-autoclaved sediment
Autoclaved sediment
Alphaproteobacteria
Anaerolineae
Bacteroidia
Chlorobia
Clostridia
Cytophagia
Deferribacteres_Incertae_Sedis
Deltaproteobacteria
Epsilonproteobacteria
Fibrobacteria
Flavobacteriia
Fusobacteriia
Gammaproteobacteria
Holophagae
Ignavibacteria
Other
Planctomycetacia
Sphingobacteriia
Spirochaetes

Figure 3.3: Root microbial communities in autoclaved sediments were less similar to the community they started with than root microbial communities in not-autoclaved sediments. (A) The distance between the initial microbial community and the final microbial community by sample type (light purple for roots in autoclaved sediments and dark purple for roots in not autoclaved sediment). (B) There was no difference in change community richness on roots between the two treatments, (C) nor was there a difference in how distinct they were from adjacent sediments at the end of the experiment.

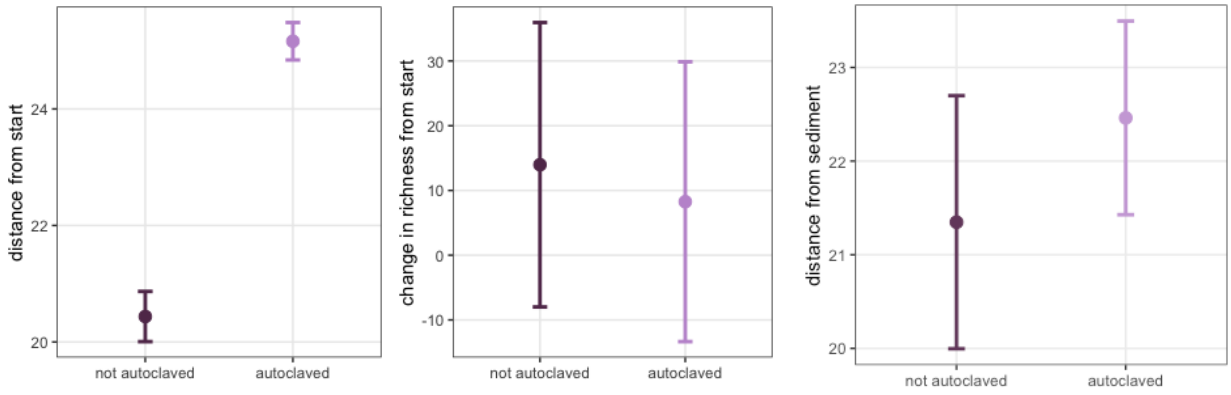

Figure 3.4: After 7.5 weeks, autoclaved and not-autoclaved sediments maintained distinct bacterial profiles. (A) Principal coordinate representation of phylogenetic isometric log-ratio transformed abundances show differences among autoclaved (light purple) and not-autoclaved (dark purple) sediments. (B) Per sample community richness by sample type. All samples are shown in jittered and means and standard errors are plotted in light purple for autoclaved sediments and dark purple for not-autoclaved sediments. Autoclaved sediments had 3-fold lower numbers of observed ASVs. (C) Pooled community richness by sample type. Here all bacteria that occurred in at least 50% of samples at at least a 0.5% detection rate pooled by sample type. Hashed bars indicate ASVs that were shared across sample types. There were more core ASVs in not-autoclaved sediments than non-autoclaved sediments (and no overlapping core ASVs). (D) Pooled community richness including all bacteria in a sample type. Hashed bars indicate ASVs that were shared across sample types. Comparing all ASVs present across samples, there were more ASVs found in not autoclaved sediments compared to autoclaved sediments. (E) Even on a rough class level, the composition of communities in autoclaved vs. not autoclaved sediments varied substantially across time. This bar graph represents the mean abundance of various bacterial classes within sample types. Autoclaved sediments contained relatively fewer bacteria in Deltaproteobacteria, Bacteroidiia, Spirochaetes, and Clostridia, and more bacteria in Gammaproteobacteria, Flavobacteria, and Sphingobacteriia. See Supplemental Table 3.S4 for individual ASVs that varied among treatments.

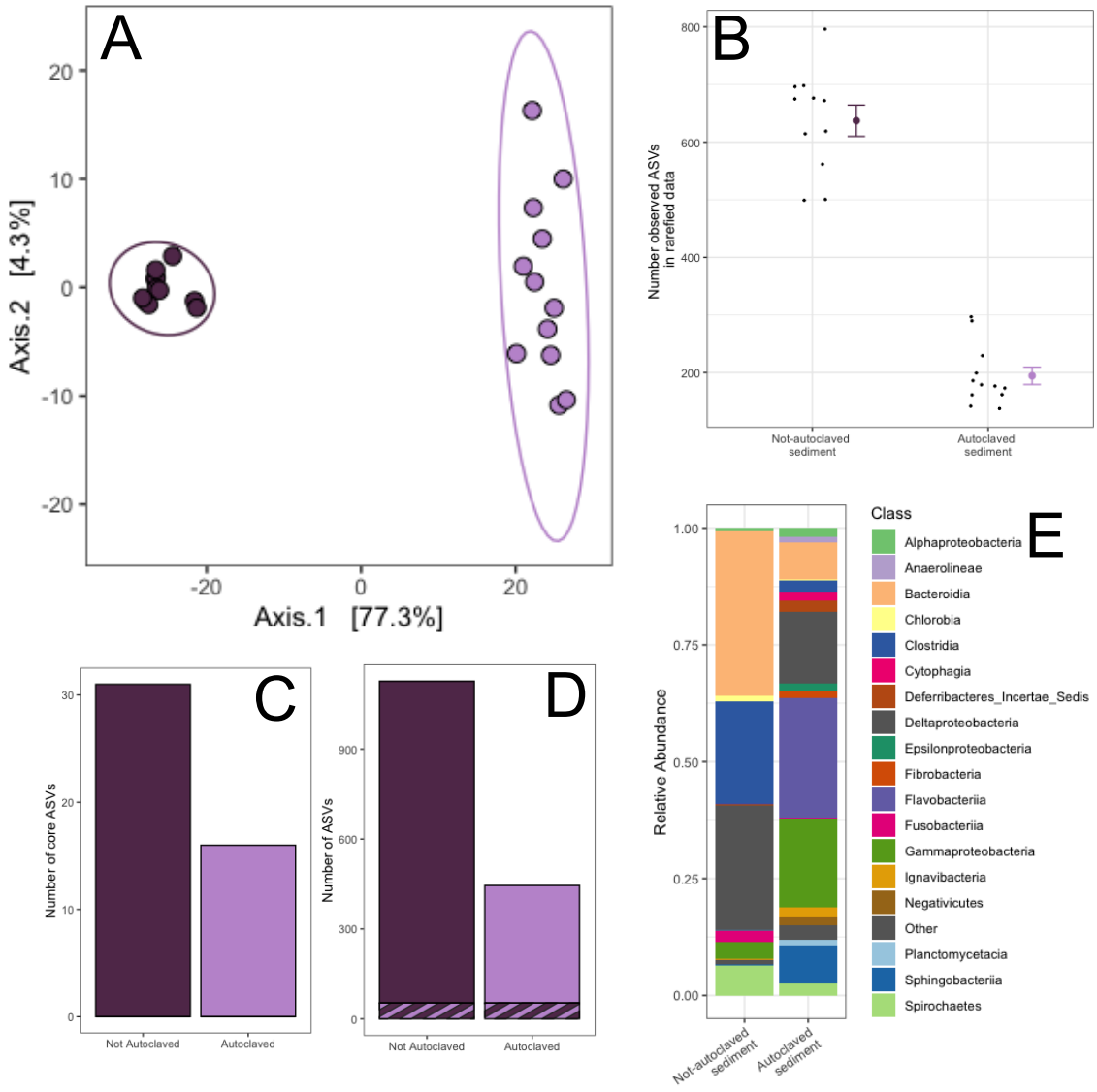
A
Axis.2 [4.3%]
Axis.1 [77.3%]
B
Number observed ASVs in rarefied data
Not-autoclaved sediment
Autoclaved sediment
C
Number of core ASVs
Not Autoclaved
Autoclaved
D
Number of ASVs
Not Autoclaved
Autoclaved
E
Relative Abundance
Not-autoclaved sediment
Autoclaved sediment
Class
Alphaproteobacteria
Anaerolineae
Bacteroidia
Chlorobia
Clostridia
Cytophagia
Deferribacteres_Incertae_Sedis
Deltaproteobacteria
Epsilonproteobacteria
Fibrobacteria
Flavobacteriia
Fusobacteriia
Gammaproteobacteria
Ignavibacteria
Negativicutes
Other
Planctomycetacia
Sphingobacteriia
Spirochaetes

Figure 3.5: While there was a strong effect of autoclaving, different genotypes also harbored different communities after 7.5 weeks. (A) Principal coordinate representation of phylogenetic isometric log-ratio transformed abundances show differences among different genotypes. Each genotype is show in its own color. Red & Green ($p = 0.036$), Purple & Blue ($p = 0.018$) and Grey and White ($p = 0.018$) are all distinct from each other. (B) Per sample community richness by sample type. All samples are shown in jittered and means and standard errors are plotted by genotype. (E) Community composition by genotype by class. The composition of communities in autoclaved vs. not autoclaved sediments varied substantially across time. This bar graph represents the mean abundance of various bacterial classes within sample types. On a course level we see that some classes were relatively more or less abundant in different genotypes. For detailed descriptions of taxa that varied among genotypes see Supplemental Figures 3.S2-S10.

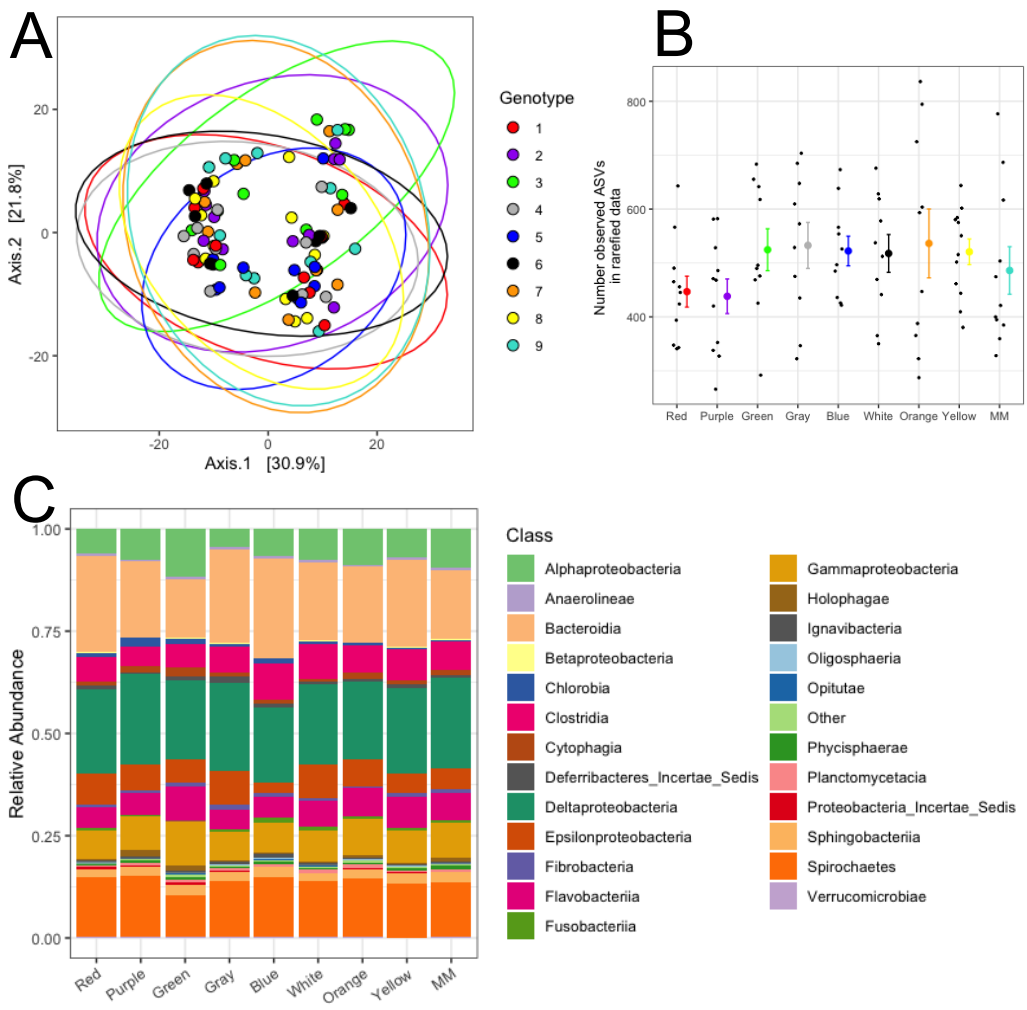
A
B
C
Axis.2 [21.8%]
Axis.1 [30.9%]
Genotype
1
2
3
4
5
6
7
8
9
Number observed ASVs in rarefied data
Red
Purple
Green
Gray
Blue
White
Orange
Yellow
MM
Relative Abundance
Class
Alphaproteobacteria
Anaerolineae
Bacteroidia
Betaproteobacteria
Chlorobia
Clostridia
Cytophagia
Deferribacteres_Incertae_Sedis
Deltaproteobacteria
Epsilonproteobacteria
Fibrobacteria
Flavobacteriia
Fusobacteriia
Gammaproteobacteria
Holophagae
Ignavibacteria
Oligosphaeria
Opitutae
Other
Phycisphaerae
Planctomycetacia
Proteobacteria_Incertae_Sedis
Sphingobacteriia
Spirochaetes
Verrucomicrobiae

Figure 3.6: A summary of significant differences in ASVs by genotype. We tested with DESeq2 to identify specific ASVs that distinguished genotypes. All genotypes had between 60 and 96 significantly different ASVs compared to the other eight genotypes. Perhaps notably, the green genotype had the most differences and the relative abundance of ASVs that differed were generally lower on the green genotype compared to other genotypes. Darker colors highlight a greater number of ASVs.

Genotype	Number of significant differences	Number higher in red genotype	Number higher in purple genotype	Number higher in green genotype	Number higher in gray genotype	Number higher in blue genotype	Number higher in white genotype	Number higher in orange genotype	Number higher in yellow genotype	Number higher in MM genotype
Red	60	NA	5	7	2	3	2	3	1	4
Purple	93	14	NA	13	22	11	11	23	14	12
Green	96	27	12	NA	16	20	10	27	23	26
Gray	92	10	19	16	NA	18	21	12	19	6
Blue	70	4	3	4	2	NA	7	2	5	4
White	66	6	11	12	13	19	NA	14	9	7
Orange	66	2	3	3	2	0	1	NA	0	3
Yellow	73	3	10	8	10	8	3	4	NA	8
MM	60	4	8	8	1	7	3	5	4	NA

Figure 3.7: The final community composition on roots reflected the environments they were in more so than individual structure. In Experiment, 2 we tested the importance of the microbial community already intact on root microbial communites. (A) Principal coordinate representation of phylogenetic isometric log-ratio transformed abundances show differences among different bleach treatments before our experiment. Bleaching roots dramatically reduced ASVs present on roots, and resulted in variable communities initially. Bleached roots microbial communities are shown in yellow and not-bleached communities are shown in blue. (B) Per sample community richness by sample type. All samples are shown in jittered and means and standard errors are plotted by genotype. Bleached roots microbial communities are shown in yellow and not-bleached communities are shown in blue. While there were differences in richness due to autoclaving at the end of experiment, there was no difference in community richness based on bleaching at the end of the experiment. Initially bleaching dramatically reduced community richness. (C&D) Principal coordinate representation of phylogenetic isometric log-ratio transformed abundances show differences among different bleach treatments in (C) not autoclaved and (D) autoclaved sediments. (E) Community composition by sample type in experiment 2. The relative abundance of different classes of bacteria, while different before and after the experiment, did not show dramatic changes due to bleaching. See Supplemental Table 3.S5 for individual ASVs that varied among treatments.

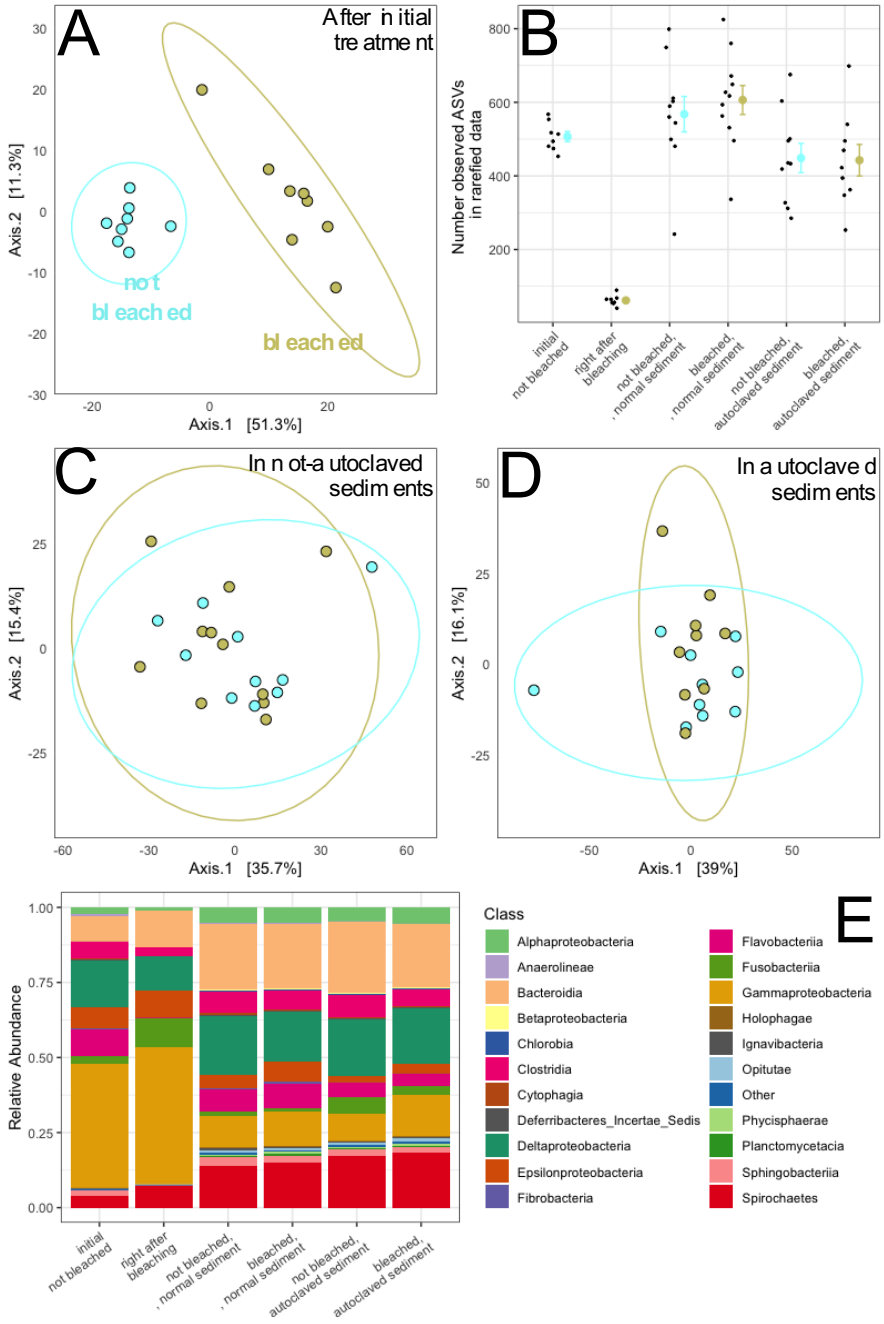
A
After initial treatment
not bleached
bleached
Axis.2 [11.3%]
Axis.1 [51.3%]
B
Number observed ASVs in rarefied data
initial not bleached
right after bleaching
not bleached, normal sediment
bleached, normal sediment
not bleached, autoclaved sediment
bleached, autoclaved sediment
C
In not-autoclaved sediments
Axis.2 [15.4%]
Axis.1 [35.7%]
D
In autoclaved sediments
Axis.2 [16.1%]
Axis.1 [39%]
E
Relative Abundance
Class
Alphaproteobacteria
Anaerolineae
Bacteroidia
Betaproteobacteria
Chlorobia
Clostridia
Cytophagia
Deferribacteres_Incertae_Sedis
Deltaproteobacteria
Epsilonproteobacteria
Fibrobacteria
Flavobacteriia
Fusobacteriia
Gammaproteobacteria
Holophagae
Ignavibacteria
Opitutae
Other
Phycisphaerae
Planctomycetacia
Sphingobacteriia
Spirochaetes

Table 3.1: Results of PERMANOVA showing differences among root microbial communities based on different plant genotypes and sediment treatments.

	df	**Sum Of Squares**	**R^2**	**F-Statistic**	**Pr(>F)**
Treatment	1	6632.187	0.212	29.650	0.004
Genotype	8	3254.209	0.104	1.819	0.001
Treatment : Genotype	8	2189.684	0.070	1.224	0.057
Residual	86	19236.908	0.614	NA	NA
Total	103	31312.988	1	NA	NA

Table 3.2: Results of PERMANOVA showing differences among root microbial communities based on different root surface sterilization and sediment treatments.

	df	Sum Of Squares	R^2	F-Statistic	Pr(>F)
Autoclaved sediment	1	4930.652	0.151	6.743	0.001
Bleached roots	1	818.487	0.025	1.119	0.304
Autoclaved sediment : Bleached roots	1	644.913	0.020	0.882	0.456
Residual	36	26324.465	0.804	NA	NA
Total	39	32718.517	1	NA	NA

Supplemental Figures

Figure 3.S1: After 7.5 weeks, roots in autoclaved (light purple) and not autoclaved sediments (dark purple) had distinct bacterial profiles, and were distinct from their initial communities as well (teal). A) Principal coordinate representation of phylogenetic isometric log-ratio transformed abundances show differences between microbial communities on roots in autoclaved and not-autoclaved sediments. (B) Per sample community richness by sample type. All samples are shown in jittered and means and standard errors are plotted in light purple for roots in autoclaved sediments and dark purple for not-autoclaved sediments. Roots in autoclaved sediments had a slightly higher number of observed ASVs than not autoclaved sediments, but neither was different from initial conditions. (C) Pooled community richness by sample type. Here all bacteria that occurred in at least 50% of samples at at least a 0.5% detection rate pooled by sample type. Hashed bars indicate ASVs that were shared across sample types. (D) Pooled community richness including all bacteria in a sample type. Hashed bars indicate ASVs that were shared across sample types. (E) On a rough class level, the composition of communities in roots in autoclaved vs. not autoclaved sediments varied substantially. This bar graph represents the mean abundance of various bacterial classes within sample types.

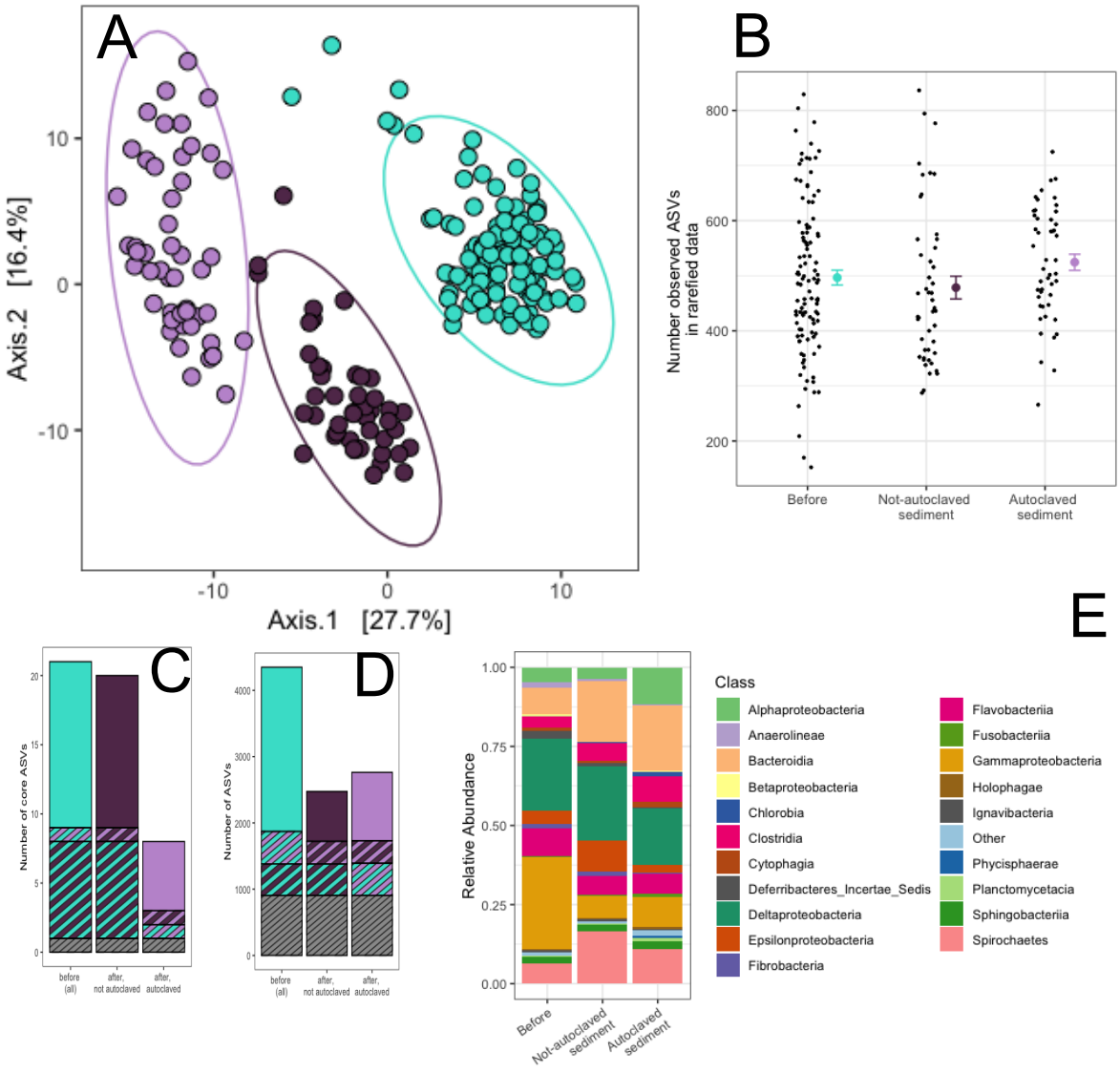
A
Axis.2 [16.4%]
Axis.1 [27.7%]
B
Number observed ASVs in rarefied data
Before
Not-autoclaved sediment
Autoclaved sediment
C
Number of core ASVs
D
Number of ASVs
E
Relative Abundance
Class
Alphaproteobacteria
Anaerolineae
Bacteroidia
Betaproteobacteria
Chlorobia
Clostridia
Cytophagia
Deferribacteres_Incertae_Sedis
Deltaproteobacteria
Epsilonproteobacteria
Fibrobacteria
Flavobacteriia
Fusobacteriia
Gammaproteobacteria
Holophagae
Ignavibacteria
Other
Phycisphaerae
Planctomycetacia
Sphingobacteriia
Spirochaetes

Figure 3.S2: Bacterial taxa that distinguish the Red genotype from other genotypes after 7.5 weeks. All other genotypes that are being compared to the Red genotype are colored. A positive value indicates higher in the Red genotype, a lower value indicates higher in the other genotype.

Figure 3.S3: Bacterial taxa that distinguish the Purple genotype from other genotypes after 7.5 weeks. All other genotypes that are being compared to the Purple genotype are colored. A positive value indicates higher in the Purple genotype, a lower value indicates higher in the other genotype.

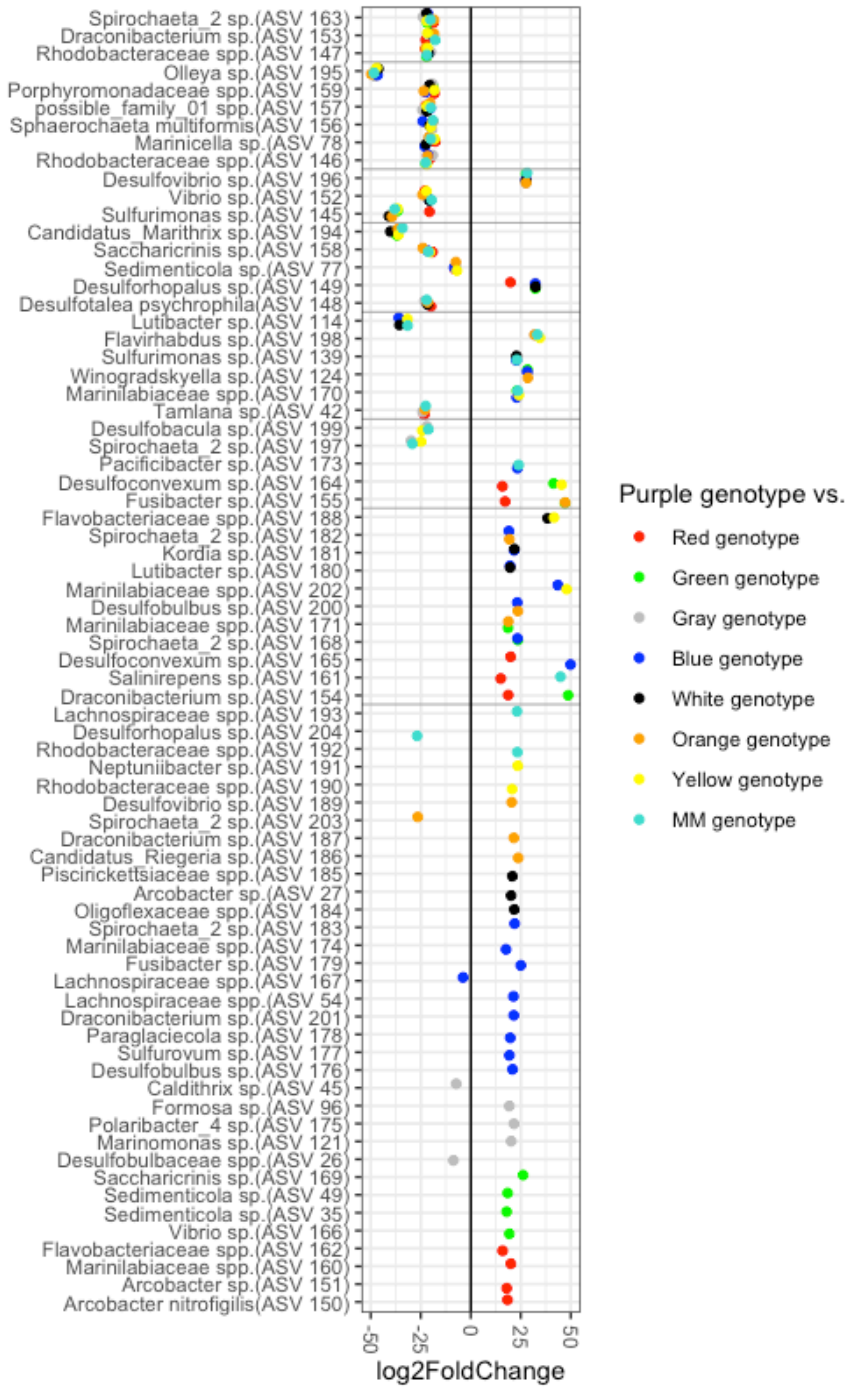

Figure 3.S4: Bacterial taxa that distinguish the Green genotype from other genotypes after 7.5 weeks. All other genotypes that are being compared to the Green genotype are colored. A positive value indicates higher in the Green genotype, a lower value indicates higher in the other genotype.

Figure 3.S5: Bacterial taxa that distinguish the Gray genotype from other genotypes after 7.5 weeks. All other genotypes that are being compared to the Gray genotype are colored. A positive value indicates higher in the Gray genotype, a lower value indicates higher in the other genotype.

Figure 3.S6: Bacterial taxa that distinguish the Blue genotype from other genotypes after 7.5 weeks. All other genotypes that are being compared to the Blue genotype are colored. A positive value indicates higher in the Blue genotype, a lower value indicates higher in the other genotype.

Figure 3.S7: Bacterial taxa that distinguish the White genotype from other genotypes after 7.5 weeks. All other genotypes that are being compared to the White genotype are colored. A positive value indicates higher in the White genotype, a lower value indicates higher in the other genotype.

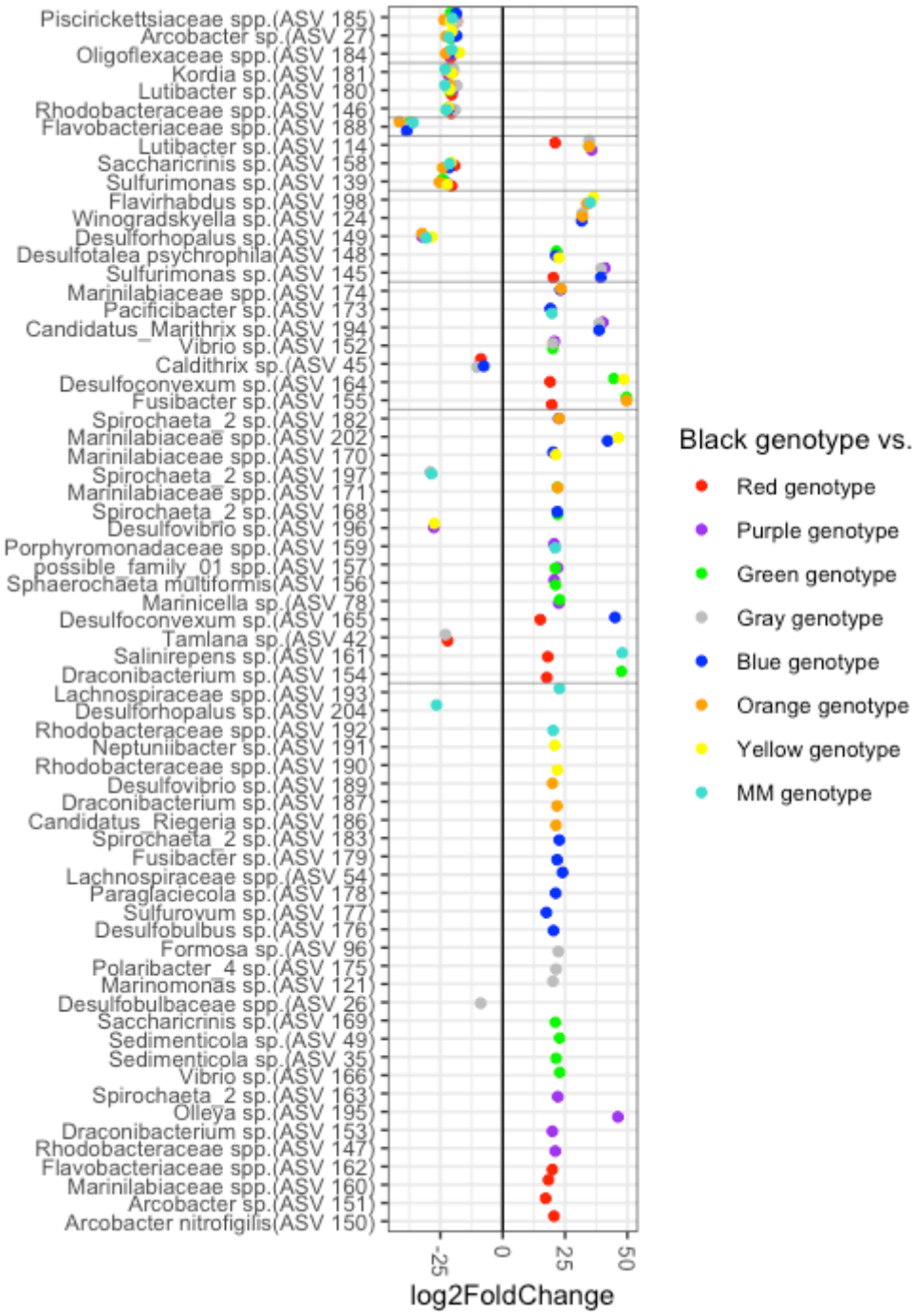

Figure 3.S8: Bacterial taxa that distinguish the Orange genotype from other genotypes after 7.5 weeks. All other genotypes that are being compared to the Orange genotype are colored. A positive value indicates higher in the Orange genotype, a lower value indicates higher in the other genotype.

Figure 3.S9: Bacterial taxa that distinguish the Yellow genotype from other genotypes after 7.5 weeks. All other genotypes that are being compared to the Yellow genotype are colored. A positive value indicates higher in the Yellow genotype, a lower value indicates higher in the other genotype.

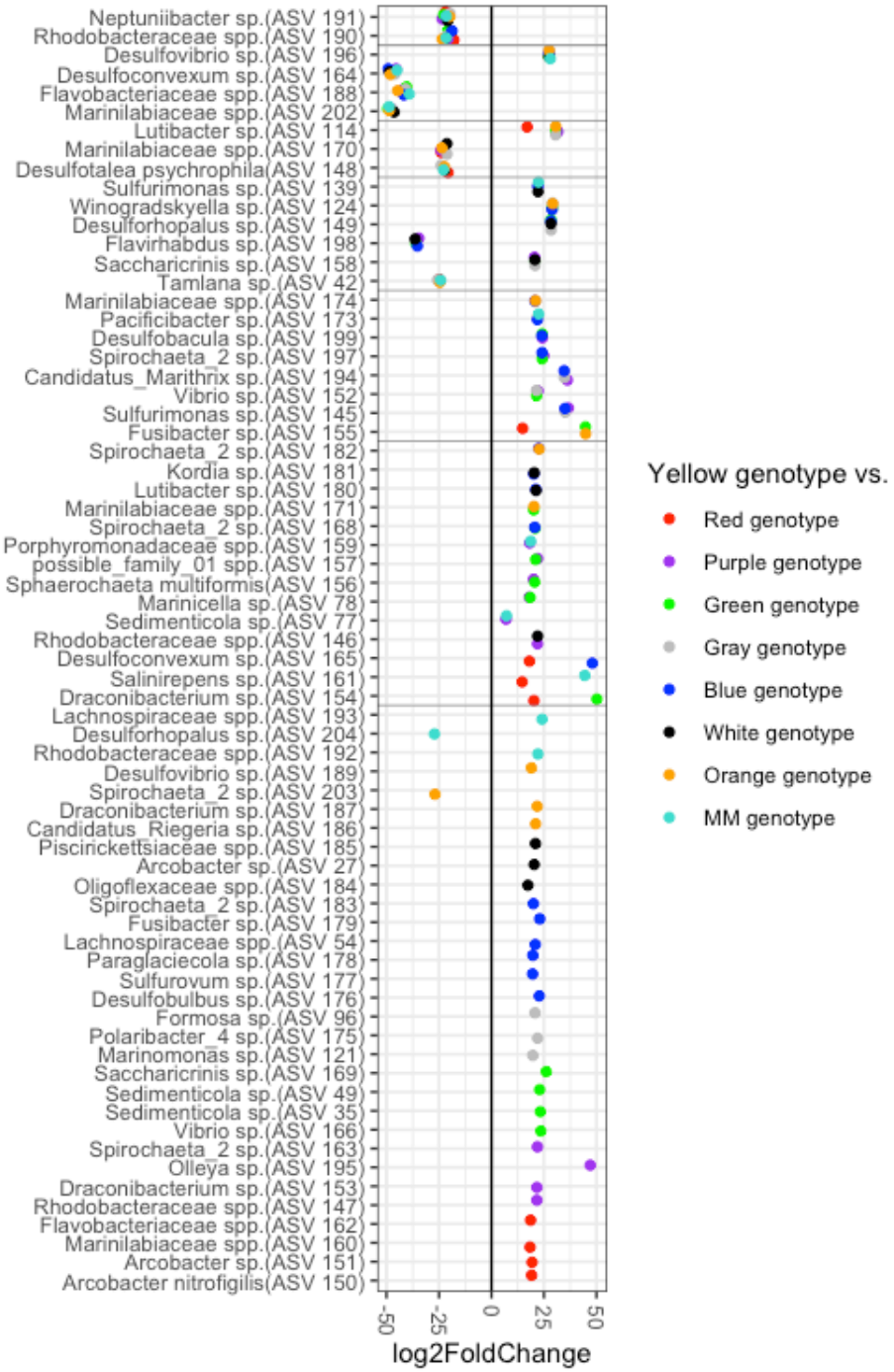

Figure 3.S10: Bacterial taxa that distinguish the MM genotype from other genotypes after 7.5 weeks. All other genotypes that are being compared to the MM genotype are colored. A positive value indicates higher in the MM genotype, a lower value indicates higher in the other genotype.

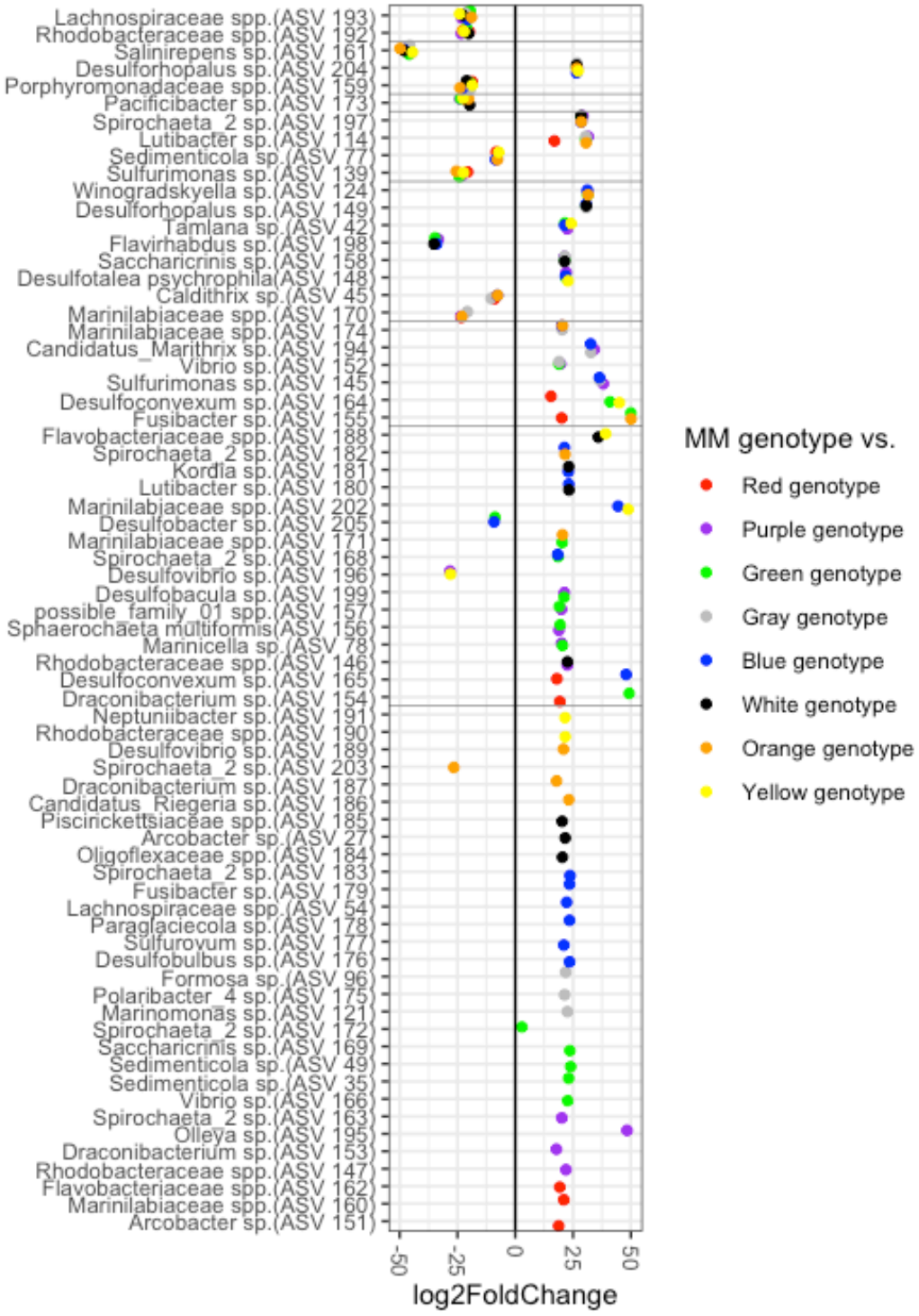

Supplemental Tables:

Supplemental Table 3.S1: Summary of sample replicates and sequencing depth for microbial communities.

Sample Type	Number of samples	Sequencing depth	ASVs per sample
Initial sediment samples			
Autoclaved sediment	13	1,384 - 38,505 (mean: 21,117.92)	50 - 186 (mean: 125.0769)
Not autoclaved sediment	15	8,512 - 21,915 (mean: 15,853.33)	430 - 830 (mean : 658.6)
At end of experiment			
Roots in autoclaved sediment	53	9665 - 40588 (mean: 24436.91)	112 - 800 (mean: 574.0377)
Roots in not autoclaved sediment	51	6542 - 41422 (mean : 21551.96)	292 - 966 (mean: 519.098)
Autoclaved sediment	13	17,403 - 63,122 (mean: 32808.85)	155 - 769 (mean: 331.3077)
Not autoclaved sediment	10	13,895 - 49,758 (mean: 23053.6)	217 - 888 (mean: 595.5)
In bleach experiment			
Bleached roots right after treatment	8	1,993 - 16,625 (mean: 5,496.625)	41 - 92 (mean: 63.5)
Non-bleached roots right after rinse	8	18,869 - 36,333 (mean: 26,767.62)	484 - 678 (mean: 568.875)
Bleached roots in autoclaved sediments	9	23,275 - 49,562 (mean: 36,299.44)	300 - 800 (mean: 507.7778)
Non-bleached roots in autoclaved sediments	10	22,626 - 47,526 (mean: 32,870.1)	332 - 753 (mean: 509.3)
Bleached roots in not autoclaved sediments	11	17,784 - 44,152 (mean: 32,437.09)	383 - 933 (mean: 692.3636)
Non-bleached roots in not autoclaved sediments	10	16,938 - 50,343 (mean: 27,616)	303 - 895 (mean: 630.1)

Supplemental Table 3.S2: Coefficients from the generalized linear model Plant growth ~ days*autoclaving.

Coefficients	***Estimates***	***Std. errors***	***t***	***Pr(>|t|)***
(Intercept)	1.294	0.079	16.301	**<0.001**
days24	0.073	0.113	0.643	0.520
days38	-0.579	0.113	-5.112	**<0.001**
days51	-0.360	0.116	-3.098	0.002
autoclave not autoclaved	-0.051	0.113	-0.456	0.649
days24 : autoclave not autoclaved	0.207	0.161	1.288	0.199
days38 : autoclave not autoclaved	0.324	0.161	2.005	**0.046**
days51 : autoclave not autoclaved	0.428	0.164	2.614	**0.009**

df = 409

Supplemental Table 3.S3: ASVs significantly different among roots in autoclaved and not autoclaved sediments after 7.5 weeks. A negative log2Fold change indicates higher in autoclaved sediments, a positive indicates higher in not-autoclaved sediments. Supplemental File SuppTab3.S3.csv

Supplemental Table 3.S4: ASVs significantly different among autoclaved and not autoclaved sediments after 7.5 weeks. A negative log2Fold change indicates higher in autoclaved sediments, a positive indicates higher in not-autoclaved sediments. Supplemental File SuppTab3.S4.csv

Supplemental Table 3.S5: ASVs significantly different initially among bleached and not bleached roots at the end of our experiment. A negative log2Fold change indicates higher on bleached roots, a positive indicates higher in not-bleached roots. Supplemental File SuppTab3.S5.csv

Appendix 3.A

This appendix describes the initial conditions of both root and sediment communities at the outset of Experiment 1. It contains information on (1) the immediate effect of autoclaving on sediments, (2) the initial community composition of root microbial communities by future treatment (to show no differences, and (3) the initial community composition of root microbial communities split by genotype

Immediate effect of autoclaving on sediments

In autoclaved sediments, total ASV richness was lower (mean of 92.65 vs 431.8 in non-autoclaved sediments, negative binomial glm, estimate = 1.540, standard error = 0.109, z-value = 14.18, $p < 0.001$) and most of the compositional differences among samples was driven by sediment treatment (PERMANOVA, $F = 34.55$, $p = 0.001$, $r = 0.57$). There was no difference in the variance of the communities in autoclaved vs control sediment (betadisper, ANOVA, $p = 0.26$).

When we examined overlapping ASVs, we found that there were no shared core ASVs (shared by by at least 50% of samples at at least a 1% detection rate) between autoclaved and non autoclaved sediments (autoclaved sediments had 21 core ASVs and not-autoclaved had 361). When we compared all ASVs in autoclaved and not-autoclaved sediments, we found 122 shared ASVs, 149 ASVs unique to autoclaved sediments, and 1182 ASVs unique to not-autoclaved sediments. When we examined which ASVs were at significantly higher or lower abundance, we found 412 ASVs at higher abundance in not-autoclaved sediments and 35 ASVs were higher in autoclaved sediments. Two thirds of ASVs higher in autoclaved sediments were Gammaproteobacteria.

Appendix Figure 3.A1: After autoclaving sediment, we saw a distinct shift in the bacterial community sequenced from sediments. These sediments had reduced per-sample alpha diversity and an overall reduction in the number of ASVs found in a sample type. A) Principal coordinate representation of phylogenetic isometric log-ratio transformed abundances show differences between microbial communities on in autoclaved and not-autoclaved sediments immediately after treatment. (B) Per sample community richness by sample type. All samples are shown in jittered and means and standard errors are plotted in light purple for autoclaved sediments and dark purple for not-autoclaved sediments. (C) Pooled community richness by sample type. Here all bacteria that occurred in at least 50% of samples at at least a 0.5% detection rate pooled by sample type. Hashed bars indicate ASVs that were shared across sample types. (D) Pooled community richness including all bacteria in a sample type. Hashed bars indicate ASVs that were shared across sample types. (E) On a rough class level, the composition of communities in autoclaved vs. not autoclaved sediments varied substantially. This bar graph represents the mean abundance of various different bacterial classes within sample types.

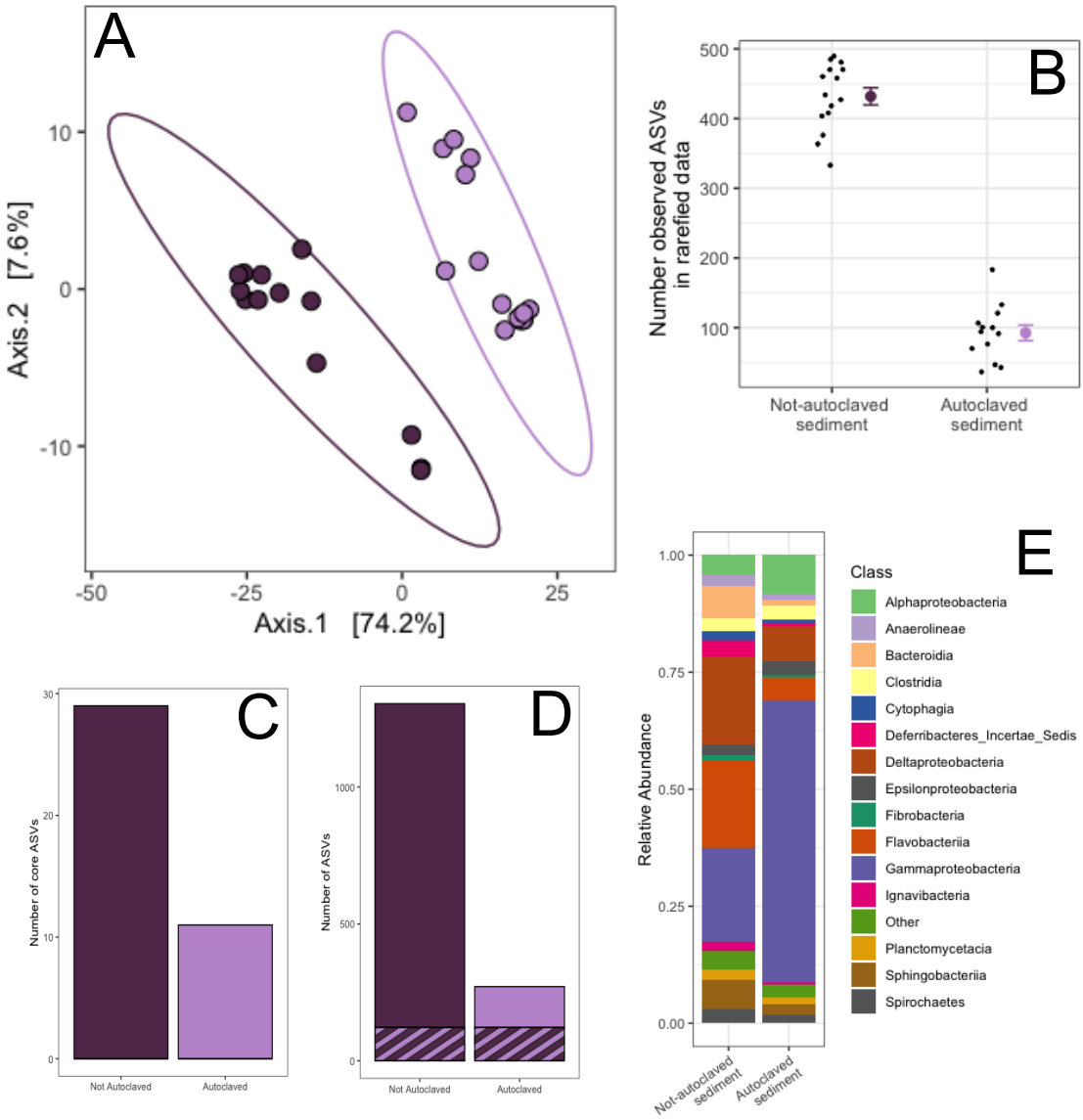
A
Axis.2 [7.6%]
Axis.1 [74.2%]
B
Number observed ASVs in rarefied data
Not-autoclaved sediment
Autoclaved sediment
C
Number of core ASVs
Not Autoclaved
Autoclaved
D
Number of ASVs
Not Autoclaved
Autoclaved
E
Relative Abundance
Class
Alphaproteobacteria
Anaerolineae
Bacteroidia
Clostridia
Cytophagia
Deferribacteres_Incertae_Sedis
Deltaproteobacteria
Epsilonproteobacteria
Fibrobacteria
Flavobacteriia
Gammaproteobacteria
Ignavibacteria
Other
Planctomycetacia
Sphingobacteriia
Spirochaetes

Initial composition of root microbial communities by future treatment

Before planting, we confirmed that there was no effect of future treatment on any aspect of community structure.

Appendix Figure 3.A2: (A) Overall community composition based on phylogenetic isometric log-transform ratios. (B) Per sample community richness by sample type. All samples are shown in jittered and means and standard errors are plotted in light purple for autoclaved sediments and dark purple for not-autoclaved sediments. (C) Pooled community richness by sample type. Here all bacteria that occurred in at least 50% of samples at at least a 0.5% detection rate pooled by sample type. Hashed bars indicate ASVs that were shared across sample types. (D) Pooled community richness including all bacteria in a sample type. Hashed bars indicate ASVs that were shared across sample types. While we saw an effect of genotype (discussed later), there was no difference in community structure (Figure 3.S2A, $r^2_{treatment} = 0.011$, $F_{treatment} = 1.465$, $p_{treatment} = 0.081$, $r^2_{genotype} = 0.204$, $F_{genotype} = 3.168$, $p_{genotype} = 0.001$, $r^2_{treatment:genotype} = 0.061$, $F_{treatment:genotype} = 0.954$, $p_{treatment:genotype} = 0.631$), richness (Figure 3.A2B, negative binomial glm p = 0.4, class composition), or ASV identity (Figure 3.A2C&D, >70% shared in all ASVs, >80% shared in core ASVs, no major differences in abundance among bacterial classes) between roots that would be planted in autoclaved or non-autoclaved sediment. (E) On a rough class level, the composition of root microbial communities that would be put into autoclaved vs. not autoclaved sediments. These communities did not look substantially different. This bar graph represents the mean abundance of various different bacterial classes within sample types.

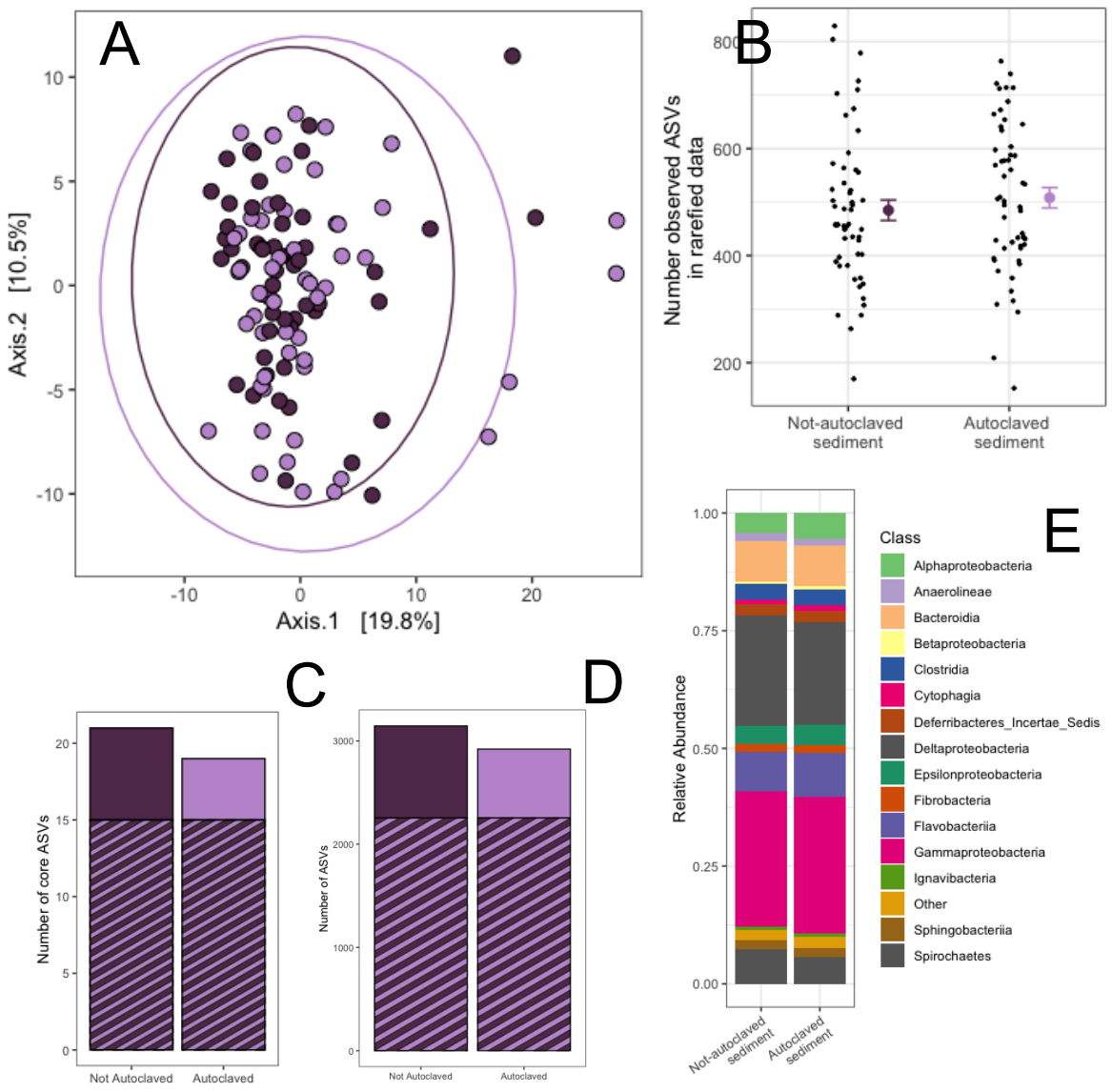
A
Axis.2 [10.5%]
Axis.1 [19.8%]
B
Number observed ASVs in rarefied data
Not-autoclaved sediment
Autoclaved sediment
C
Number of core ASVs
Not Autoclaved
Autoclaved
D
Number of ASVs
Not Autoclaved
Autoclaved
E
Relative Abundance
Not-autoclaved sediment
Autoclaved sediment
Class
Alphaproteobacteria
Anaerolineae
Bacteroidia
Betaproteobacteria
Clostridia
Cytophagia
Deferribacteres_Incertae_Sedis
Deltaproteobacteria
Epsilonproteobacteria
Fibrobacteria
Flavobacteriia
Gammaproteobacteria
Ignavibacteria
Other
Sphingobacteriia
Spirochaetes

Initial composition of root microbial communities by genotype

Figure 3.A3: Different genotypes harbored different communities at the time of planting. (A) Principal coordinate representation of phylogenetic isometric log-ratio transformed abundances show differences among different genotypes. Each genotype is show in its own color. All genotypes were distinct from each other except Orange & Yellow and White & MM (each pair was indistinguishable) (pairwise PERMANOVA with fdr corrected p-values < 0.05). (B) Per sample community richness by sample type. All samples are shown in jittered and means and standard errors are plotted by genotype. (E) Community composition by genotype by class. The composition of communities in autoclaved vs. not autoclaved sediments varied substantially across time. This bar graph represents the mean abundance of various different bacterial classes within sample types. On a course level we see that some classes were relatively more or less abundant in different genotypes. For detailed descriptions of taxa that varied among genotypes see Figures 3.A4-A12.

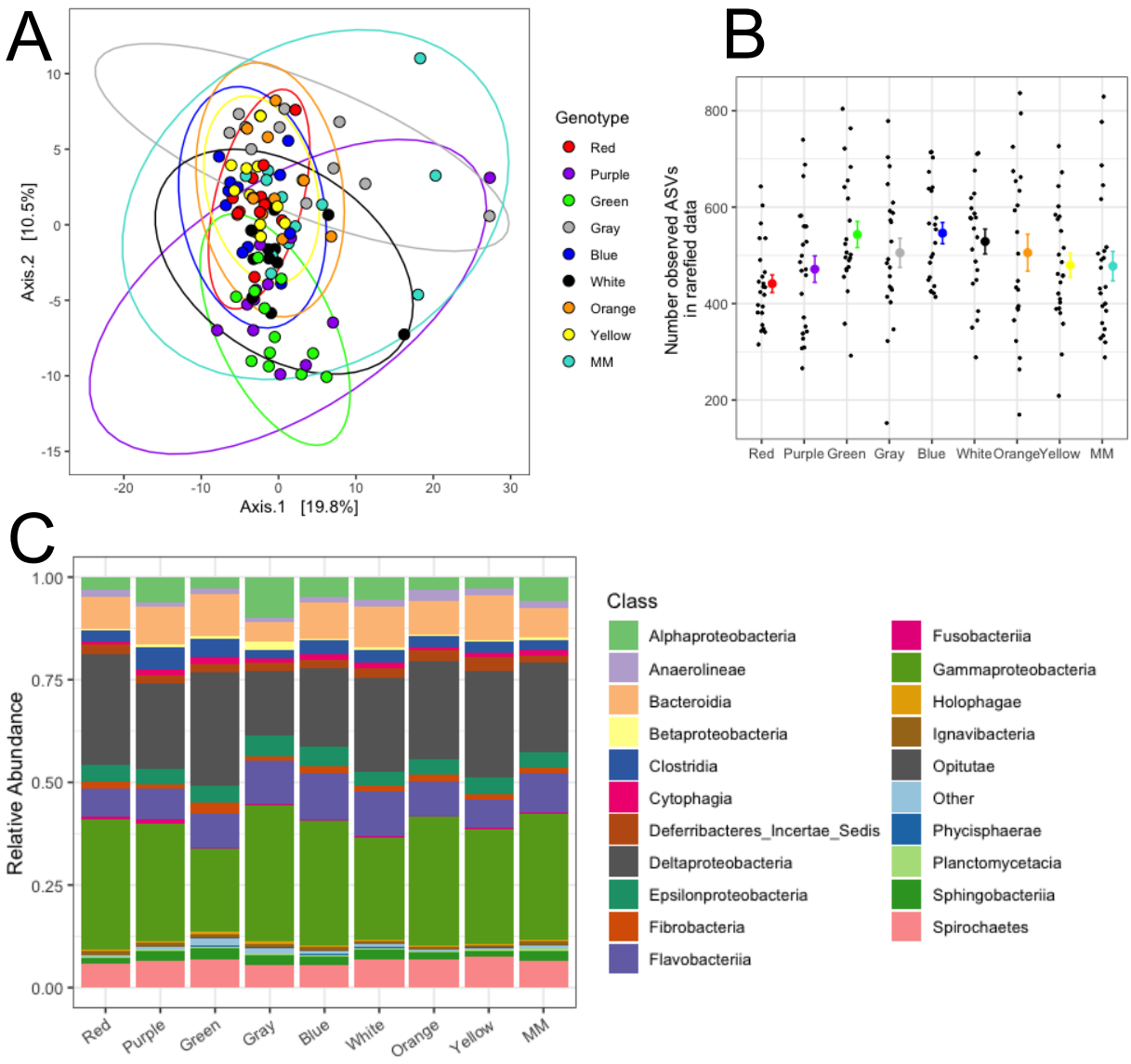
A
B
C
Axis.1 [19.8%]
Axis.2 [10.5%]
Genotype
Red
Purple
Green
Gray
Blue
White
Orange
Yellow
MM
Number observed ASVs in rarefied data
Relative Abundance
Class
Alphaproteobacteria
Anaerolineae
Bacteroidia
Betaproteobacteria
Clostridia
Cytophagia
Deferribacteres_Incertae_Sedis
Deltaproteobacteria
Epsilonproteobacteria
Fibrobacteria
Flavobacteriia
Fusobacteriia
Gammaproteobacteria
Holophagae
Ignavibacteria
Opitutae
Other
Phycisphaerae
Planctomycetacia
Sphingobacteriia
Spirochaetes

Figure 3.A4: Bacterial taxa that distinguish the Red genotype from other genotypes before our sediment treatments. All other genotypes that are being compared to the Red genotype are colored. A positive value indicates higher in the Red genotype, a lower value indicates higher in the other genotype.

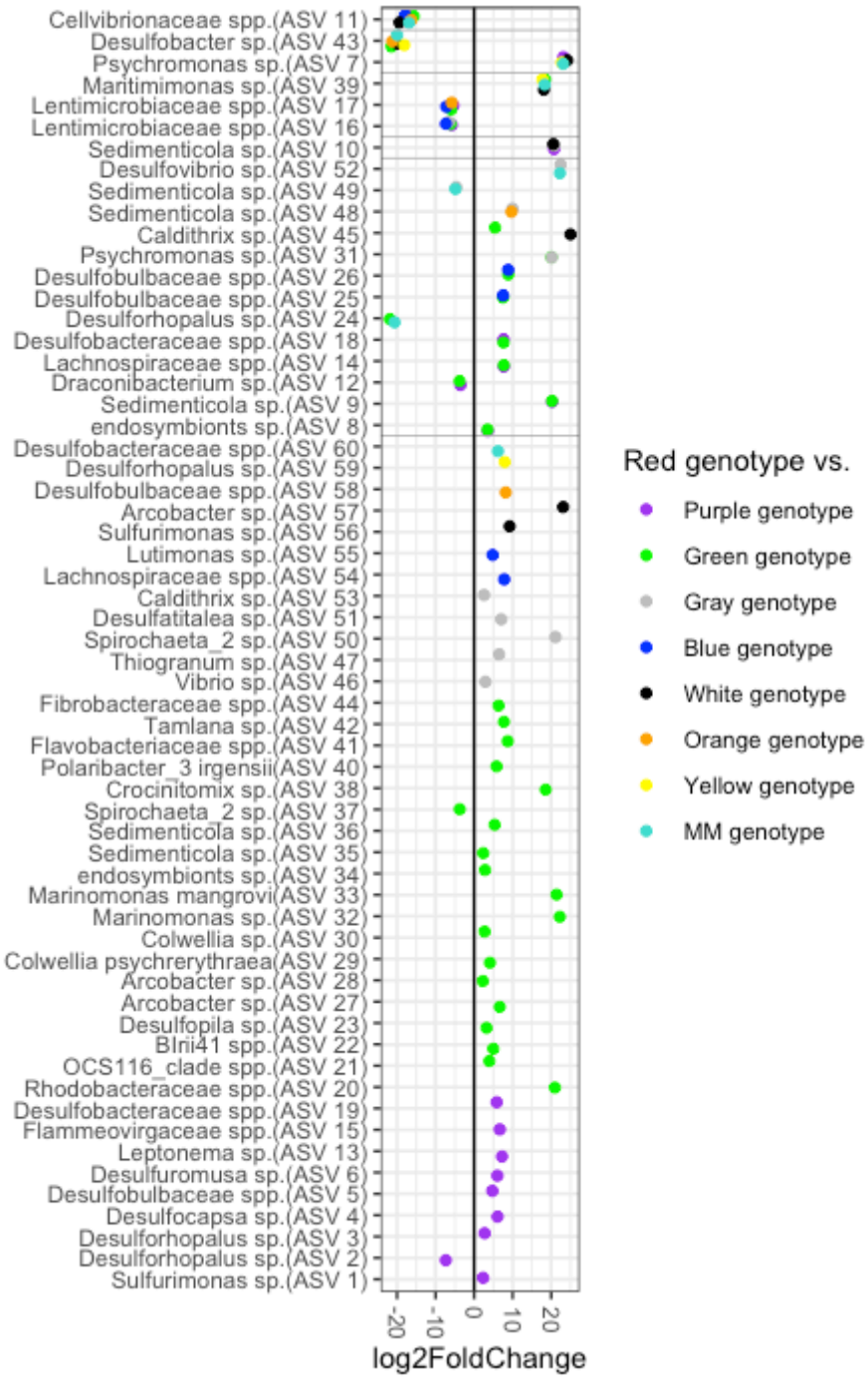

Figure 3.A5: Bacterial taxa that distinguish the Purple genotype from other genotypes before our sediment treatments. All other genotypes that are being compared to the Purple genotype are colored. A positive value indicates higher in the Purple genotype, a lower value indicates higher in the other genotype.

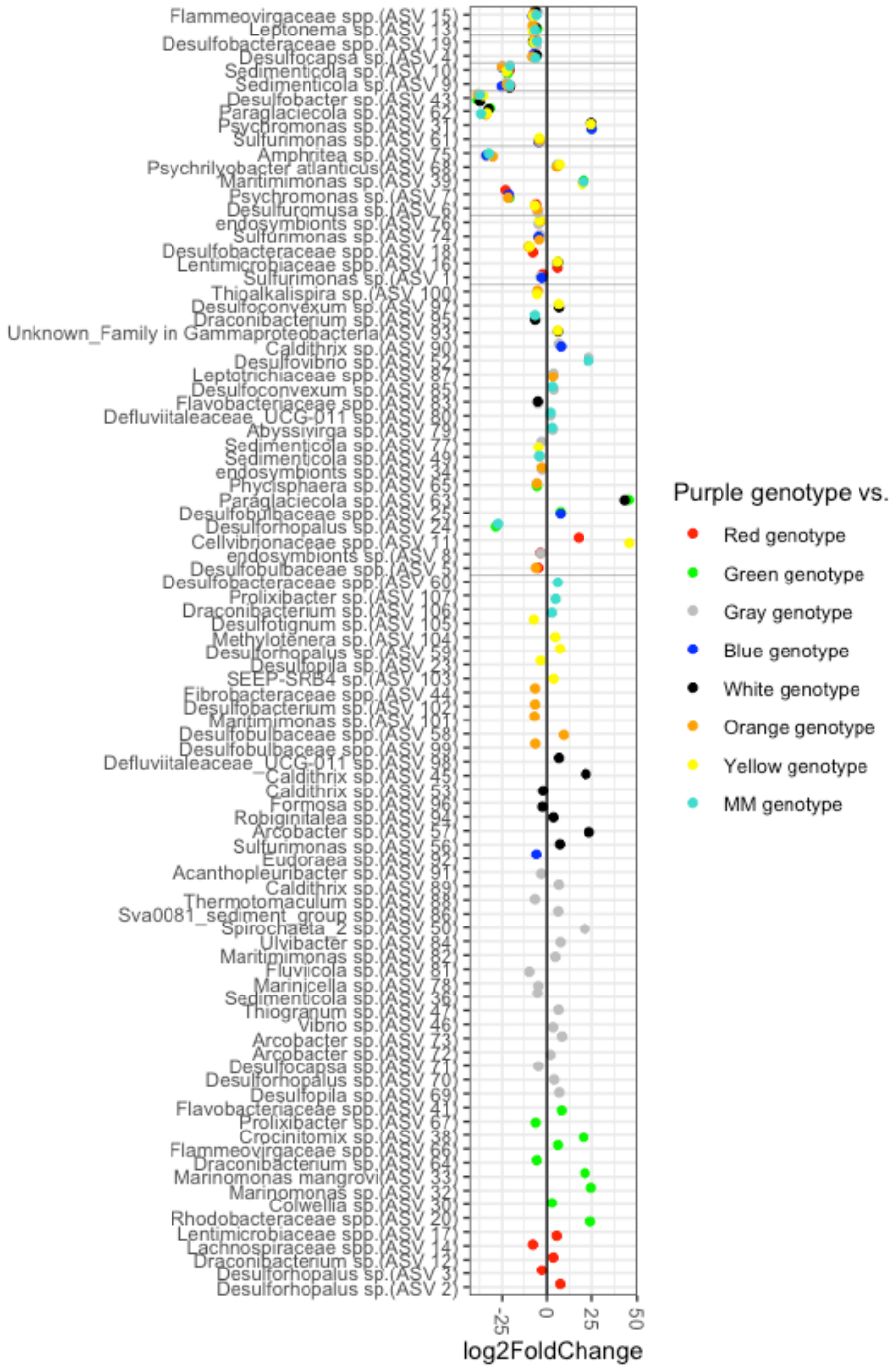

Figure 3.A6: Bacterial taxa that distinguish the Green genotype from other genotypes before our sediment treatments. All other genotypes that are being compared to the Green genotype are colored. A positive value indicates higher in the Green genotype, a lower value indicates higher in the other genotype.

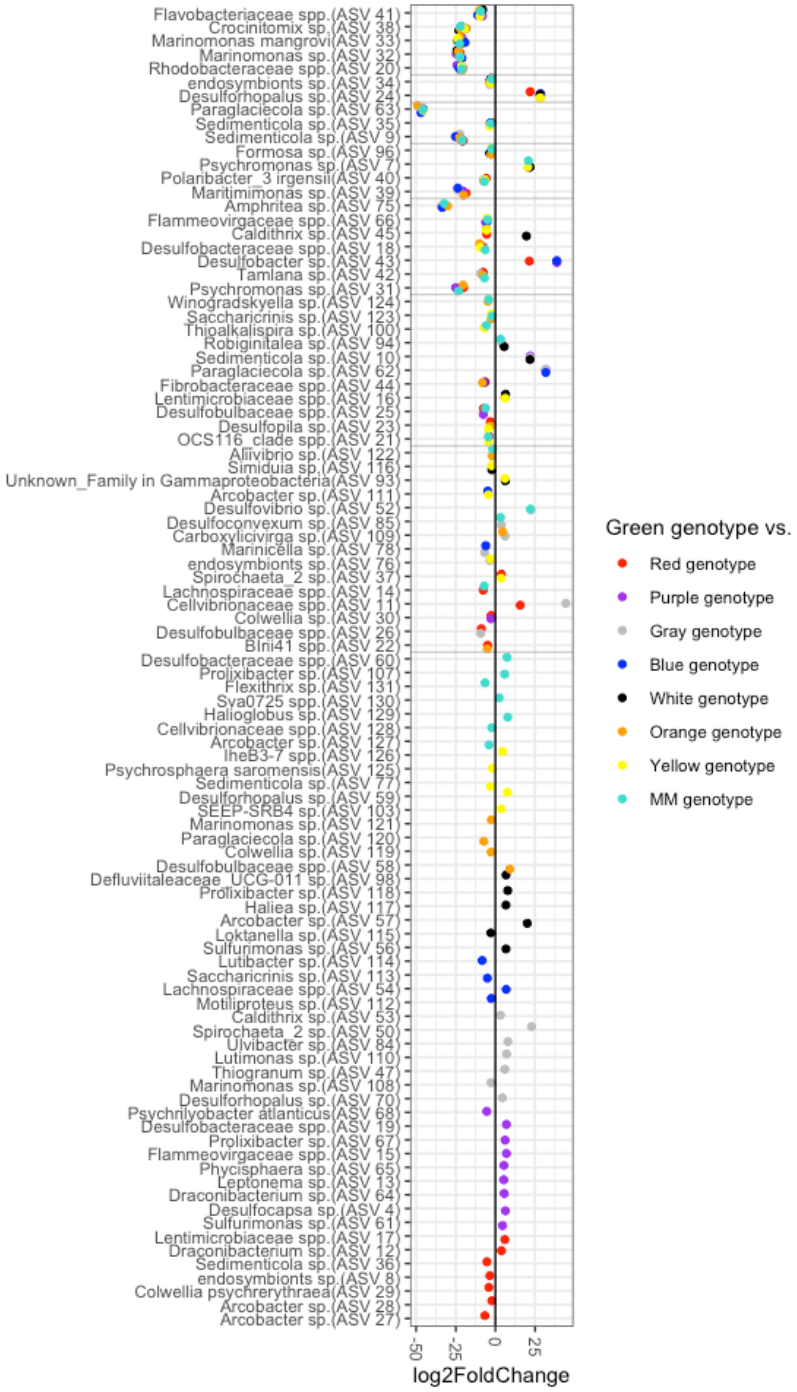

Figure 3.A7: Bacterial taxa that distinguish the Gray genotype from other genotypes before our sediment treatments. All other genotypes that are being compared to the Gray genotype are colored. A positive value indicates higher in the Gray genotype, a lower value indicates higher in the other genotype.

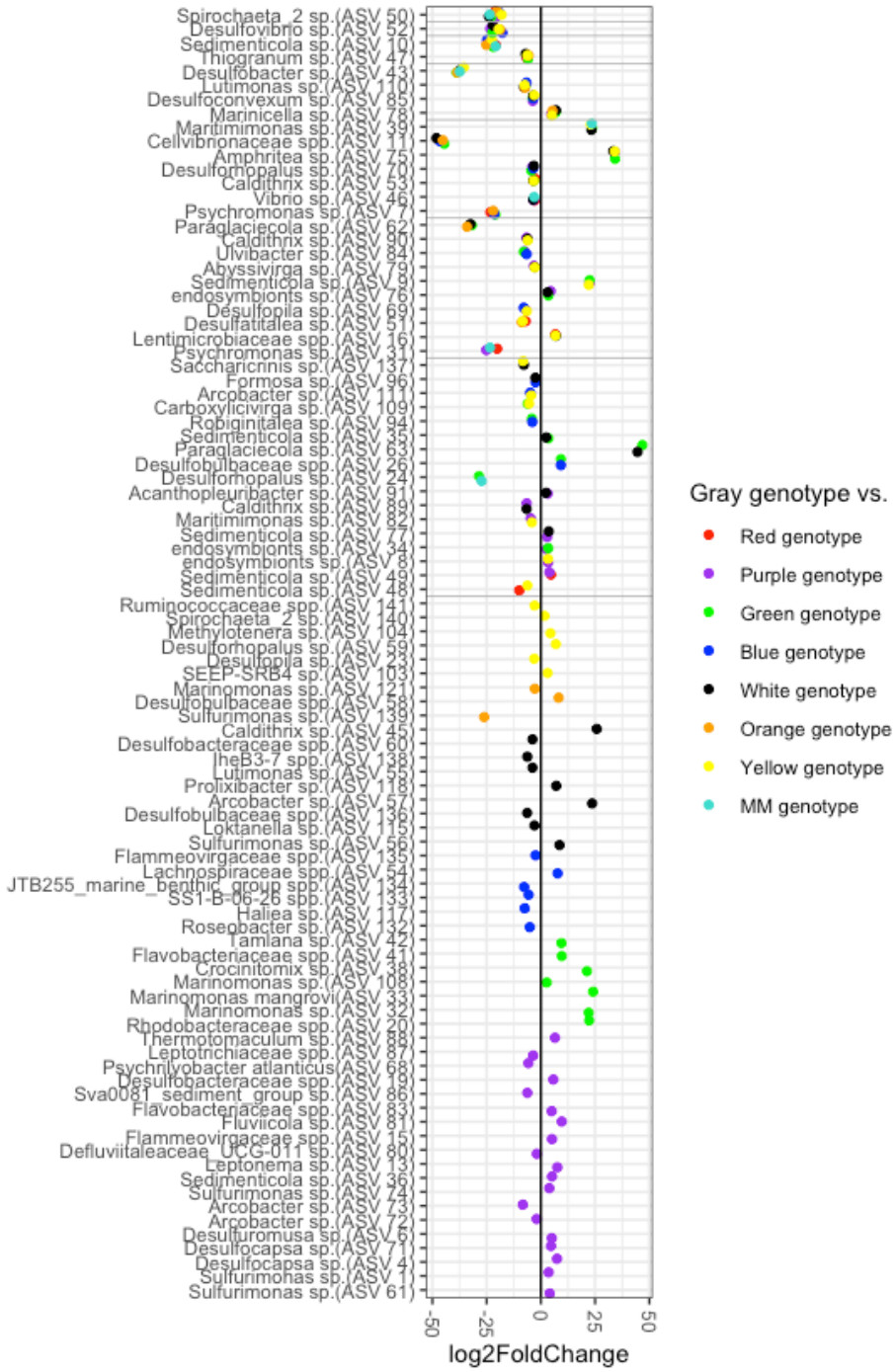

Figure 3.A8: Bacterial taxa that distinguish the Blue genotype from other genotypes before our sediment treatments. All other genotypes that are being compared to the Blue genotype are colored. A positive value indicates higher in the Blue genotype, a lower value indicates higher in the other genotype.

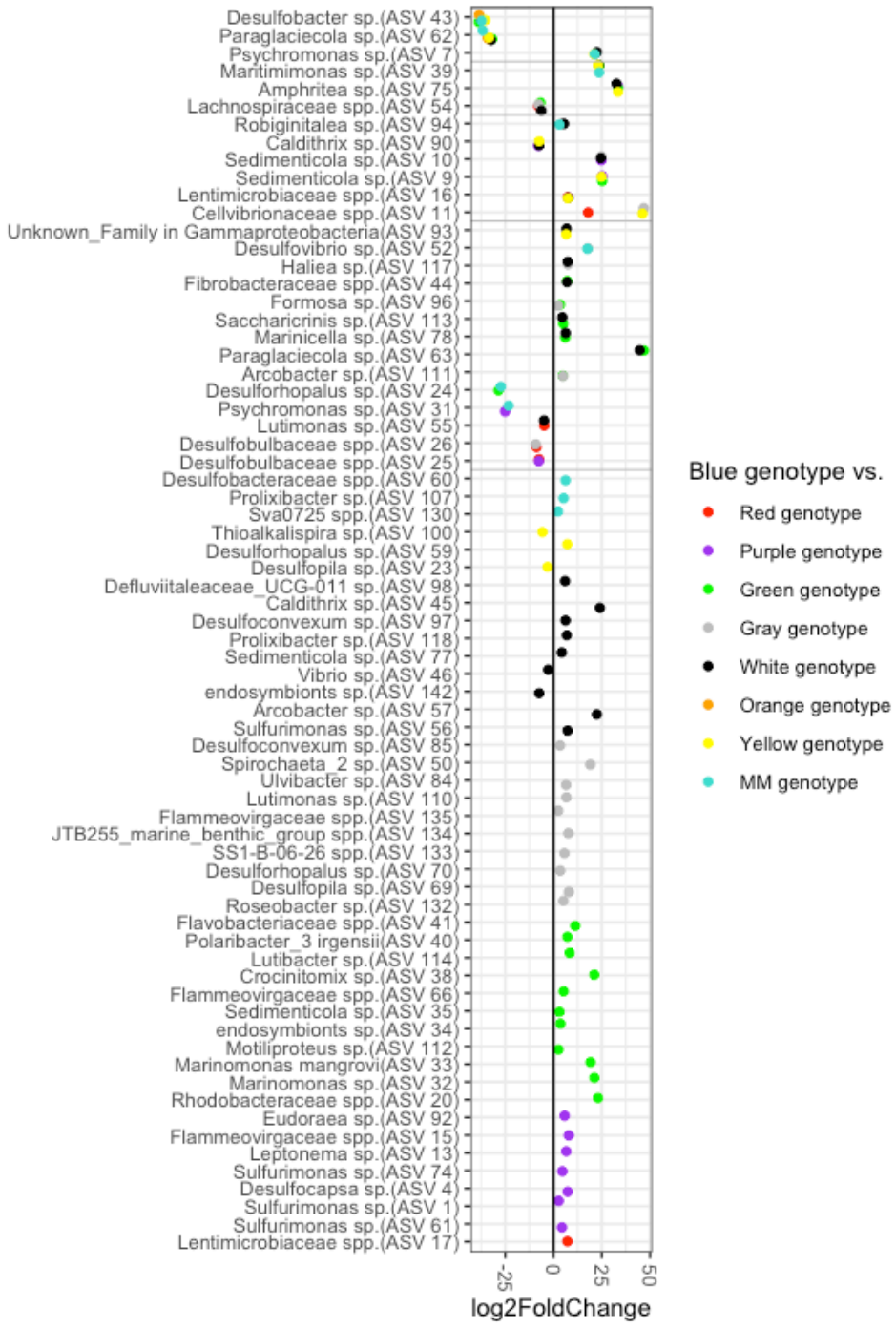

Figure 3.A9: Bacterial taxa that distinguish the White genotype from other genotypes before our sediment treatments. All other genotypes that are being compared to the White genotype are colored. A positive value indicates higher in the White genotype, a lower value indicates higher in the other genotype.

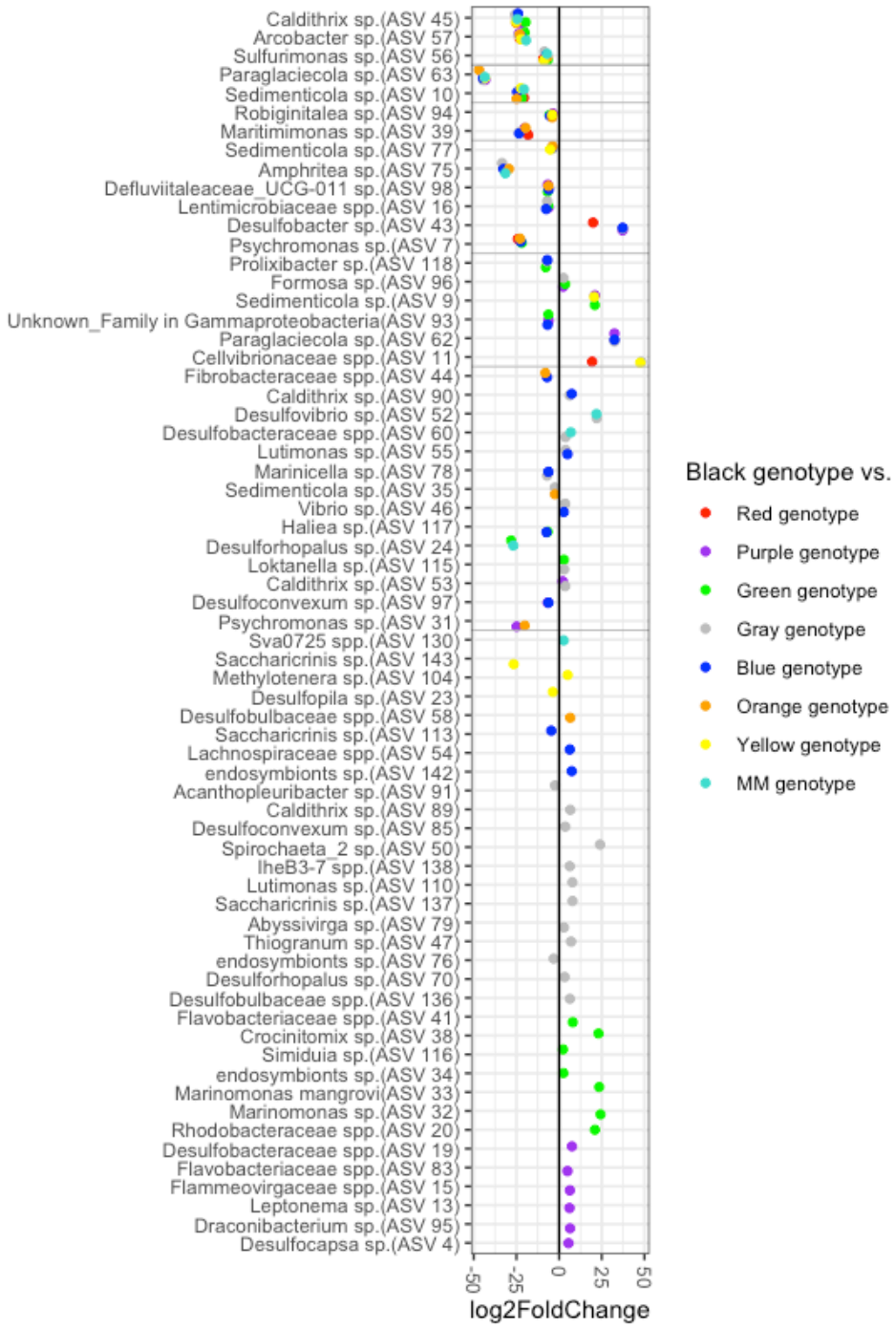

Figure 3.A10: Bacterial taxa that distinguish the Orange genotype from other genotypes before our sediment treatments. All other genotypes that are being compared to the Orange genotype are colored. A positive value indicates higher in the Orange genotype, a lower value indicates higher in the other genotype.

Figure 3.A11: Bacterial taxa that distinguish the Yellow genotype from other genotypes before our sediment treatments. All other genotypes that are being compared to the Yellow genotype are colored. A positive value indicates higher in the Yellow genotype, a lower value indicates higher in the other genotype.

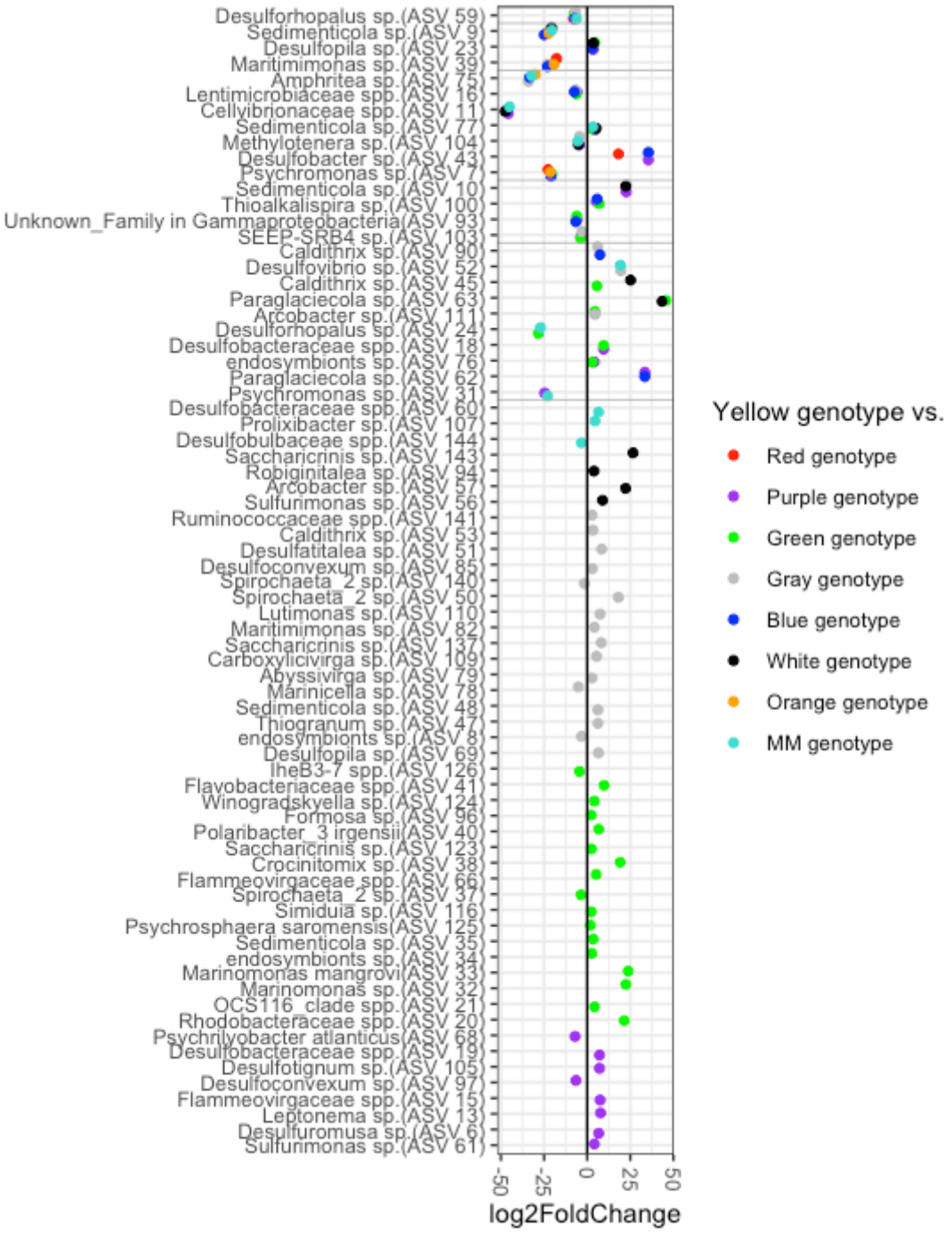

Figure 3.A12: Bacterial taxa that distinguish the MM genotype from other genotypes before our sediment treatments. All other genotypes that are being compared to the MM genotype are colored. A positive value indicates higher in the MM genotype, a lower value indicates higher in the other genotype.